Final Report 1999-35

PB2000-105144

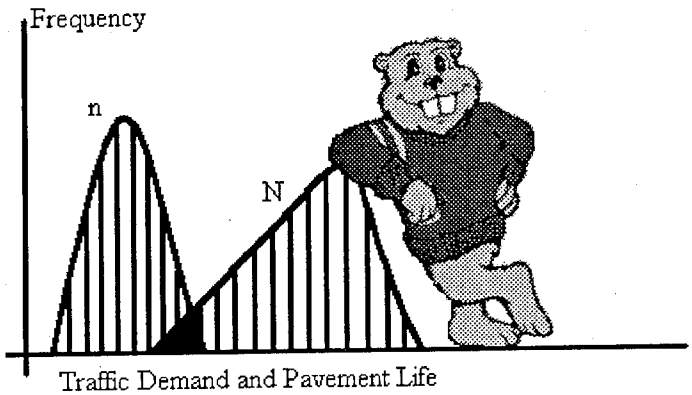

Incorporation of Reliability into the Minnesota Mechanistic - Empirical Pavement Design Method

Technical Report Documentation Page

1. Report No.	2.	3. Recipients Accession No.
MN/RC - 1999-35		

4. Title and Subtitle	5. Report Date
INCORPORATION OF RELIABILITY INTO THE MINNESOTA MECHANISTIC-EMPIRICAL PAVEMENT DESIGN METHOD	July 1999
	6.

7. Author(s)		8. Performing Organization Report No.
David H. Timm	Bjorn Birgisson	
David E. Newcomb	Theodore V. Galambos	

9. Performing Organization Name and Address	10. Project/Task/Work Unit No.
University of Minnesota Department of Civil Engineering 122 CivE Bldg., 500 Pillsbury Dr., S.E. Minneapolis, Minnesota 55455-0220	11. Contract (C) or Grant (G) No. 74708 TOC # 63

12. Sponsoring Organization Name and Address	13. Type of Report and Period Covered
Minnesota Department of Transportation 395 John Ireland Boulevard, Mail Stop 330 St. Paul, Minnesota 55155	Final Report 1997 - 1999
	14. Sponsoring Agency Code

15. Supplementary Notes

16. Abstract (Limit: 200 words)

This report documents the research that incorporated reliability analysis into the existing mechanistic-empirical (M-E) flexible pavement design method for Minnesota. Reliability in pavement design increases the probability that a pavement structure will perform as intended for the duration of its design life.

The report includes a comprehensive literature review of the state-of-the-art research. The Minnesota Road Research Project (Mn/ROAD) served as the primary source of data, in addition to the literature review. This research quantified the variability of each pavement design input and developed a rational method of incorporating reliability analysis into the M-E procedure through Monte Carlo simulation.

Researchers adapted the existing computer program, ROADENT, to allow the designer to perform reliability analysis for fatigue and rutting. A sensitivity analysis, using ROADENT, identified the input parameters with the greatest influence on design reliability. Comparison designs were performed to check ROADENT against the 1993 AASHTO guide and the existing Minnesota granular equivalency methods. Those comparisons showed that ROADENT produced very similar design values for rutting. However, data suggests that the fatigue performance equation will require further modification to accurately predict fatigue reliability.

17. Document Analysis/Descriptors		18. Availability Statement
Pavement design	Monte Carlo Simulation	No restrictions. Document available from:
Flexible pavement design	Reliability	National Technical Information Services,
Mechanistic-empirical design	ROADENT	Springfield, Virginia 22161

19. Security Class (this report)	20. Security Class (this page)	21. No. of Pages	22. Price
Unclassified	Unclassified	128	

INCORPORATION OF RELIABILITY INTO THE MINNESOTA MECHANISTIC – EMPIRICAL PAVEMENT DESIGN METHOD

Final Report

Prepared by
David H. Timm
David E. Newcomb
Bjorn Birgisson
Theodore V. Galambos

University of Minnesota
Department of Civil Engineering
122 CivE Building
500 Pillsbury Dr SE
Minneapolis, MN 55455-0220

July 1999

Published by

Minnesota Department of Transportation
Office of Research Services
First Floor
395 John Ireland Boulevard, MS 330
St Paul, Minnesota 55155

ACKNOWLEDGEMENTS

The authors would like to acknowledge the Minnesota Department of Transportation and the Office of Materials and Road Research for their support, cooperation, and contributions toward this research. The following people deserve special recognition: Glenn Engstrom, George Cochran, Duane Young and Graig Gilbertson provided guidance, leadership, and valuable insight throughout the project. Roger Olson, Dave Van Deusen, Dave Rettner, Shongtao Dai and John Siekmeier contributed their technical review and expertise. Jill Ovik's research was critical to the seasonal characterization of the material properties and her work was much appreciated. Curt Dahlin was of great assistance in the characterization of the Mn/ROAD traffic and his work on the WIM data was invaluable. Craig Schrader, Greg Johnson and Dave Palmquist provided vital data pertaining to in-situ conditions and pavement performance at the Mn/ROAD site. Warren Kalsow's technical assistance in maintaining access to the Mn/ROAD database was much appreciated.

TABLE OF CONTENTS

LIST OF TABLES

LIST OF FIGURES

EXECUTIVE SUMMARY

This report documents the research that incorporated reliability analysis into the existing mechanistic-empirical (M-E) flexible pavement design method for Minnesota. In fact, this report is an extension of a previous report entitled, "Mechanistic-Empirical Flexible Pavement Thickness Design, The Minnesota Method."

M-E methods are gaining more acceptance and greater use both nationally and internationally since they are more robust than traditional empirically-based design methods. For example, M-E methods can adapt to new design conditions (e.g., heavier loads, new pavement materials) by relying primarily upon mechanistic pavement modeling. Empirically-based procedures, however, are limited to the original test conditions encountered during procedure development.

The previous report, mentioned above, assumed that the input parameters used for design were deterministic, but virtually every design parameter has some associated variability. Consequently, for the M-E procedure to be complete there must be an accounting for the inherent variability within the design process. Reliability analysis allows for a rational accounting of the variability in the design parameters. Other advantages of using reliability include the calibration of new design methods, developing rational design specifications, optimizing resources, and assessing the damage and remaining life of the pavement structure. Given these statements, the objectives of this research were to:

1. Develop a rational method of incorporating reliability into the existing M-E pavement thickness design framework for Minnesota.

2. Identify and statistically characterize the design input parameters.
3. Assess the effects of the design parameters and their variability on pavement design reliability.
4. Incorporate the research findings into the existing computer program, ROADENT, to facilitate reliability-based designs in a user-friendly environment.

The project began with a comprehensive literature review that examined pavement design in the context of reliability analysis. The following topics were investigated in the literature review: definitions of reliability, methods of reliability analysis, reliability in the 1993 American Association of State Highway and Transportation Officials (AASHTO) Design Guide, and variability of the design input parameters used in ROADENT.

Once the literature review was complete, it was possible to proceed with the incorporation of reliability into the M-E method. The first task was to characterize the variability of the design input parameters used in ROADENT. This was accomplished by synthesizing data from the literature and from the Minnesota Road Research Project (Mn/ROAD) into a coherent representation of input variability. The second task was to formulate the reliability analysis scheme. It was found that Monte Carlo simulation was a straightforward means of incorporating reliability into the existing M-E framework. Consequently, ROADENT was modified to accommodate Monte Carlo simulation and reliability analysis.

After the input parameters had been statistically characterized and ROADENT had been modified, it was necessary to perform a sensitivity analysis to achieve the third

objective of this project. The sensitivity analysis examined the effects of one parameter variability, combined variability, and combined variability with axle weight variability on the distribution of predicted fatigue and rutting life. The results of the sensitivity analysis are summarized below:

(a) Fatigue variability is most affected by the inputs closer to the pavement surface. Namely, asphalt modulus, asphalt thickness and base thickness.

(b) Rutting variability is most affected by the stiffness of the subgrade material and the thicknesses of the overlying materials.

(c) The other parameters' variability should not be discounted since they each contribute to the so-called baseline variability.

(d) Axle weight distributions have an overwhelming effect on the output variability in terms of fatigue and rutting. Therefore, these deserve careful characterization.

(e) The fatigue and rutting probability density functions may be approximated with an extreme-value type I function.

(f) The number of Monte Carlo cycles that should be used in design is 5,000.

The final task in the project was to compare the results obtained from ROADENT versus those obtained from the 1993 AASHTO Design Guide and those obtained from the current Minnesota granular equivalency (G.E.) methods. It was generally found that ROADENT provides consistent results with AASHTO and the G.E. method with respect to rutting. However, it was clearly evident that further calibration of the fatigue transfer function is required to more accurately predict fatigue life.

While the objectives of this project were met, it is important to reemphasize the need to continually refine this design procedure. One of the fundamental principles of M-E design is that it must be calibrated to local conditions. This was evident in the fatigue performance predictions made by ROADENT. Further investigations and calibration are required to fine-tune the design procedure. Additionally, the calibration database should be expanded beyond the realm of Mn/ROAD to better represent conditions around the state of Minnesota. However, with the framework in place, the calibration process is relatively straightforward and changes may be implemented without great difficulty.

CHAPTER 1

INTRODUCTION

Background

The role of reliability in pavement design is to quantify the probability that a pavement structure will perform, as intended, for the duration of its design life. Many of the parameters associated with pavement design and construction exhibit natural variability. Therefore, in order for a thickness design methodology to be complete, there must be an accounting of variability within the process. Reliability analysis allows for a rational accounting of the variability in the design parameters. Other advantages of using reliability include the calibration of new design methods, developing rational design specifications, optimizing resources, and assessing the damage and remaining life of the pavement.

A mechanistic-empirical (M-E) flexible design methodology has been proposed for use in Minnesota (*1*). A flow chart depicting the procedure is shown in Figure 1.1 and a brief summary of the process is described below:

Material properties, initial layer thicknesses, and load configurations are entered into a load-displacement model that calculates stresses and strains at critical locations. The calculated stresses and strains are used to compute the number of allowable loads until failure, while the number of expected loads for each particular condition must also be determined. This process is then iterated for each seasonal condition and load configuration and the accumulated damage is summed. Failure occurs when damage exceeds unity, in which case the layer thicknesses are increased. If damage is much less than unity, the pavement has been over-designed and the layer thicknesses should

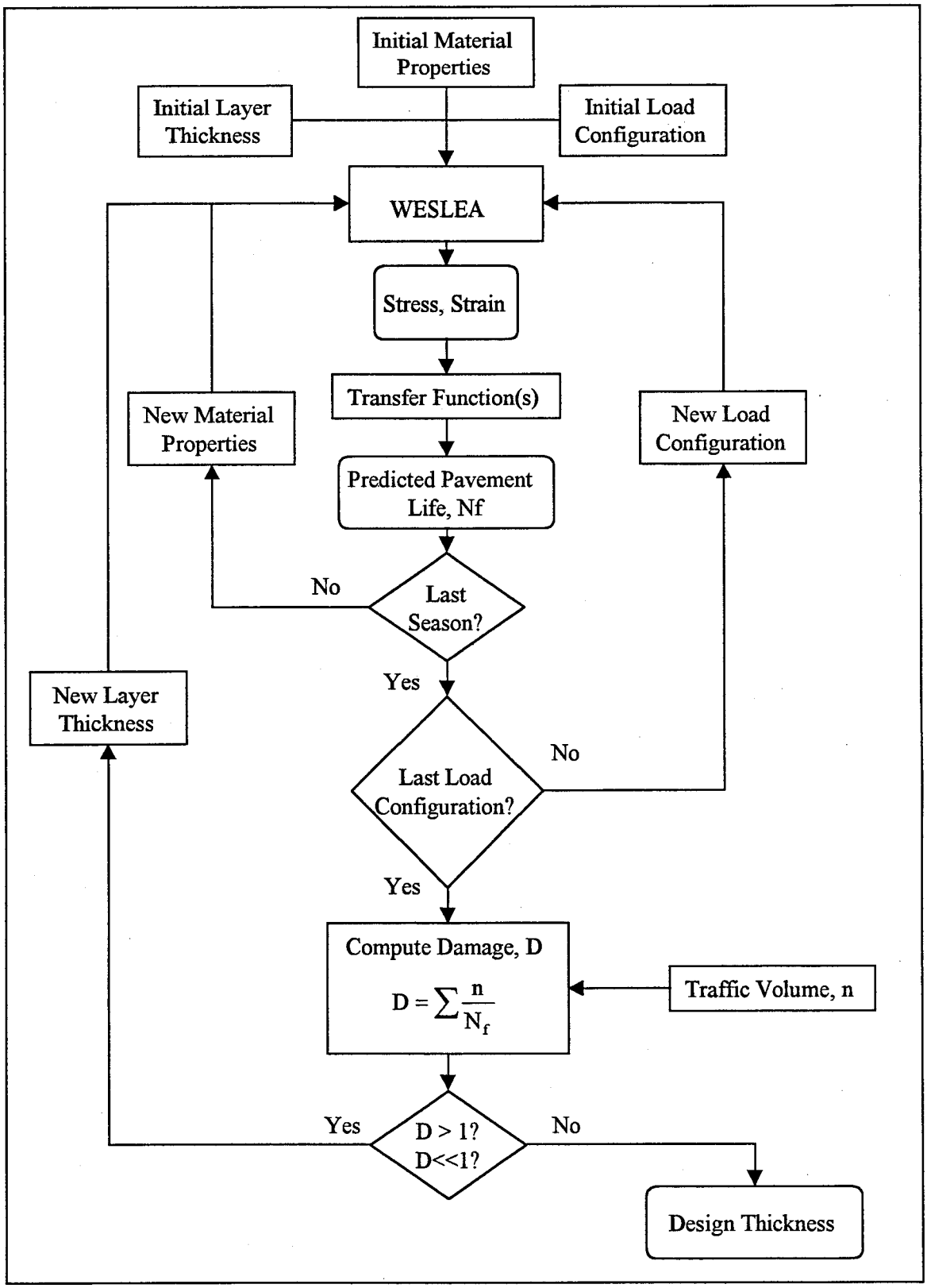

Figure 1.1 Mechanistic-Empirical Design Flow Chart (*1*).

be decreased. When damage is near but not exceeding unity the design thickness has been achieved.

The component missing from the above methodology is reliability. There is statistical variation in the input parameters. Consequently, there is variability in the calculated stresses and strains that lead to variations in the number of allowable loads. There is also variability in the number of expected loads during the design period. Finally, there is variability in regard to the transfer functions that predict pavement life.

A simple example of how the variability of the inputs can be related to the variability of the output, and ultimately reliability, is depicted in Figure 1.2. In this example, the predicted pavement life is a function of the pavement strain, which is a function of the asphalt stiffness, which is a function of the asphalt temperature. Since the asphalt temperature is variable, it follows that the pavement life would also exhibit variability. The reliability may then be interpreted as the probability of the pavement structure exceeding some level of predicted pavement life. In actual pavement design, there are many more input parameters to consider which all contribute to the stochastic nature of the design methodology. Therefore, the incorporation of reliability in flexible pavement thickness design is the focus of this research project.

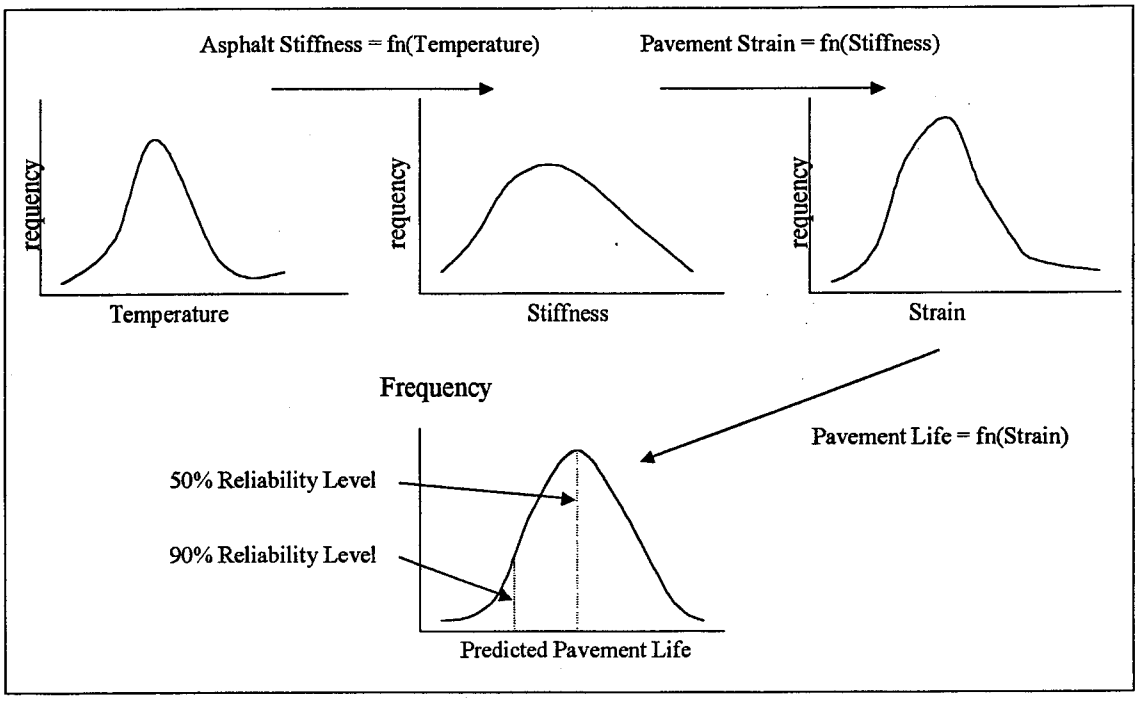

Figure 1.2 Example of Variability and Reliability.

Objectives

The main objective of this research was to develop a rational method of incorporating reliability into the existing M-E pavement thickness design framework for Minnesota. In order to achieve this objective, the relevant design input variables needed to be identified and their variability statistically characterized. Assessing the effects of the design parameters and their statistical variability on pavement design reliability was an additional objective. The final objective was to incorporate the research findings into the existing computer program, ROADENT (*1*), in order to facilitate reliability-based designs in a user-friendly environment.

Scope

A literature review was conducted to investigate issues in reliability-based pavement design. Information was obtained regarding Monte Carlo simulation and other reliability analysis techniques, pseudo-random number generation, and statistical characterization of the relevant design variables. Data obtained from the literature and the Minnesota Road Research Project (Mn/ROAD) were used in the statistical characterization.

The computer program, ROADENT, was enhanced to incorporate Monte Carlo simulation in the design process. This allowed for an in-depth sensitivity analysis regarding the relative effects of each input parameter's variability on the design reliability. For the purposes of this project, the transfer functions, which predict pavement life from pavement response, were assumed to be deterministic. Example designs were developed to demonstrate the application of reliability in flexible pavement thickness design and to compare the results of the M-E method against established design procedures.

CHAPTER 2

LITERATURE REVIEW

Definitions of Reliability

There are many definitions concerning the term "reliability." In the general sense, reliability implies trustworthiness or dependability. When applied to structural pavement design, the 1993 AASHTO Guide defines reliability in this way (*2*):

> "The reliability of a pavement design-performance process is the probability that a pavement section designed using the process will perform satisfactorily over the traffic and environmental conditions for the design period."

Other definitions of reliability include, "...the probability that:"

> "... serviceability will be maintained at adequate levels from a user's point of view, throughout the design life of the facility" (*3*).
>
> "... the load applications a pavement can withstand in reaching a specified minimum serviceability level is not exceeded by the number of load applications that are actually applied to the pavement" (*4*).
>
> "... the pavement system will perform its intended function over its design life (or time) and under the conditions (or environment) encountered during operation" (*5*).
>
> "... any particular type of distress (or combinations of distress manifestations) will remain below or within the permissible level during the design life" (*2*).
>
> "... a pavement as designed will withstand the actual number of load applications on it during a selected design life while maintaining its structural integrity" (*6*).

The first four definitions imply pavement failure as a serviceability loss (e.g., loss of ride quality). Serviceability is often viewed as a subjective measure of pavement performance, while more objective measures include evaluating the fatigue cracking and rut depth of the pavement in question. For example, pavement failure may be defined as a specific amount of rutting or fatigue cracking. Regardless of the type of failure, it is

critical to establish a failure threshold since in the strictest sense, reliability is one minus the probability of failure:

$$R = 1 - P[\text{failure}] \qquad \text{Equation 2.1}$$

As cited by Kulkarni (*6*), a common basis for comparison between pavement types is essential in estimation of life cycle costs. Since flexible and rigid pavements exhibit different types of distress, defining failure by distress could lead to erroneous conclusions. Therefore, Kulkarni defines reliability in terms of traffic that is the same regardless of pavement type:

> "To provide uniformity, pavement design reliability is defined as the probability that the pavement's traffic load capacity exceeds the cumulative traffic loading on the pavement during a selected design life."

The above statement may be expressed mathematically as (*6*):

$$R = P[N > n] \qquad \text{Equation 2.2}$$

Where "N" is the traffic load capacity of the pavement structure and "n" is the actual number of load applications. This definition is consistent with definitions in structural mechanics where reliability is the probability that the resistance provided by the structure is greater than the load effects. A graphical representation of the equation is shown in Figure 2.1. The shaded area in the figure concerns reliability but is not the explicit representation of reliability. Kulkarni explains that the figure simply illustrates how the two distributions may overlap and moving them further apart increases the reliability.

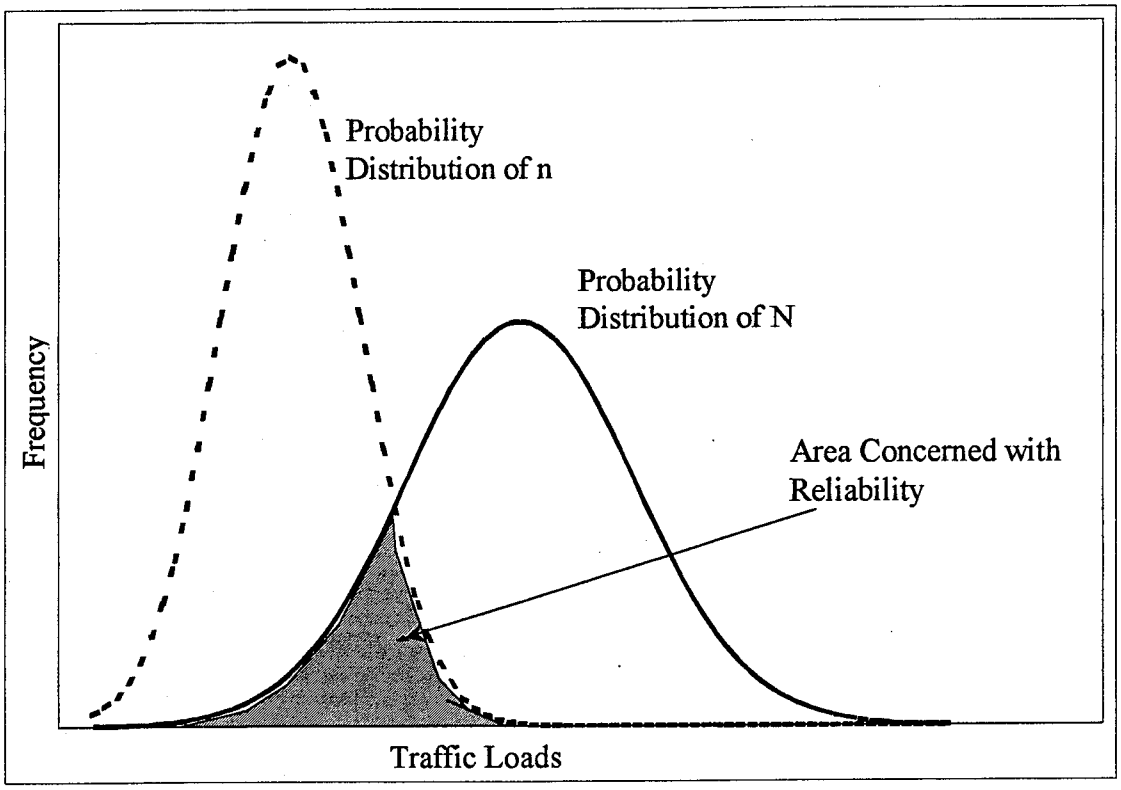

Figure 2.1 Probability Distributions of N and n (*6*).

It is important to keep in mind that N and n are drawn from probability distributions in Equation 2.2. In other words, N and n are random variables. Consequently, in order to quantify reliability, the distribution of each must be determined. Typically, N and n are determined from functions that utilize relevant input parameters. The variability of the input parameters causes N and n to exhibit variation. For example, say that N may be expressed as a function of three input parameters; x_1, x_2, and x_3. Since each of the x values exhibit variability, N must also be variable. Therefore, the characterization of N and n are critical to reliability.

Reliability Analysis

In order to accurately quantify reliability (as in Equation 2.2), reliability analysis must be performed. The objective of reliability analysis, as described by Harr (*7*), is to determine the probability distribution of a function's output given a number of variable input parameters.

There are three general categories of reliability analysis cited by Harr and each yields a representation of the output probability distribution:

- First-Order, Second Moment (FOSM) Methods
- Point-Estimate Method (PEM)
- Exact Methods

FOSM Methods

First-Order, Second Moment (FOSM) methods are based on the truncation of the Taylor series expansion of the function in question (*7*). In contrast to exact methods, the inputs and outputs are expressed as expected values and standard deviations rather than entire distributions. While this reduces the reliance upon computers, the mathematical requirements in terms of the derivatives associated with the Taylor series may be prohibitively complicated. This is especially true when dealing with a load-displacement model including iterative steps and complicated functions that calculate pavement response.

PEM Methods

The second category presented by Harr (*7*) was the point-estimate method (PEM), which was originally developed by Rosenblueth (*8*). This method avoids the issue of obtaining derivatives required by the FOSM method and most calculations may be handled by a pocket calculator. The method relies upon knowing the mean, variance, and skewness of each input parameter. Two points, drawn from each of the input distributions, are then selectively chosen about the mean and their associated probabilities are determined. The parameters are then transformed by the function and the mean and variance of the function are determined. Other researchers, including Van Cauwelaert (*9,10*) expanded the original work of Rosenblueth to include a three-point estimation for better accuracy. A disadvantage of this method is that although the selected points are transformed by the function, the probabilities are not, they are simply associated with each point. Eckmann (*11*) demonstrated, however, that if the transforming function could be modeled by a polynomial with a certain degree (generally second or third order) then the Rosenblueth method provides accurate results.

Exact Methods

The final category cited by Harr (*7*), exact methods, includes numerical integration and Monte Carlo simulation. Harr uses the term "exact" in the context that entire distributions are input into the function rather than representative points. Therefore, the probability distributions of all the component variables must be initially specified. Briefly, the Monte Carlo method involves artificially reproducing each input distribution, entering the values into the function, and obtaining the output distribution.

The primary advantage of an exact method is that the complete probability distribution of the dependent random variable is determined (*7*). This proves especially useful when examining the "tails" of the distribution. Additionally, Monte Carlo simulation is straightforward, involving nothing more than generation of random numbers and transforming these into particular distributions. A more detailed explanation is provided in the Research Methodology Chapter. The relative simplicity of the method was the primary motivation for using Monte Carlo simulation in this project.

As described by Harr (*7*), numerous Monte Carlo cycles may be required for an accurate approximation of the true distribution. In order to determine the number of required cycles, M, he proposed using a normal approximation of a binomial distribution. When generating the output distribution consisting of M cycles there are "P" correct and "1-P" incorrect values. With a large M, this binomial distribution may be approximated as normal. This approach leads to an equation that estimates the number of required cycles given an acceptable level of error and number of input parameters:

$$M = \left(\frac{z_{\frac{\alpha}{2}}^2}{4\varepsilon^2} \right)^m \qquad \text{Equation 2.3}$$

where: M = number of required cycles

ε = acceptable level of error

$z_{\alpha/2}$ = associated z-statistic from standard normal table

m = number of input parameters to function

This equation will escalate the number of required cycles very quickly. For example, assuming only one parameter (m=1) and 99% confidence ($\varepsilon = 0.01$, $z_{\alpha/2} = 2.58$), the required number of cycles is 16,641. This number of cycles would already be somewhat

prohibitive, and with the addition of more variables (increasing m), the number would currently be unreasonable for a personal computer. Another method of estimating the precision of a Monte Carlo distribution involves checking the repeatability of the results for a given number of cycles, M (*12*).

Reliability in the 1993 AASHTO Pavement Design Method

Method of Reliability Analysis in the AASHTO Guide

An examination of either the flexible or rigid pavement design algorithms in the AASHTO 1993 Guide (*2*) reveals that reliability is accounted for in the procedure. For design purposes, the reliability term is straightforward to use and guidance is given in selecting the relevant parameters. However, it is useful to investigate the origins of reliability in the AASHTO method because it lends insight into the general formulation of reliability in pavement design.

In the AASHTO guide, pavement section designs are governed by a performance equation. It is inherently assumed that the equation is an explicit mathematical formula that predicts the number of equivalent single axle loads (ESALs) the pavement can endure before reaching the specified minimum serviceability. When designed, the pavement must be able to withstand the expected applied traffic multiplied by a reliability design factor, F_R ($F_R \geq 1$). Mathematically speaking, predicted performance may be expressed as:

$$W_t = F_R * w_T \qquad \text{Equation 2.4}$$

or

$$\log W_t = \log F_R + \log w_T \qquad \text{Equation 2.5}$$

where W_t is the predicted number of ESALs the structure can withstand, F_R is the reliability design factor, and w_T is the predicted ESALs that will be applied to the pavement for the design period.

It is the "reliability design factor" that accounts for the sources of uncertainty in the AASHTO procedure, which is often referred to as the "positive spacing factor" between log W_t and log w_T:

$$\log F_R = (\log W_t - \log w_T) \geq 0 \qquad \text{Equation 2.6}$$

F_R is the only probability component that the designer "controls" by selecting a design level of reliability. Basically, F_R provides some probabilistic assurance that the actual pavement performance exceeds the actual design period traffic. The other sources of deviation ($\pm\delta$) in the design procedure are:

1. Prediction error in the design period traffic:

$$(\log w_T - \log N_T) = \pm\delta(N_T, w_T) \qquad \text{Equation 2.7}$$

The difference between the predicted and actual design period ESAL the pavement will experience.

2. Prediction error in pavement performance:

$$(\log N_t - \log W_t) = \pm\delta(W_t, N_t) \qquad \text{Equation 2.8}$$

The difference between the actual number of ESALs and the predicted ESALs the structure can withstand before reaching terminal serviceability.

3. Overall deviation of actual section performance from actual design period traffic, expressed as the algebraic and geometric sum of equations 2.6, 2.7 and 2.8:

$$(\log N_t - \log N_T) = \pm\delta_0 \qquad \text{Equation 2.9}$$

The difference between the actual number of ESALs the pavement can withstand

before reaching terminal serviceability and the actual number of ESALs applied to the pavement structure.

Figure 2.2 illustrates the above deviations in terms of present serviceability index.

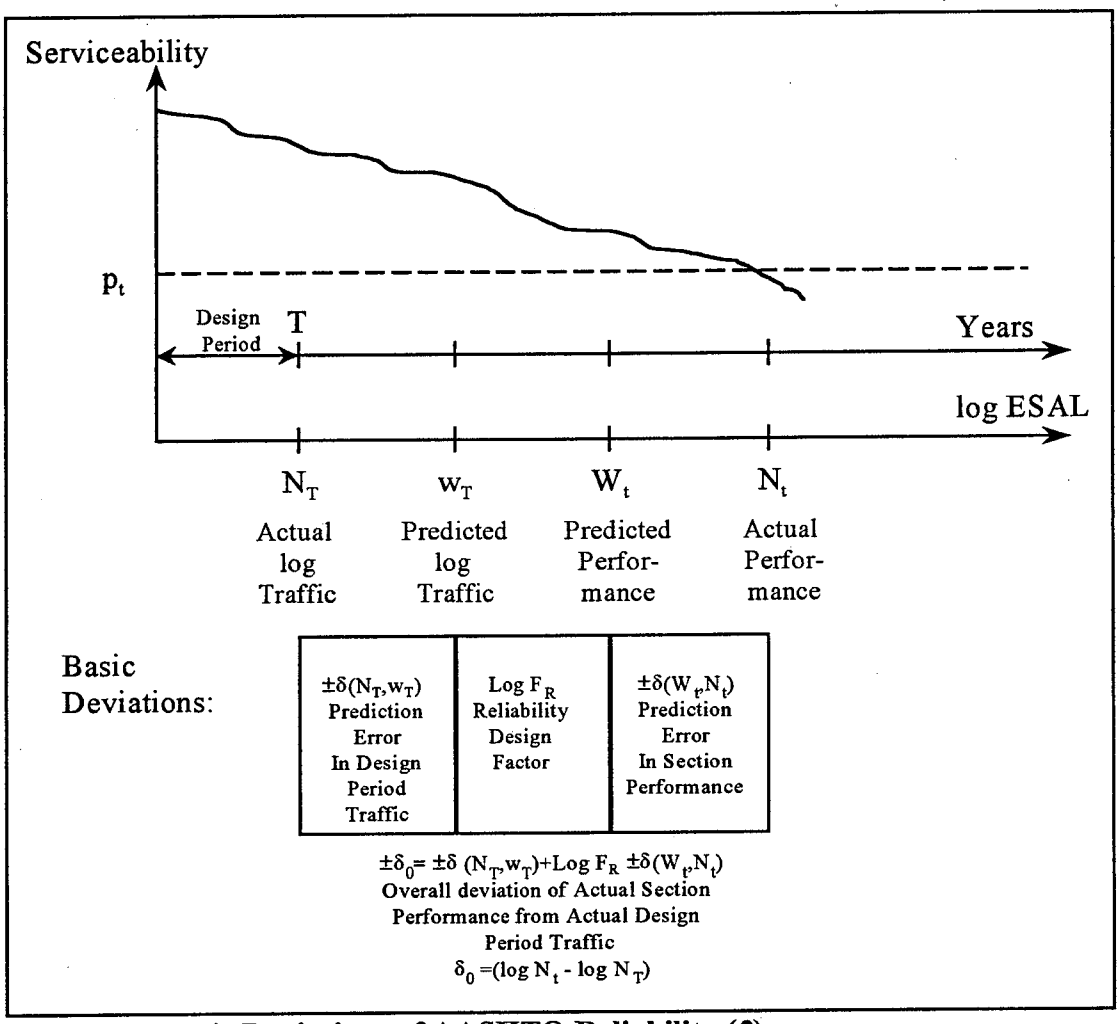

Figure 2.2 Basic Deviations of AASHTO Reliability (*2*).

AASHTO assumes that the set of all possible outcomes for each of the chance deviations would produce a normal probability distribution. Therefore the overall deviation, δ_0, would also have a normal probability distribution with a mean as the sum of the three deviate means and variance as the sum of the three deviate variances. Furthermore, assuming no bias in the prediction procedure, the set of all possible chance deviations will have an average value of zero:

$$\bar{\delta}_0 = \bar{\delta}(N_T, w_t) + \log(F_R) + \bar{\delta}(W_t, N_t)$$
$$\bar{\delta}_0 = 0 + \log(F_R) + 0 = \log(F_R) \qquad \text{Equation 2.10}$$

The variance of the above distribution is then the sum of the squares of the variances from each source of chance variation. Since the reliability factor, F_R, is not random, its variance is zero. Mathematically:

$$S_0^2 = S_w^2 + 0 + S_N^2 \qquad \text{Equation 2.11}$$

Thus far, a normal random variable (δ_0) has been defined. The variable is a performance predictor that encompasses the error in predicting the design period traffic, the reliability design factor, and the error in predicting pavement performance. The mean of the distribution is the log of the reliability factor, while the variance is the sum of the squares of traffic prediction variance and pavement performance prediction variance. The area of concern associated with this distribution is when δ_0 equals zero. At this point the number of actual ESALs applied equals the number of allowable ESALs and failure is imminent. Figure 2.3 illustrates the above concepts.

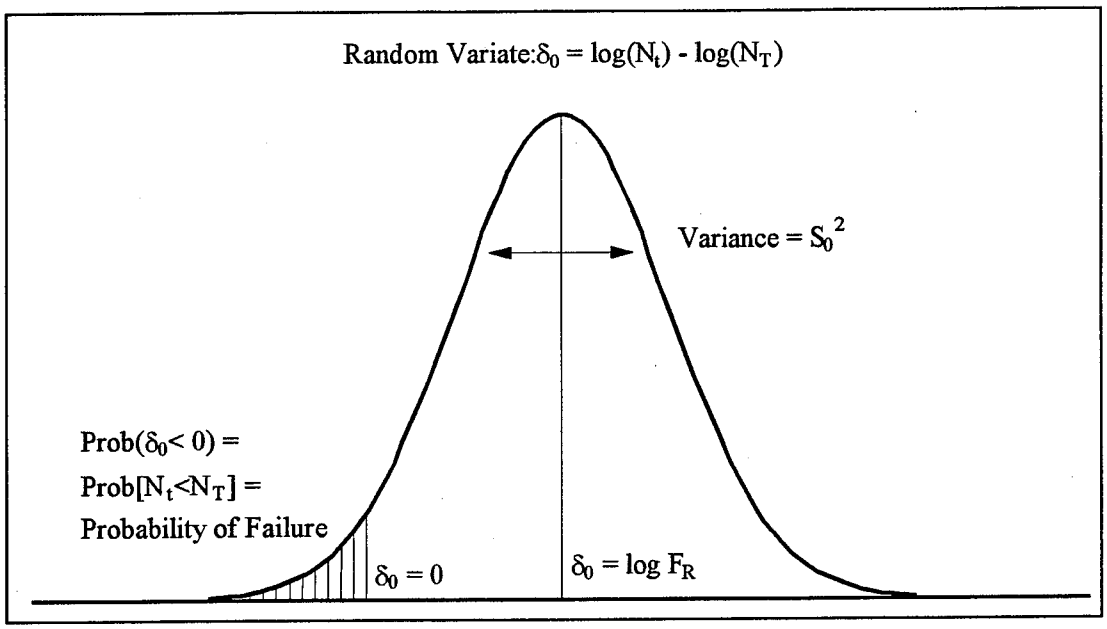

Figure 2.3 Definition of AASHTO Reliability (*2*).

The final steps in the AASHTO reliability method involve the transformation of δ_0 to the standard unit normal variable. The equations below outline the process.

$$Z = \frac{\delta_0 - \bar{\delta}_0}{S_0} = \frac{\delta_0 - \log(F_R)}{S_0} \qquad \text{Equation 2.12}$$

Taking δ_0 at zero, the point of failure, Equation 2.12 becomes:

$$Z_R = \frac{-\log(F_R)}{S_0} \qquad \text{Equation 2.13}$$

$$F_R = 10^{-Z_R * S_0} \qquad \text{Equation 2.14}$$

where Z_R may be obtained from a standard normal table for a specified level of reliability, and F_R is incorporated into the design equations as a positive spacing factor. Therefore, accurate predictions of reliability depend primarily on the selection of S_0. AASHTO provides a range of values and an appendix to help select S_0, while it is emphasized that the designer should develop an S_0 to suit the given design conditions.

Consequently, the problem involves determining the variability of the associated input parameters followed by a statistical exercise to determine the design reliability.

Levels of Reliability in the AASHTO Guide

The design nomograph in the 1993 AASHTO Guide (*2*) allows the designer to select a level of reliability. However, a decision must be made regarding the appropriate level of reliability for a given design scenario. The AASHTO guide recognizes that different classifications of roads require different levels of reliability and states:

"Generally, as the volume of traffic, difficulty of diverting traffic, and public expectation of availability increases, the risk of not performing to expectations must be minimized. This is accomplished by selecting higher levels of reliability."

The recommended levels of reliability, shown in Table 2.1, are the result of a survey of the AASHTO Pavement Design Task force. The wide range of recommended design reliability suggests that there is currently some debate regarding this matter and that the design engineer's judgement must be employed on a case-by-case basis.

Table 2.1 Suggested Levels of Reliability for Various Functional Classifications (*2*).

Functional Classfication	Recommended Level of Reliability, %	
	Urban	Rural
Interstate and Other Freeways	85 - 99.9	80 - 99.9
Principal Arterials	80 – 99	75 - 95
Collectors	80 – 95	75 - 95
Local	50 – 80	50 - 80

Note: Results based on a survey of the AASHTO Pavement Design Task Force.

Design Input Parameters

In order to incorporate reliability into the M-E design process, the relevant input parameters needed to be statistically characterized. The following subsections discuss information found in the literature regarding the variability of: layer modulus, Poisson's ratio, layer thickness, and load characteristics.

Layer Modulus

Modulus is the stiffness of a material that may be defined, in the strictest sense, as the slope of the stress-strain curve that results when either load or displacement are applied to the material in its elastic range. The materials of concern for flexible pavement design are asphalt concrete, granular base and subgrade materials.

Asphalt Concrete

Although much research has been devoted to the determination of asphalt concrete resilient modulus, less has been focused upon measuring the variability of this parameter. There are two general methods of obtaining modulus for an asphalt concrete mixture. The first is the diametral resilient modulus test with American Society for Testing and Materials test designation ASTM D4123. The second method, backcalculation of falling weight deflectometer (FWD) measurements, tests in-situ conditions and is considered non-destructive. The falling-weight deflectometer test consists of dropping a known weight from a known height onto a pavement surface. Deflection sensors measure the vertical deflections at points under and away from the

load. A mechanistic pavement model is then used to estimate the modulus values that would be needed to obtain the measured deflection values for the FWD load.

Several studies evaluated the variation associated with measured resilient modulus (M_R) by diametral testing (ASTM D4123). Al-Sugair and Almudaiheem (*13*) tested laboratory-prepared asphalt concrete samples at different load levels, moisture conditions (wet or dry) and mix designs. They found the coefficient of variation to range between 7% and 16%, although they recommended using between 10% and 20% in practice. Brown and Foo (*14*) conducted a similar study on asphalt concrete using different mix designs and found the COV to range between 6% and 10%. A study that obtained asphalt pavement cores from 32 Strategic Highway Research Program (SHRP) Long Term Pavement Performance (LTPP) sites found the coefficient of variation to range between 1% and 45% (*15*).

Another study (*16*) also investigated the variability of asphalt concrete resilient modulus as tested by ASTM D4123. Asphalt materials from Mn/ROAD, including mix design samples, specimens obtained from behind-the-paver, and cores taken from the in-place pavement were tested at -18°C, 1°C, 25°C and 40°C. Although the COV did not vary significantly between the three types of samples, it did vary with temperature as shown in the second column of Table 2.2. The relative increase in variability at the coldest and warmest temperatures were cited as a function of sensor noise and the mixture's soft binders, respectively. An important finding of this research was that a log transformation of the data was necessary to achieve a normally distributed data set. In other words, Stroup-Gardiner and Newcomb suggested that the resilient modulus of asphalt concrete be treated as a lognormal random variable. Their final report (*17*)

contained statistical information of the un-transformed modulus data (Table 2.2, column 3). It should be pointed out that the values in the third column represented different mix designs from column two. Additionally, the range of the COV for column three (un-transformed data) was 5% to 15%.

Table 2.2 COV of Asphalt Concrete Modulus with Temperature (*16,17*).

Temperature, °C	COV (Log-Transformed)	COV (Un-transformed)
-18	3.5%	11.2%
1	2.0%	8.9%
25	2.0%	10.6%
40	6.0%	Unable to Test

Allen and Graves (*18*) examined the spatial variability of asphalt concrete modulus as back-calculated from falling weight deflectometer data. Test sections 150 m long were evaluated at 7.5 m intervals on twelve projects in Kentucky and coefficients of variation were calculated. The COV ranged between 15% and 76%, with the majority of variance around 30%. Allen and Graves cited the sources of spatial variability as pavement cracking, presence of water, and decoupling of the asphalt concrete from the granular base material. An FWD study by Noureldin (*19*) used different load levels, tested in different air temperatures, and evaluated 1000 m sections at 50 m intervals. Noureldin found the COV of asphalt concrete to range between 20% and 40%, and showed that the variation increased slightly with load level and considerably with temperature. This evidence was consistent with the trend shown by Stroup-Gardiner and Newcomb where the COV of laboratory samples increased with test temperature (Table 2.2). A summary of the research findings is provided in Table 2.3.

Table 2.3 Summary of Asphalt Concrete Modulus Variability.

Reference	Test Method Type(s) of Samples	COV
13	ASTM D4123 Mix Design	10%-20%
14	ASTM D4123 Mix Design	6%-10%
15	ASTM D4123 Cores	1%-45%
16	ASTM D4123 Mix Design, Behind Paver, Cores	5%-15% Temperature Dependent
18	Backcalculation of FWD Data In-Place	15%-76%
19	Backcalculation of FWD Data In-Place	20%-40%

Granular Base and Subgrade Materials

Soils may be grouped into two general categories, either coarse or fine-grained. According to the Unified Soils Classification System (USCS), coarse-grained soils have more than 50% retained on a 0.075 mm sieve while fine-grained soils have 50% or more passing the 0.075mm sieve. The distinction is important in the context of resilient modulus because fine-grained soils tend to decrease in resilient modulus with an increase in applied stress while coarse-grained soils tend to exhibit the opposite behavior. As with the measurement of asphalt modulus, the resilient modulus of soils may be determined in the field or in the laboratory.

The laboratory test method commonly used to determine the resilient modulus of soils is the standard triaxial compression test (AASHTO T274-82 or SHRP Protocol P46). Basically, the test is performed in a triaxial cell on cylindrical granular samples 10 cm to 15 cm in diameter. Different stress levels are applied and the resulting deformation is measured. The resilient modulus, M_R, is then:

$$M_R = \frac{\sigma_d}{\varepsilon_r}$$ Equation 2.15

where σ_d is the deviator stress (axial stress minus confining pressure) and ε_r is the recoverable axial strain. After the testing has been completed, the resulting M_R data are generally used in a regression analysis to determine the material property constants for the particular material so that resilient modulus may be predicted from the applied stress. A common model predicts resilient modulus from the bulk stress, θ (sum of the applied principal stresses):

$$M_R = K_1 \theta^{K_2}$$ Equation 2.16

where K_1 and K_2 are regression constants. A study by Rada and Witczak (*20*) synthesized existing laboratory resilient modulus data, found in the literature, and performed additional tests to build up a database. Rather than reporting the actual resilient modulus values, Rada and Witczak provided statistical information pertaining to K_1 and K_2 of Equation 2.16 for six different unbound materials. Table 2.4 summarizes their findings.

Table 2.4 Summary of K_1 and K_2 Parameters for Unbound Materials (*20*).

	K1			K2		
Material Class	Mean	Stdev.	Range	Mean	Stdev.	Range
Silty Sand	1620	780	710-3,830	0.62	0.13	0.36-0.80
Sand Gravel	4480	4,300	860-12,840	0.53	0.17	0.24-0.80
Sand & Aggregate	4350	2,630	1,880-11,070	0.59	0.13	0.23-0.82
Crushed Stone	7210	7,490	1,705-56,670	0.45	0.23	-0.16-0.86
Limerock	14,030	10,240	5,700-83,860	0.40	0.11	0.0-0.54
Slag	24,250	19,910	9,300-92,360	0.37	0.13	0.0-0.52

An investigation performed at the Minnesota Road Research Project (Mn/ROAD) served as an initial characterization of the subgrade materials at the project site (*21*). The project site was divided into four major areas consisting of the 5-year, 10-year, low-volume south, and low-volume north sections. Each group constituted a different design level, for example, the 5-year sections were designed to fail in 5 years. A more detailed discussion of Mn/ROAD is provided in Chapter 3, Research Methodology. Both laboratory and field testing were performed on the Mn/ROAD soils, primarily a silty clay, and the variability was characterized. Resilient modulus was measured in the laboratory using SHRP Protocol P46, while back-calculation techniques were used on the FWD data for field determination. Undisturbed laboratory samples were obtained using thin-walled tubes and tested while disturbed "bag subgrade" soil samples were reconstituted in the laboratory prior to testing. Table 2.5 shows the measured variability for each of the laboratory soil tests and the back-calculated modulus values. The bag subgrade samples exhibited the lowest amount of variability, which is logical since the samples were compacted in the lab as opposed to the undisturbed and back-calculated data, which represent field conditions. The authors found that the back-calculated modulus was consistently higher than the measured laboratory resilient modulus.

Table 2.5 COV of Subgrade Soil Modulus at Mn/ROAD (*21*).

Section	Undisturbed	Bag Subgrade	Back-Calculated
5-Year	39%	18%	28%
10-Year	59%	20%	39%
LVR – North	43%	20%	29%
LVR – South	42%	17%	26%

Barnes, Jankovic and Colom (*22*) performed a comprehensive statewide investigation of FWD data from 1983 to 1993 in Minnesota. The end result of their work was a statistical subgrade atlas that may be used to determine the design values of

subgrade modulus. The atlas represents 120,000 back-calculated subgrade modulus values and the corresponding statistical information broken down into highway district, highway number, mile post, and year. The data demonstrate that the subgrade modulus may be considered as a log-normal random variable and is treated as such in the atlas.

Poisson's Ratio

Poisson's ratio (ν) is the ratio of transverse strain (ε_t) to axial strain (ε_a) when a material is axially loaded:

$$\nu = \frac{\varepsilon_t}{\varepsilon_a} \qquad \text{Equation 2.17}$$

Although Poisson's ratio is likely a random variable that potentially could be described by a particular distribution, it has traditionally been difficult to measure and the values have usually been assumed. Yoder and Witczak (*23*) cite that, for most pavement materials, the influence of many factors on ν is generally small. Although for asphalt concrete they do report a change in ν with temperature, where ν varies between 0.25 at cooler temperatures (4°C) to 0.5 at warmer temperatures (60°C), with a typical value of 0.35. Table 2.6 summarizes Yoder and Witczak's recommendations pertaining to Poisson's ratio. A further breakdown of unbound materials by soil type is shown in Table 2.7, which was taken directly from Das (*24*). The range of values for soft clay appear somewhat low, as reported by Das, especially when compared with the typical value given by Yoder and Witczak for a cohesive unbound granular material. It is commonly accepted that soft clay has a Poisson's ratio approaching 0.45.

Table 2.6 Poisson's Ratio of Paving Materials (*23*).

Material	Range	Typical
Asphalt Concrete	Temp. Dependent 0.25 at 4°C 0.50 at 60°C	0.35 at 25°C
Cement-Treated	0.1-0.25	0.15
Unbound Granular	0.2-0.5	0.5 (cohesive) 0.3 (non-cohesive)

Table 2.7 Poisson's Ratio of Soils (*24*).

Soil Type	Poisson's Ratio
Loose Sand	0.2-0.4
Medium Sand	0.25-0.4
Dense Sand	0.3-0.45
Silty Sand	0.2-0.4
Soft Clay	0.45*
Medium Clay	0.2-0.5

*The range reported by Das (0.15-0.25) was replaced by the value given by Yoder and Witczak.

Layer Thickness

The purpose of M-E flexible pavement design is to determine the thickness of each pavement layer to withstand the traffic and environmental conditions during the design period. Ideally, the design thickness would be a deterministic parameter, but construction inherently causes layer thickness to be variable.

Ground-penetrating radar (GPR) was used in Kansas (*25*) to determine the overall structural thickness of pavements. Eleven pavement sites, 305 m long, were tested for thickness in the inner wheelpath of the outside lane at 1.5 m intervals. The COV for this data ranged from 1.1% to 18.2%. A more descriptive breakdown of variability by layer was provided in a synthesis from Saudi Arabia (*26*). The authors combined construction records from Saudi Arabia with information from the literature (*23, 27, 7*) to arrive at the information in Table 2.8.

Table 2.8 COV of Pavement Layer Thickness (*26*).

Material Type	Position in Structure	COV
Asphalt Concrete	Surface	3%-12%
Asphalt Concrete	Base	5%-15%
Granular	Base	10%-15%
Granular	Subbase	10%-20%

Another aspect concerning pavement thickness is the design versus as-built thickness. A study conducted in Minnesota (*28*) found that the as-built mean surface thickness may be up to 2.5 cm thicker than designed, while the mean base thickness may be 5 cm greater than its design thickness. In effect, more material than was originally designed is being constructed.

The shape of the respective thickness distributions has not yet been addressed. However, a study of I-85 in South Carolina (*29*) found the surface thickness to be log-normally distributed. It remains to be proven if this statistical classification may be applied to all pavement construction.

Load Characteristics

In a broad sense, the type of traffic applied to the pavement structure defines load characteristics. The traffic, in turn, is comprised of a wide array of vehicle types which designers must somehow translate into values suitable for design. In past empirically-based thickness design methods the concept of load equivalency was used to quantify the load effects. For example, the damage done by one type of axle would be converted into an equivalent number of standard axles to cause the same amount of damage. This approach becomes inaccurate when the loading configurations or material characteristics differ from those used to establish the empirical database. However, M-E approaches may dissect the load effects into its components: wheel load magnitude, contact area

between tire and pavement, and tire spacing. As with material properties, quantifying the variability of each parameter is vital to the incorporation of reliability into the design process.

Wheel Load Magnitude

Most mechanistic-based load-displacement models require that the tire loads be applied vertically to the pavement. Additionally, an individual load magnitude for each tire in the configuration must be specified. However, traditional traffic load data have been gathered on a per-vehicle or per-axle basis. For example, many static weigh stations measure gross vehicle weight (GVW) although some weigh axles or axle groups individually. Weigh-in-motion (WIM) stations also determine GVW but more typically measure axle weights.

It has been well documented that the GVW probability distribution function of heavy vehicles is bi-modal. Figure 2.4 illustrates typical truck load distributions measured on I-74 near Danville, Illinois (*30*). Similar distributions were observed by Liu, Cornell and Imbsen when GVW data were analyzed from 18 WIM sites in Florida and 23 WIM sites in Wisconsin (*31*). It is commonly speculated that the two peaks represent loaded and unloaded heavy vehicles. A more detailed analysis, performed by Chia-Pei and Ching examined weights on an axle-by-axle basis (*32*). A total of 186,034 heavy vehicles were measured and the weights were divided into single and tandem axles. Figure 2.5 illustrates the findings, which show that the bi-modality lies in the tandem axles. This makes sense because it is the tandem axles that primarily carry the truck freight, which could be in a loaded or unloaded state.

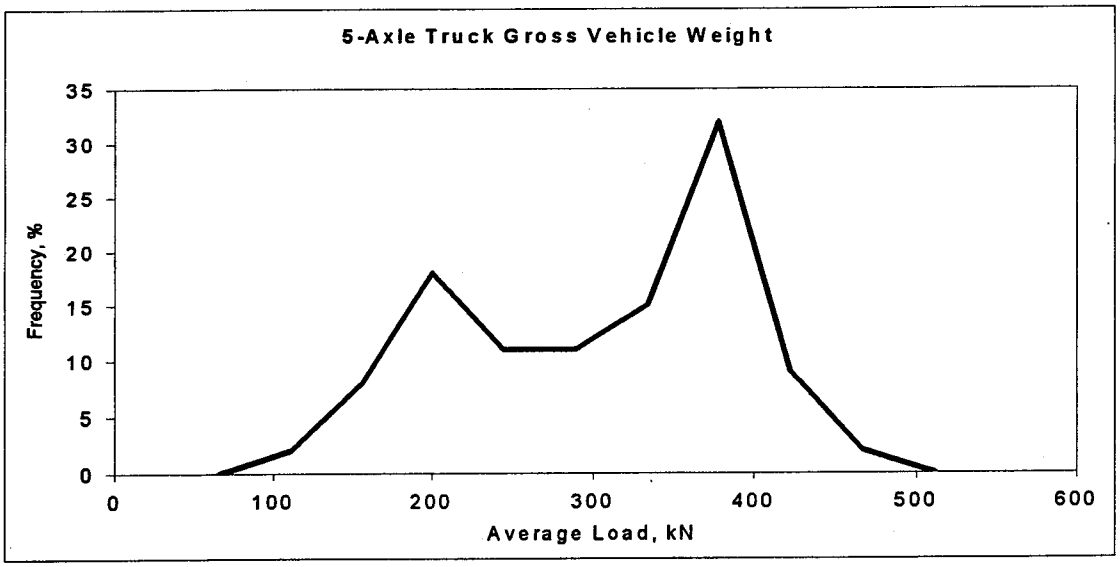

Figure 2.4 Gross Vehicle Weight Distribution (*30*).

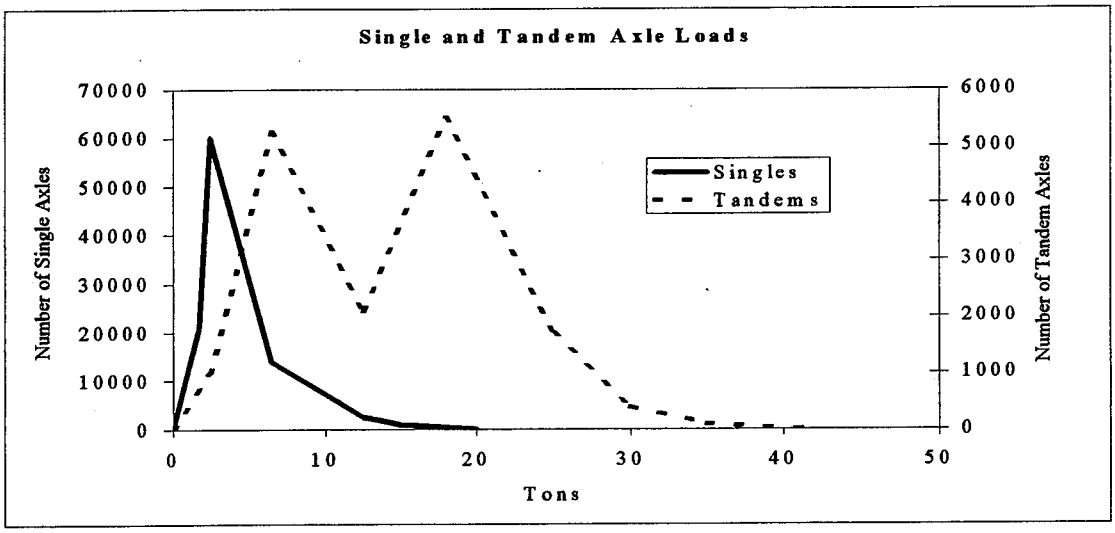

Figure 2.5 Single and Tandem Axle Load Distributions (*32*).

The next logical step, after gathering traffic weight data, is to determine a characteristic distribution function for the data. Mohammadi and Shah performed Chi-Squared goodness-of-fit tests to determine the characteristic distribution that would best model the data and they pointed out that the tests did not pass at any significant level, but were used simply as a relative measure of the accuracy of a particular distribution (*33*). For the data examined by Mohammadi and Shah, a beta distribution model worked best.

The study by Liu, Cornell and Imbsen, which focused on the second peak of the distribution (e.g., overloads), found the upper tail to be log-normal (*31*). They stated that this was similar to earlier studies but did not identify those studies.

Contact Area Between Tire and Pavement

The second load characteristic critical to mechanistic analysis is the contact area between the tire and the pavement which defines the interface conditions. This variable is important since a small contact area with corresponding higher stress will be more damaging than if the weight is spread over a larger area. There were two main types of tires cited in the literature, radial and bias ply. A bias-ply tire is constructed with crossed layers of ply-cord set diagonally to the center line of the tread while radial tires have ply cords approximately 90 degrees to the center line of the tread.

A common assumption used in pavement design is that the tire inflation pressure nearly equals the pressure applied to the pavement beneath the wheel. The assumption is based upon the membrane theory for tire-pavement interaction, which states that if an inflated membrane lacking any bending stiffness is in contact with a flat surface, the contact pressure at each point will equal the inflation pressure of the membrane (*34*).

Various state departments of transportation have conducted surveys to characterize loading mechanisms and their magnitudes, which included a measure of tire inflation pressure (Table 2.9). Studies conducted in Wisconsin (*35*), Texas (*36*), Montana (*37*) and Illinois (*38*) generally found that tire inflation pressures varied according to tire type, size, and manufacturer.

Wisconsin tested 6,780 truck tires and found the manufacturer recommended cold inflation pressures to range between 620 kPa and 760 kPa (*35*). Approximately 12% of the tested population were inflated more than 70 kPa above the upper limit. Texas tested a total of 1,486 tires of which radial tires were more common than bias tires and also inflated to a higher pressure (*36*). The maximum pressure encountered in the Texas study was 1,035 kPa. The Montana Department of Highways encountered 81% steel belted radials inflated to an average 725 kPa (*37*). Bias ply tires constituted 17% of the tested tires, with an average inflation of 580 kPa. Approximately 11% of the tires had inflation pressures exceeding 760 kPa. Unpublished data from the Illinois Department of Transportation showed an average inflation pressure of 670 kPa (*38*). The values ranged from 360 kPa to 900 kPa.

While the numbers above give an indication of average values and ranges of tire pressures, they do not indicate the shape of the distribution associated with tire pressures. A tire survey was conducted in 1986 near Woodburn, Oregon on Interstate 5 (*39*). The data showed that 87% of the tires were radial with an average inflation pressure of 705 kPa. The bias tires made up 13% with an average inflation pressure equaling 565 kPa. Figure 2.6 illustrates the frequency histogram by tire type of the Oregon study, the COV for this data varied between 9% and 20%. By inspection, it appears that tire pressure may be considered a normally distributed random variable.

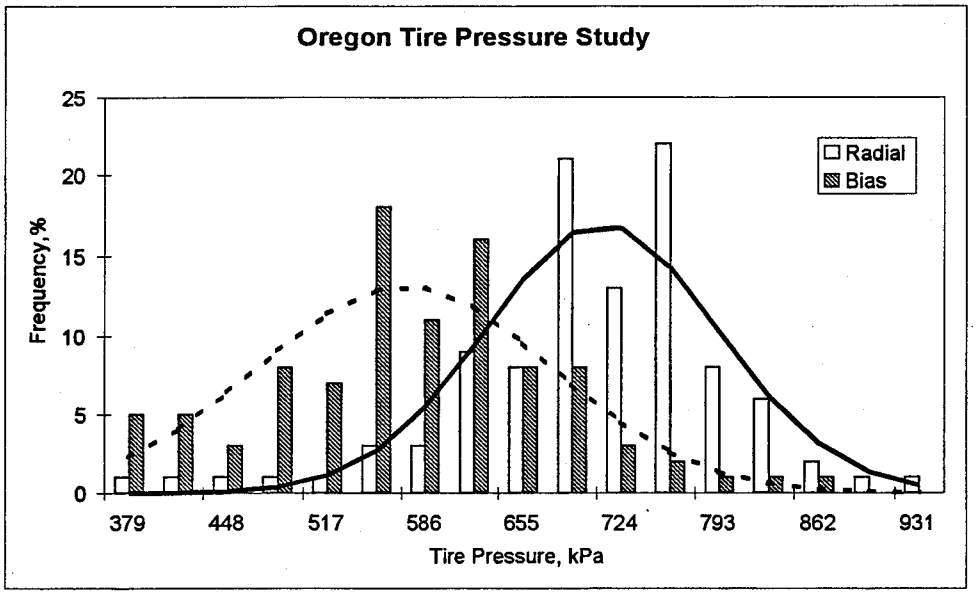

Figure 2.6 Tire Pressure Distribution by Tire Type (*39*).

One final issue deals with the dependence of tire pressure on wheel load. Another report of truck tire pressures in Texas found, through regression analysis, that the axle weight is statistically significant in explaining the variability in tire pressures (*40*). However, the authors pointed out that the regression equations require that the axle load increase by more than 6,000 N for a tire pressure increase of only 7 kPa. The authors concluded that the magnitude of this pressure-weight relationship may be considered practically non-significant. Additionally, the report showed the mean tire pressures of radial and bias-ply tires to be 670 kPa and 590 kPa, respectively. The COV for the data varied between 15% and 20%.

Table 2.9 Summary of Tire Pressure Information.

State (*Reference*)	Research Findings
Texas (*36*)	Maximum Pressure: 1,035 kPa Radial tires more frequent than bias ply tires
Montana (*37*)	81% Radials inflated to an average of 725 kPa 17% Bias ply inflated to an average of 580 kPa
Illinois (*38*)	Average pressure: 670 kPa Range of Pressure: 360 kPa - 900 kPa
Oregon (*39*)	87% Radials inflated to an average of 705 kPa 13% Bias ply inflated to an average of 565 kPa COV range: 9% - 20% Pressure normally distributed
Texas (*40*)	Radial average pressure: 670 kPa Bias ply average pressure: 590 kPa COV range: 15% - 20% Tire pressure - tire weight relationship insignificant

Tire and Axle Spacing

Tire and axle spacing refers to the distance between tires within a single configuration. This characteristic is important since the pavement may react differently to wheel configurations comprised of different spacings. Figure 2.7 illustrates typical axle groupings and the important distances. The reason for requiring closely spaced tires is to take advantage of the compressive forces at the bottom of the pavement surface layer some distance away from the center of the tire. If the tires are spaced closely enough, the compressive zone of one tire may overlap the tensile zone of another for a net reduction in tensile stress. This tends to work better on portland cement concrete than on asphalt as shown by Gillespie and Karamihas (*41*). In fact, they stated that the zone of compressive influence for 5 cm to 17 cm thick asphalt pavements is so narrow, for a minimum axle spacing of 1.3 m common for most truck tires, that there is no beneficial effect at the bottom of the asphalt layer, where fatigue cracking originates. With thicker

surfaces or when examining locations deeper in the pavement structure, there will be a net effect of overlapping stresses which should be taken into consideration.

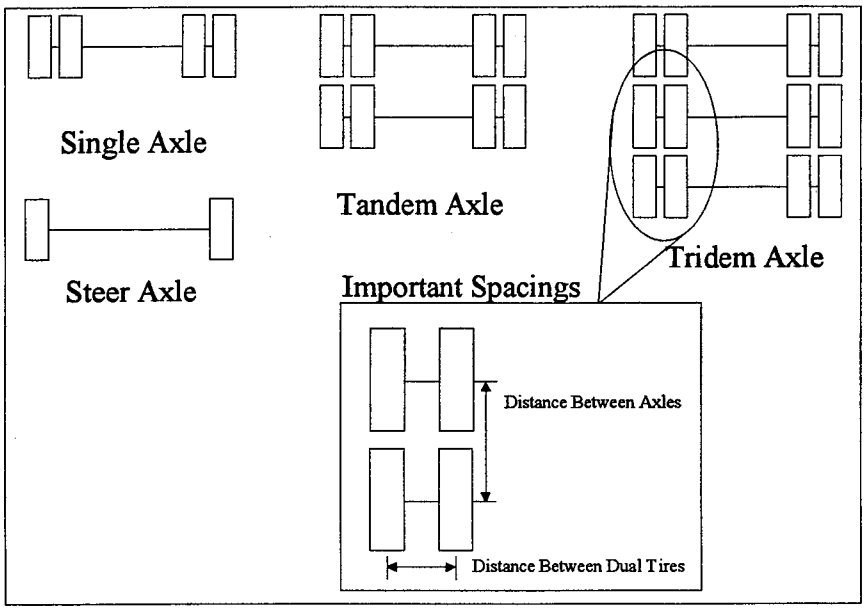

Figure 2.7 Typical Axle Groups and Important Tire Spacings.

There was little information concerning the variability of tire and axle spacing in the literature. The references cited here reported either minimum or typical spacing. Yoder and Witczak tabulated the minimum tandem axle spacing for the 50 U.S. states (*23*). The smallest allowable, 91 cm, was found in Pennsylvania while the largest minimum was 122 cm in Delaware, Maine, North Carolina and Vermont. The typical minimum value, also reported in Minnesota, was 102 cm. It would be logical to assume that these spacings also pertain to tridem axles.

The distances between dual tires were reported by Gerrard and Harrison (*42*). They classified wide dual tire spacing as 34 cm, average spacing as 30 cm and close spacing as 27 cm. Further, Gerrard and Harrison defined wide axle spacing as 140 cm, average spacing as 120 cm and 102 cm as close spacing.

CHAPTER 3

INPUT DATA CHARACTERIZATION AND RELIABILITY FORMULATION

The challenge of incorporating reliability into mechanistic-empirical (M-E) design was handled in several phases. The first phase involved gathering information regarding the design input parameters and associated variability. These values formed the basis of design inputs for the mechanistic load-displacement model. The second phase required the development of a computer program that included Monte Carlo simulation, a mechanistic load-displacement model, and reliability analysis. The third phase involved a sensitivity analysis to determine the number of required Monte Carlo cycles and to develop a better understanding of the input's effect on output reliability. Finally, example designs were performed to draw comparisons between the reliability based M-E design procedure and current empirical methods. Phases one and two are discussed in this chapter, while Chapter 4 discusses the sensitivity analysis and Chapter 5 contains the example designs.

Phase I - Input Data Characterization

The Minnesota Road Research Project (Mn/ROAD) served as a primary source of data. Mn/ROAD is a pavement test facility located on I-94 near Monticello, Minnesota. The facility is divided into two subsections comprised of a number of pavement test cells. The main line section contains 23 test cells approximately 150 m long and the low-volume subsection has 17 test cells of the same length. The mainline is subjected to westbound interstate traffic, while the low-volume section experiences repetitions of a

calibrated five-axle truck with known axle weights. There are over 4,500 sensors embedded in the pavement that record pavement responses (e.g., pavement strain) and pavement condition (e.g., state of moisture). The mainline is also equipped with a weigh-in-motion (WIM) device that measures the half-axle weight in each wheelpath of both westbound lanes. The information produced at Mn/ROAD is available through an Oracle database and can be partially accessed over the Internet. The Mn/ROAD database was utilized in this research to examine axle weight, axle type distribution, and pavement layer thicknesses. Each investigation is discussed below. Data concerning the other input variables came from the literature review, as discussed in Chapter 2.

Layer Modulus

The resilient modulus of all the materials (asphalt concrete, granular base, subgrade) was taken to be log-normally distributed. This conclusion was taken directly from data obtained through the literature review. Since the input variability for a particular design would depend upon those specific conditions, this report was intended only to quantify the range of practical variability for each of the materials. This was done by first identifying the characteristic shape of the distribution followed by establishing a practical range of coefficient of variation (COV). COV may be defined as the ratio of the standard deviation to the mean value.

Asphalt Concrete

Information regarding asphalt moduli and variability was taken directly from the literature review. Based upon the synthesis of information presented in Table 2.3, a

practical range of modulus COV is 10% to 40%. Additionally, the research by Stroup-Gardiner and Newcomb show that asphalt modulus is a lognormal random variable (*16*).

Granular Base and Subgrade Materials

A log-normal distribution was also used to characterize the modulus of the unbound materials. The Minnesota subgrade atlas served as the primary indicator of the log-normal characteristics of the subgrade materials (*22*). The study of Mn/ROAD soils, summarized in Table 2.5, indicated that a practical range of COV is 20% to 60%. These numbers are consistent with those obtained from the subgrade atlas.

Since the asphalt and subgrade materials are log-normally distributed with respect to modulus, it is logical to conclude that the base modulus is also log-normally distributed. Furthermore, base materials are "engineered" (i.e., the gradation is specified and constituent materials are selectively chosen). Therefore, it is a rational conclusion that the variability of a particular base would lie somewhere between that of the asphalt concrete layer and the subgrade layer. Based upon these deductions, a practical COV range for base materials is 15% to 50%.

Poisson's Ratio

As discovered in the literature review, the influence of many factors on Poisson's ratio is generally small. Consequently, it was decided to fix the Poisson's ratios for the three general types of materials to be consistent with that found in the literature review. The following values were selected:

- Asphalt Concrete: 0.35

- Base (Granular Soil): 0.40
- Subgrade (Cohesive Soil): 0.45

Pavement Layer Thickness

On July 7, 1994, ground penetrating radar was used to evaluate the pavement surface thickness at Mn/ROAD. Unfortunately, the Mn/ROAD database did not contain measurements of the other pavement layers. Data obtained from the database show that measurements were taken at 0.3 m to 2 m intervals along the length of each test section (approximately 100 data points per test cell). For the purposes of this project, only the flexible pavement sections were investigated and the sections were grouped according to surface thickness design. For example, cells one through three had surface design thicknesses of 14.5 cm.

Table 3.1 summarizes the investigation of the Mn/ROAD surface thicknesses. Excluding cell 26, the average measured thicknesses were 0.3 cm to 1 cm greater than the design thickness, even though there were no penalties to the contractor for insufficient thickness. Recall the study by Lukanen, which also showed the as-built thickness to be greater than the design thickness (*28*). Another aspect is the relative consistency of the standard deviation, regardless of the design thickness. This indicates uniformity of the construction practice. Approximately 95% of the thickness values are within two standard deviations of the mean; therefore 95% of the thickness values, for each design, are within 1.9 cm to 2.45 cm of the mean. The COV of cells 24, 27, 28 and 31 appeared to indicate higher variability. This, however, was the effect of the lowest mean value combined with a standard deviation comparable to the other designs.

Table 3.1 Surface Thickness Variability at Mn/ROAD.

	Surface Thickness, cm			
Cell(s)	Design	Average	Standard Deviation	COV
1-3	14.5	15.5	0.969	6.27%
4, 23	22	23.2	1.211	5.21%
14, 15	27	28.0	1.072	3.83%
16-22	20	20.0	1.071	5.36%
24, 27, 28, 31	7.5	8.2	1.160	14.12%
25, 29, 30	12.5	13.1	0.971	7.42%
26	15	15	0.992	6.61%

The data in Table 3.1, for the most part, fell within the range of 3% to 12% (see Table 2.8) estimated by Noureldin, Sharaf, Arafah and Al-Sugair (*26*). The data were also in the range found by the Kansas study (*25*). Figure 3.1 illustrates the surface thickness histogram for cells 16 through 22 overlaid with a normal distribution curve. The data appear, for the most part, normally distributed. The thinner pavement sections, as shown in Figure 3.2 also could be approximated with a normal curve.

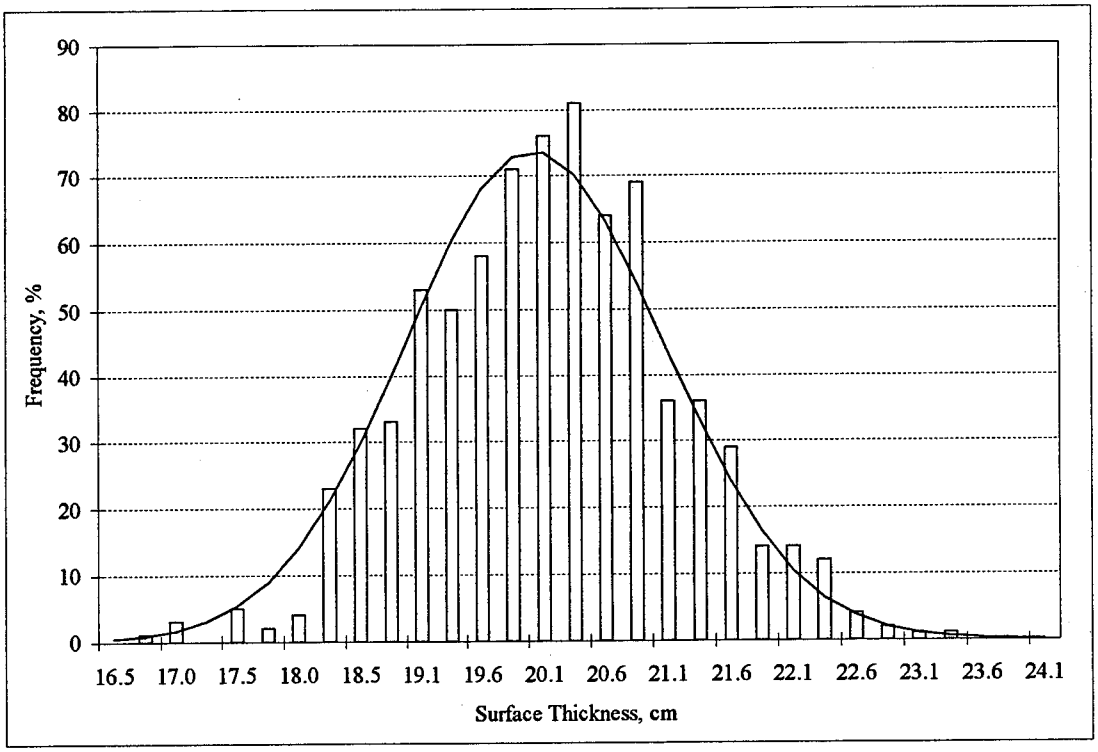

Figure 3.1 Surface Thickness Distribution of Cells 16-22 at Mn/ROAD.

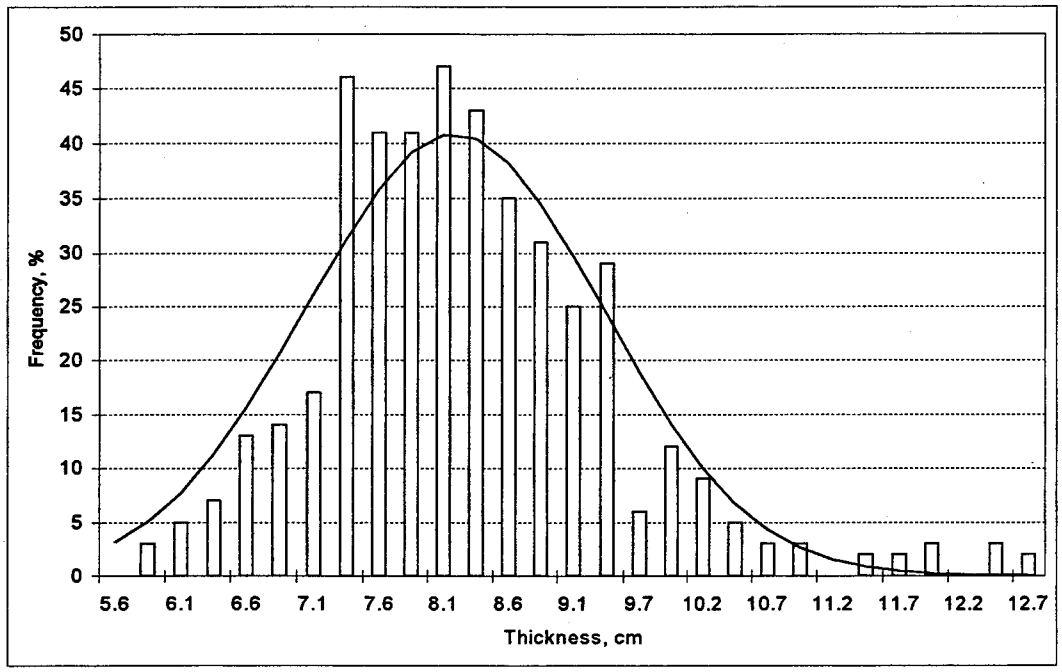

Figure 3.2 Surface Thickness Distribution of Cells 24, 27, 28, 31 at Mn/ROAD.

Since the investigation of the Mn/ROAD cells corresponded well to the information regarding surface thickness in Table 2.8, it was decided to use the other information in the table as well. The respective thicknesses were taken as normally distributed (based on the Mn/ROAD surface study) with the following ranges of COV:

- Asphalt Surface Thickness: 3% to 12%
- Granular Base Thickness: 10% to 15%
- Granular Subbase Thickness: 10% to 20%

Axle Weight and Axle Type

Axle weight and axle type measurements were obtained from a weigh-in-motion (WIM) station at Mn/ROAD. The WIM at Mn/ROAD was built by International Road Dynamics and consists of four platforms in a sealed frame, four loop detectors and a microcomputer. The WIM was set up to measure weights in each wheelpath of the two

westbound lanes. Although the WIM can be used to determine vehicle classifications, vehicle speed and length, the measurements of primary interest for M-E design are axle weights, axle spacing and axle classifications.

WIM data from the Mn/ROAD database were downloaded and organized on a 24-hour basis. A total of 70 days in 1995 were selected for the study. Data from two of the days were unusable which brought the total down to 68. Table 3.2 lists each date investigated according to the month and day of the week. The days were selected on the basis of belonging in the same week of the month. The following traffic characteristics were obtained from the WIM located in the outer (truck) lane:

- Time of the axle event (seconds)
- Left half-axle weight (kN)
- Right half-axle weight (kN)
- Axle classification by axle spacing

Table 3.2 1995 Mn/ROAD WIM - Days Investigated.

Month	Mon.	Tue.	Wed.	Thur.	Fri.	Sat.	Sun.
January	23	No data	25	26	27	28	29
February	13	14	15	16	17	18	19
March	20	21	22	23	24	25	26
April	17	18	19	20	21	22	23
May	6	7	8	9	10	11	12
June	12	13	14	15	16	17	18
July	17	18	19	20	21	22	23
August	21	22	23	24	25	26	27
September	18	19	20	21	No data	23	24
October	16	17	18	19	20	21	22

After the WIM load data had been downloaded, a means of analysis was required. Since each data file contained between 4,000 and 16,000 data points,

histograms were used as an analysis tool. An average weight was calculated from the two half-axle measurements per axle event and frequency histograms of daily half-axle weights were created. As seen in the literature review, weight histograms are not easily described by characteristic distributions (e.g., normal, log-normal); therefore, a comparison of percentiles was used to evaluate the differences on a day to day basis. Specifically, the 25th, 50th, 75th, and 99th percentiles for each of the 68 days were determined from their respective histograms. In other words, the half axle weight for which 25% of the values fall at or below that weight was determined for each day and the same was done for each of the other percentiles. The standard deviation was determined for each weight percentile to determine the spread of the data.

The axle spacing and classification provided the necessary information to break down the histogram into histograms according to axle types. This was done to better define the axle weights associated with different load configurations. The three dominant axle types were:

1. Steer (Front) Axle.
2. Tandem Axle.
3. Single, Non-Steer, Axle.

Figure 3.3 illustrates a typical half-axle weight histogram obtained from the Mn/ROAD WIM. There are two distinct peaks, as seen in the literature, and an additional third peak (≈10 kN) which was not cited in the literature. The additional peak is likely a local condition that may not be present at other sites. Table 3.3 contains the statistical information regarding the percentile weight values. The data represent 68 different days in 1995 but the spread of the data is remarkably small. The 50th percentile

exhibited the greatest amount of variation, but two standard deviations (approximately 95% of the values) is only ±4.66 kN. In other words, the histogram depicted in Figure 3.3 is a reasonably accurate representation of the half-axle weight probability density function on any day in 1995.

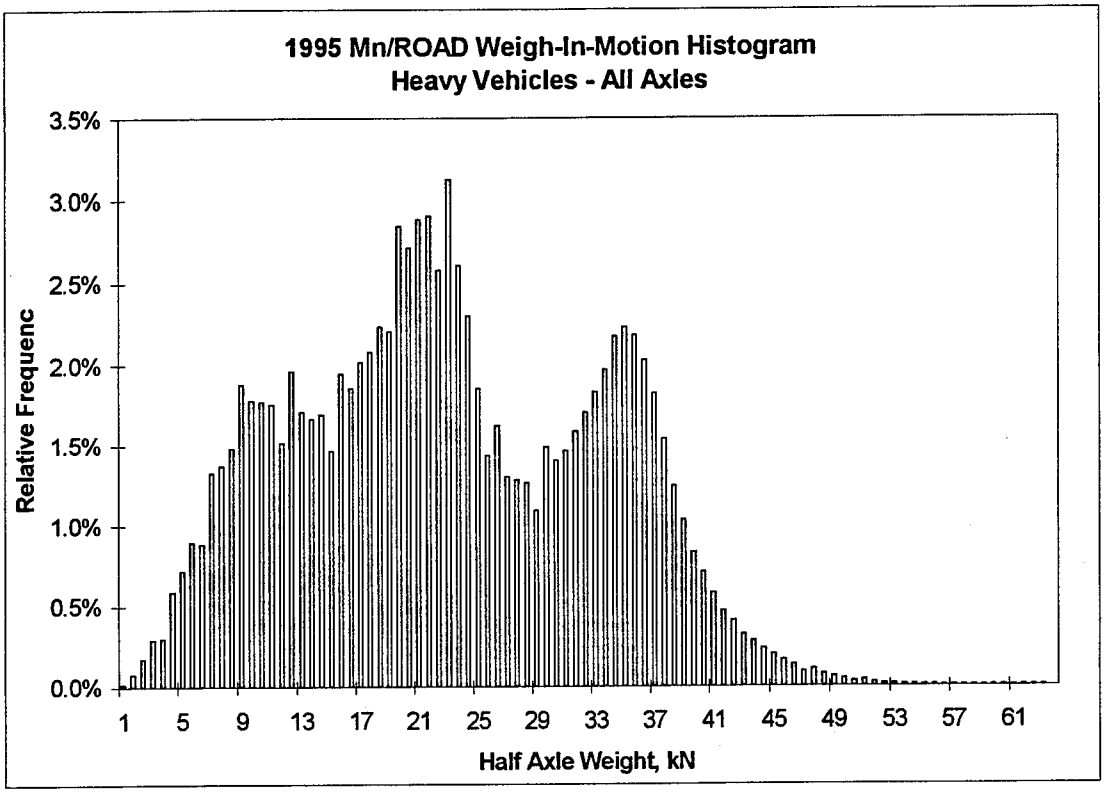

Figure 3.3 Half-Axle Weight Distribution at Mn/ROAD.

Table 3.3 Half-Axle Percentile Weight Statistics from Mn/ROAD.

Percentile	Average, kN	Standard Deviation, kN
25th	15.9	1.45
50th	22.7	2.33
75th	32.4	0.91
99th	45.6	1.16

The axle spacing data and axle classification provided by the WIM enabled a breakdown of Figure 3.3 into the respective axle configurations. Figure 3.4 shows the weight distributions of various axle types for one day in 1995. It should be noted that the

half-axle weight is for each particular axle. For example, reading 36 kN for a tandem axle means 36 kN per half-axle within the axle group. The total axle group weight would be:

$$\frac{36\ \text{kN}}{\text{Half - Axle}} * \frac{2\ \text{Half - Axle}}{\text{Whole Axle}} * \frac{2\ \text{Whole Axles}}{\text{Tandem Axle Group}} = \frac{144\ \text{kN}}{\text{Tandem Axle Group}}$$

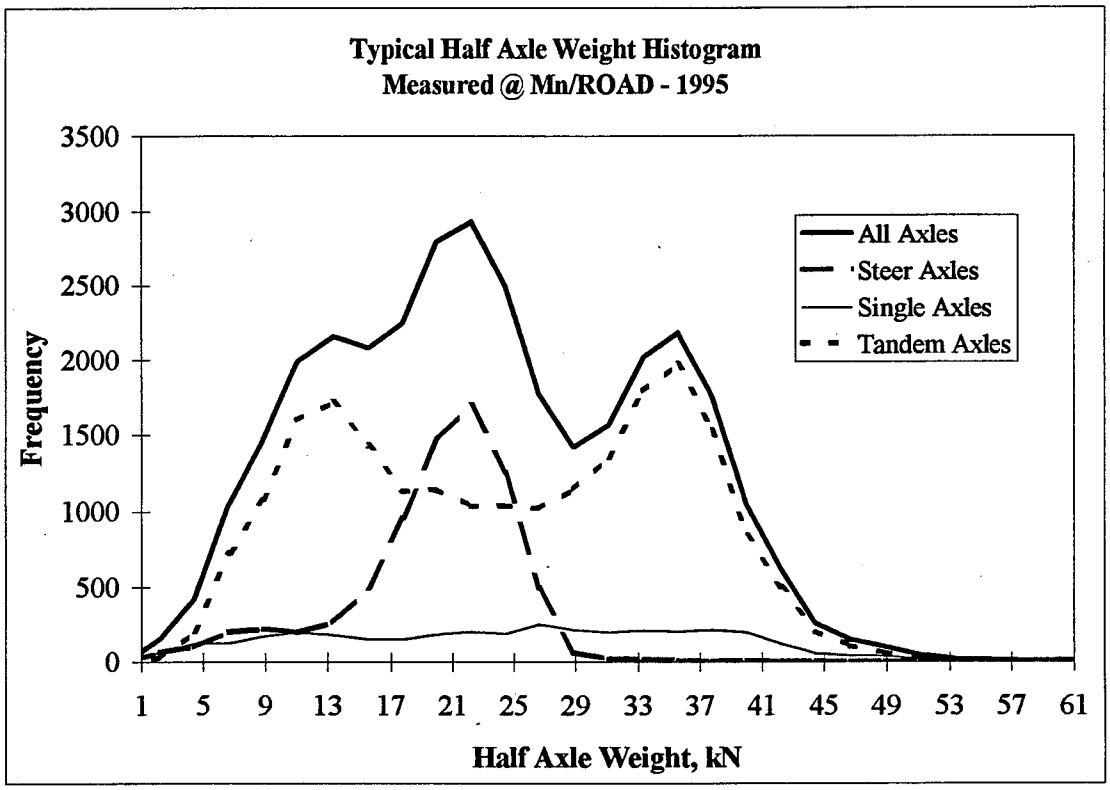

Figure 3.4 Weight Distributions by Axle Configuration.

Single axles, steer axles, and tandem axles were dominant while tridem axles were virtually non-existent. The tandem axles were responsible for the first and third peaks while the steer axles represented the second peak. The bi-modality of the tandem axles was consistent with the findings of Chia-Pei and Ching (*32*). The single, non-steer, axles were nearly uniformly distributed and were much less frequent than the other axle types.

Since the overall histogram (Figure 3.3) was consistent with time, it was reasonable to deduce that the individual axle-type histogram (Figure 3.4) was also

consistent. Therefore, only several days were analyzed to obtain axle proportions and determine the cumulative distribution function for each axle type. Three representative days, April 21 , July 17 and September 19, were drawn from the original 68 days and the cumulative distribution functions for each type of axle were determined. Figures 3.5, 3.6, and 3.7 depict the cumulative distribution functions for the single, tandem, and steer axles, respectively. The figures show that there was not a large amount of change in the function on a day-to-day basis, as was deduced. Therefore, the averages of each cumulative distribution function provided a reasonable estimate of the axle weight.

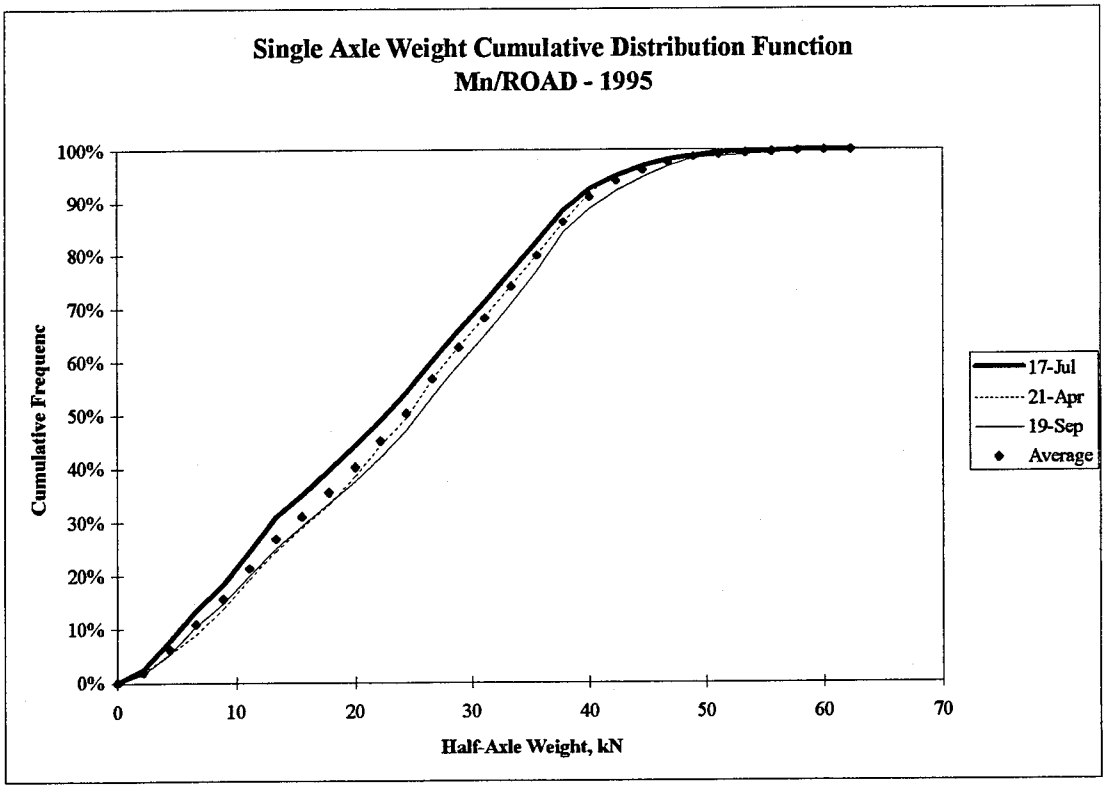

Figure 3.5. Single Axle Weight – Cumulative Distribution Function.

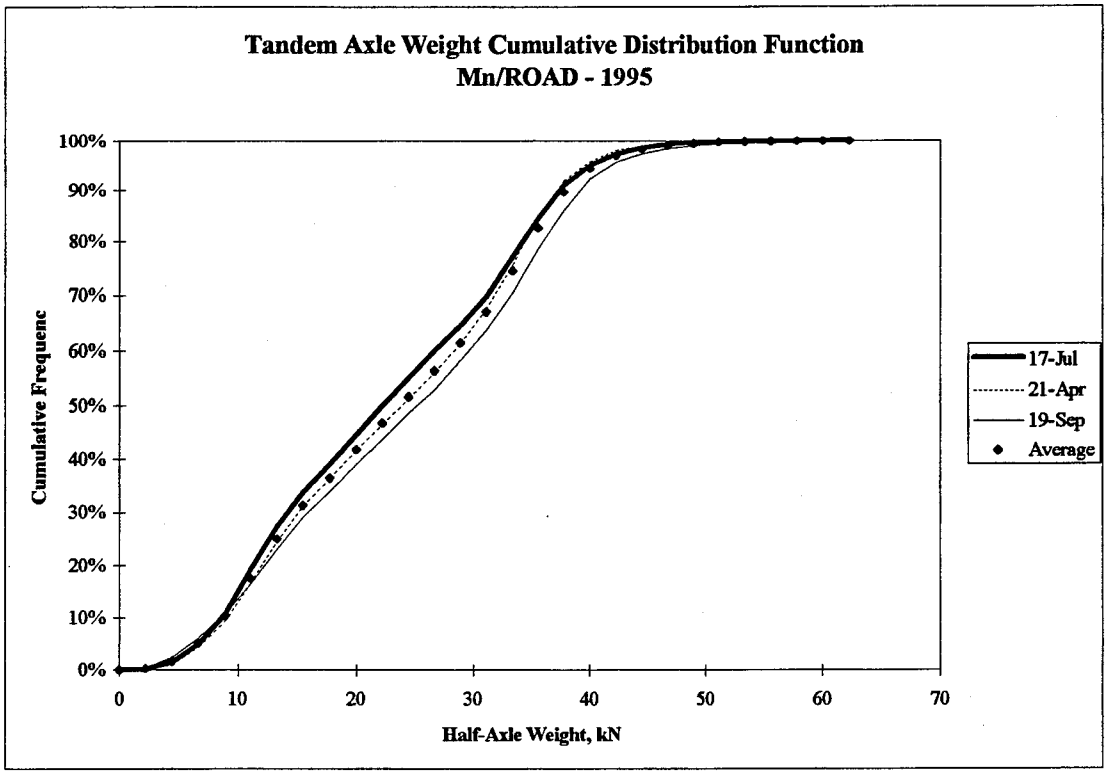

Figure 3.6 Tandem Axle Weight – Cumulative Distribution Function.

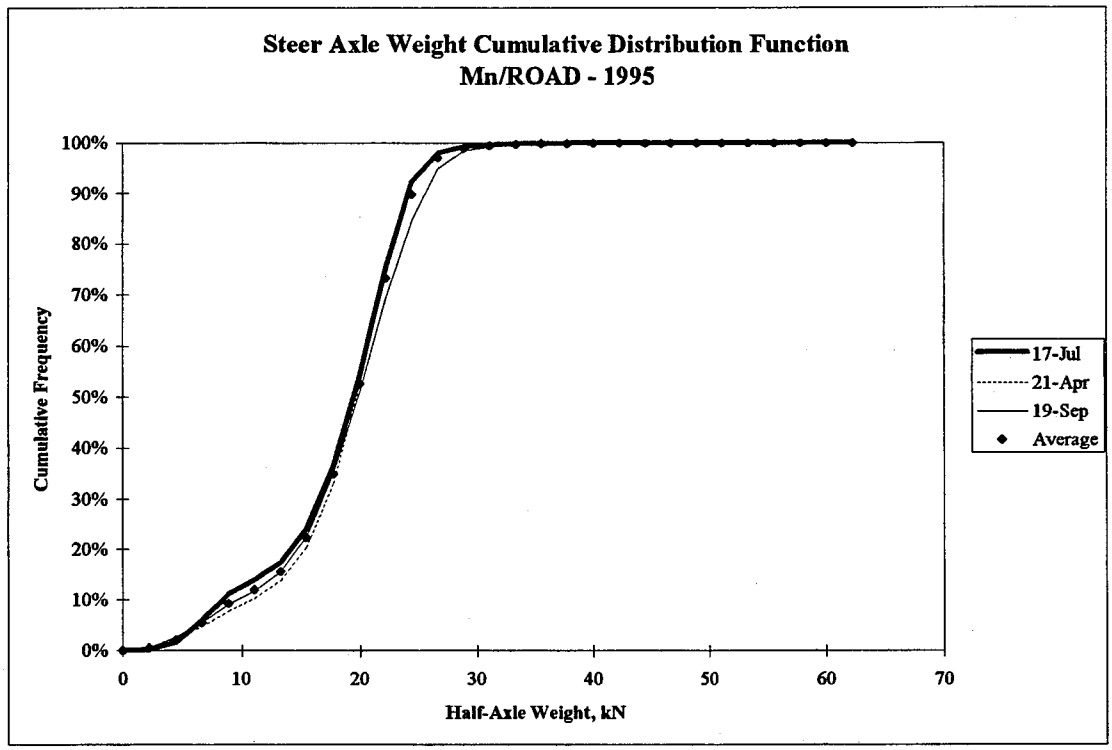

Figure 3.7 Steer Axle Weight – Cumulative Distribution Function.

The data were also used to determine the frequency of each axle type. Table 3.4 lists the relative percentages on each of the investigated days. Additionally, three weekend days were selected to determine if there was a difference between weekday and weekend traffic. As seen with all of the load data, there was consistency between the days investigated.

An important distinction should be made between the WIM data obtained from Mn/ROAD and that of other sites around the state or country. Sites on low-volume roads or roads subjected to seasonal traffic will not likely exhibit the same consistency as Mn/ROAD.

Table 3.4 Relative Frequency of Mn/ROAD Axle Groups - 1995.

Date	Day of Week	Single Axle	Steer Axle	Tandem Axle
April 21st	Friday	15.9%	34.5%	49.7%
July 17th	Monday	17.6%	34.7%	47.7%
September 19th	Tuesday	16.2%	34.3%	49.5%
January 29th	Sunday	15.8%	33.8%	50.4%
August 27th	Sunday	13.4%	23.4%	63.2%
September 23rd	Saturday	15.2%	34.5%	50.2%
Average		**15.7%**	**32.5%**	**51.8%**

It is important to keep in mind that the data presented here are only valid for the Mn/ROAD site. However, they do demonstrate how the traffic may be characterized in order to facilitate reliability analysis.

Tire Pressure and Tire Spacing

There was no means of measuring tire pressure or transverse tire spacing at Mn/ROAD. Therefore, information regarding these values came directly from the

literature. The longitudinal (axle) spacing measured at Mn/ROAD was used simply to determine the type of axle group.

There was a general consensus from the literature review that radial tires were more frequent than bias tires. The Montana (*37)* and Oregon (*39*) studies showed that radial tires comprised approximately 85% of all tires while bias ply tires constituted about 15% of the total tires. The Oregon study also depicted tire pressure as a normal random variable with COV on the order of 9% to 20%. It was decided to use the Oregon tire pressure data as input to the simulation procedure with average radial tire pressure of 700 kPa and average bias ply pressure of 550 kPa. The COV for each type of tire was taken as 15%.

Although the literature review showed ranges of tire spacing, it was decided to fix these spacings because the ranges were decidedly small. The spacings were set at the distances currently accepted in Minnesota and consistent with the data presented by Yoder and Witczak (*23*) and Gerrard and Harrison (*42*):

Distance between dual tires: 34 cm

Distance between axles: 137 cm

Although not discussed in the literature, it was assumed that all single and tandem axles had dual tires. It was further assumed that the steer axle had only single tires. These assumptions were made for the sake of the mechanistic simulations in order to specify the loading configuration.

Phase II –Monte Carlo Simulation and Reliability Formulation

A previous research project had developed the computer program, ROADENT, which utilized mechanistic pavement modeling (*1*). ROADENT was based upon information obtained from Mn/ROAD and utilized WESLEA as the mechanistic pavement model. Therefore, it was only necessary to incorporate Monte Carlo simulation into the existing software. The following subsections discuss the technical details of Monte Carlo simulation and the explicit formulation of reliability in this project.

Monte Carlo Simulation

The process used in this research for utilizing the probability distributions of the input design parameters to determine the distributions of pavement lives was Monte Carlo simulation. As described by Hart (*43*) and referenced by Galambos (*44*), Monte Carlo simulation is a straightforward method of randomly combining each of a function's input variables and producing a distribution of output. The general process follows:

1. Define "x" as a random variable with some known cumulative distribution function F_x=Probability($X \leq x$) = $P(X \leq x)$.
2. Define "u" as a standard uniform variate with cumulative distribution function, F_u. By the definition of a standard uniform variate, F_u=Probability($U \leq u$) = u.
3. A random number, u, is generated between 0 and 1.
4. By the definition in step 2, $F_u = u = F_x$.
5. Then x is found so that F_x=$P(X \leq x)$ is true for the value u.

6. The process of generating random numbers and finding the x-values is repeated for each input variable, until a set of input variables has been achieved.

7. The set of input variables is entered into the function, in this case WESLEA. The output of the function is stored and this constitutes one Monte Carlo cycle. The critical steps in the process (steps 3, 4, and 5) are illustrated in Figure 3.8. New sets of inputs are generated and run through the function until the required number of cycles has been achieved.

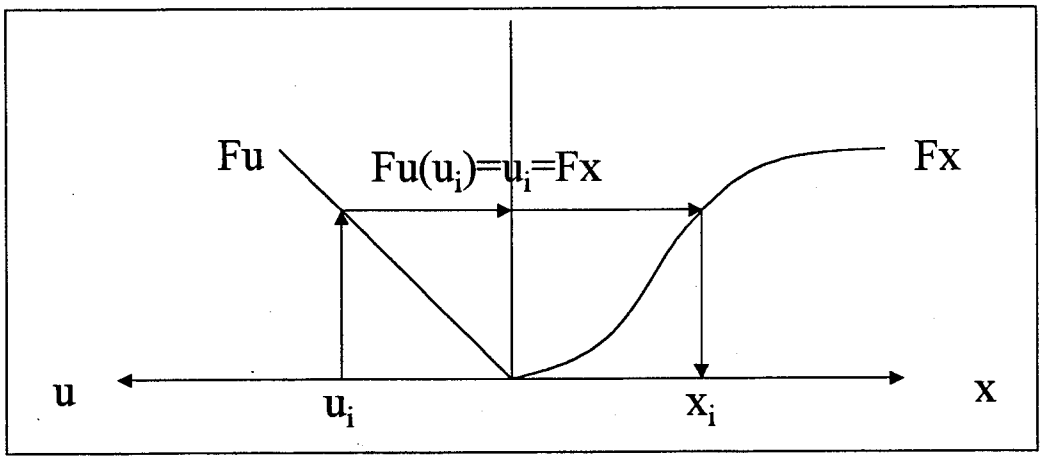

Figure 3.8 Steps 3, 4 and 5 of Monte Carlo Simulation.

When a distribution is characterized by a well-known function (e.g., normal or lognormal), as seen in the literature review regarding some of the variables, it is possible to work directly with equations to artificially generate the distribution. Box and Muller (*45*) have shown that if U_1 and U_2 are two independent standard uniform variates, then

$$S_1 = \sqrt{-2\ln U_1} * \cos 2\pi U_2 \qquad \text{Equation 3.1}$$
$$S_2 = \sqrt{-2\ln U_1} * \sin 2\pi U_2$$

are a pair of statistically independent standard normal variates. Therefore, a pair of random numbers from a normal distribution ($N(\mu,\sigma)$) may be obtained by:

$$x_1 = \mu + \sigma S_1$$
$$x_2 = \mu + \sigma S_2$$ Equation 3.2

In other words, to generate a normally distributed random variable with some mean and standard deviation, two standard uniform random numbers are generated. The numbers are then transformed by equation 3.1 to standard normal values. The final step (equation 3.2) uses the standard normal values and transforms them to the desired normal distribution. The benefit of equations 3.1 and 3.2 lies in the fact that two x values may be generated from two random numbers, which improves computing efficiency.

Lognormal random variables are generated in much the same fashion. For a log-normal variable (x) the following hold true when the mean (μ_x) and standard deviation (σ_x) are known:

$$Y = \ln X$$
$$\sigma_y = \sqrt{\text{variance of Y}} = \sqrt{\ln\left[\left(\frac{\sigma_x}{\mu_x}\right)^2 + 1\right]}$$ Equation 3.3
$$\mu_y = \text{ mean of Y} = \ln(\mu_x) - \frac{\sigma_y^{\,2}}{2}$$

Therefore, the mean and standard deviation of ln(X) are first determined from the mean and standard deviation of X. The results from Equation 3.1 then generate two standard normal values. Finally, two x values (log-normally distributed) are calculated by:

$$x_1 = e^{\mu_y + \sigma_y S_1}$$
$$x_2 = e^{\mu_y + \sigma_y S_2}$$ Equation 3.4

There are instances when the characteristic distribution is not easily described. The bimodal weight histogram, for example, is more difficult to depict and generate

random values for the distribution. However, a straightforward solution is to approximate the cumulative distribution function as a series of straight lines and use linear interpolation to determine the x-values. This is the essence of Monte Carlo simulation, where x-values are found to satisfy F_x. Although this approach requires more computation, it can also be very accurate when the cumulative distribution function is finely discretized.

A key element in either method, and critical to Monte Carlo simulation as a whole, is the generation of uniform random numbers. Entire books have been published that contain tables of random numbers. However this does not suit the microcomputer very well, therefore pseudo-random numbers must be used. The C^{++} language contains a function that will generate a pseudo-random number when given a seed value. If the seed value is the same each time the function is called, it will generate the same set of random numbers. To avoid this, the time function (also provided by C^{++}) is used to generate the seed value. Because no two points in time are ever the same, the random number function will generate a new set of pseudo-random numbers.

The above concepts were incorporated into the existing computer program, ROADENT. Briefly, the program enables the designer to set levels of input variability and evaluate their effects on the design reliability. A more detailed discussion of the program is provided in Appendix A (ROADENT User's Guide).

Reliability Formulation

In this project, the definition of reliability is consistent with that proposed by Kulkarni (*6*). Specifically, reliability is the probability that the number of allowable traffic loads exceeds the number of applied traffic loads. Mathematically speaking:

$$R = P[N > n] \qquad \text{Equation 3.5}$$

where: N = number of allowable loads until either fatigue or rutting failure

n = number of load repetitions during life of pavement

As previously discussed, the distribution of N may be determined from the mechanistic pavement model and transfer functions via Monte Carlo simulation. However, the traffic demand (n) is typically a more difficult number to quantify and relies primarily upon established traffic forecasting procedures. Therefore, for the purposes of this project, n was considered to be a deterministic design parameter. In other words, the value n was taken to be some pre-determined service life that the pavement must accommodate. Equation 3.5 then quantifies the probability that the pavement structure will exceed the demand. Figure 3.9 is a graphical representation of Equation 3.5 where N is stochastic parameter and n is a deterministic parameter. Figure 3.10 illustrates the reliability-based design procedure. Notice the similarities to Figure 1.1 which utilized Miner's hypothesis to compute pavement damage. This flowchart accomplishes the same goal of determining design thicknesses, however it has the advantage of quantifying the risk associated with the design.

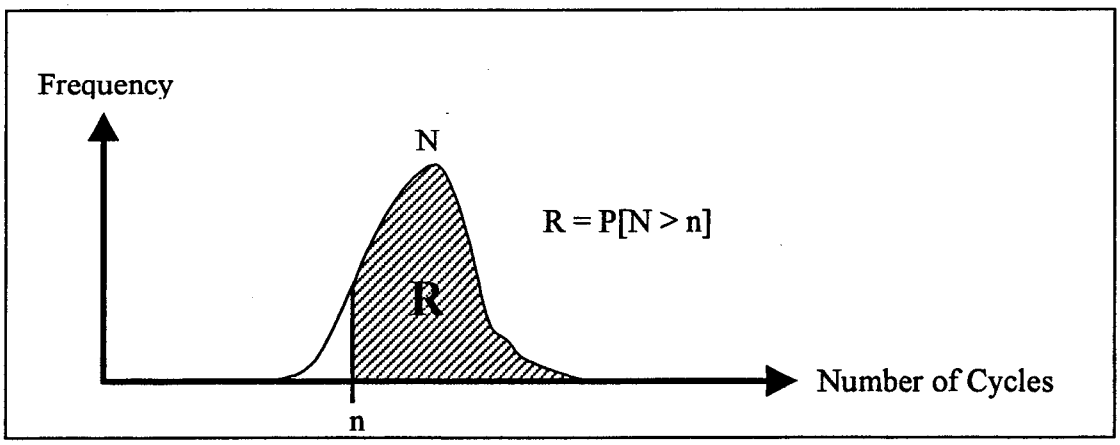

Figure 3.9 Reliability Where N is Stochastic and n is Deterministic.

The definition of reliability is relatively straightforward. If the distribution of N, pictured in Figure 3.9, were always described by the same characteristic function (e.g. normal curve) then the integration required to calculate the reliability would also be straightforward. If, however, the shape of the distribution of N were unpredictable then a numerical integration scheme would probably need to be employed.

To answer the question regarding the shape of the N distribution a parametric study and sensitivity analysis were conducted. The study also served to identify the input parameters that have the greatest influence upon the reliability calculation. The study is described in greater detail in the next chapter.

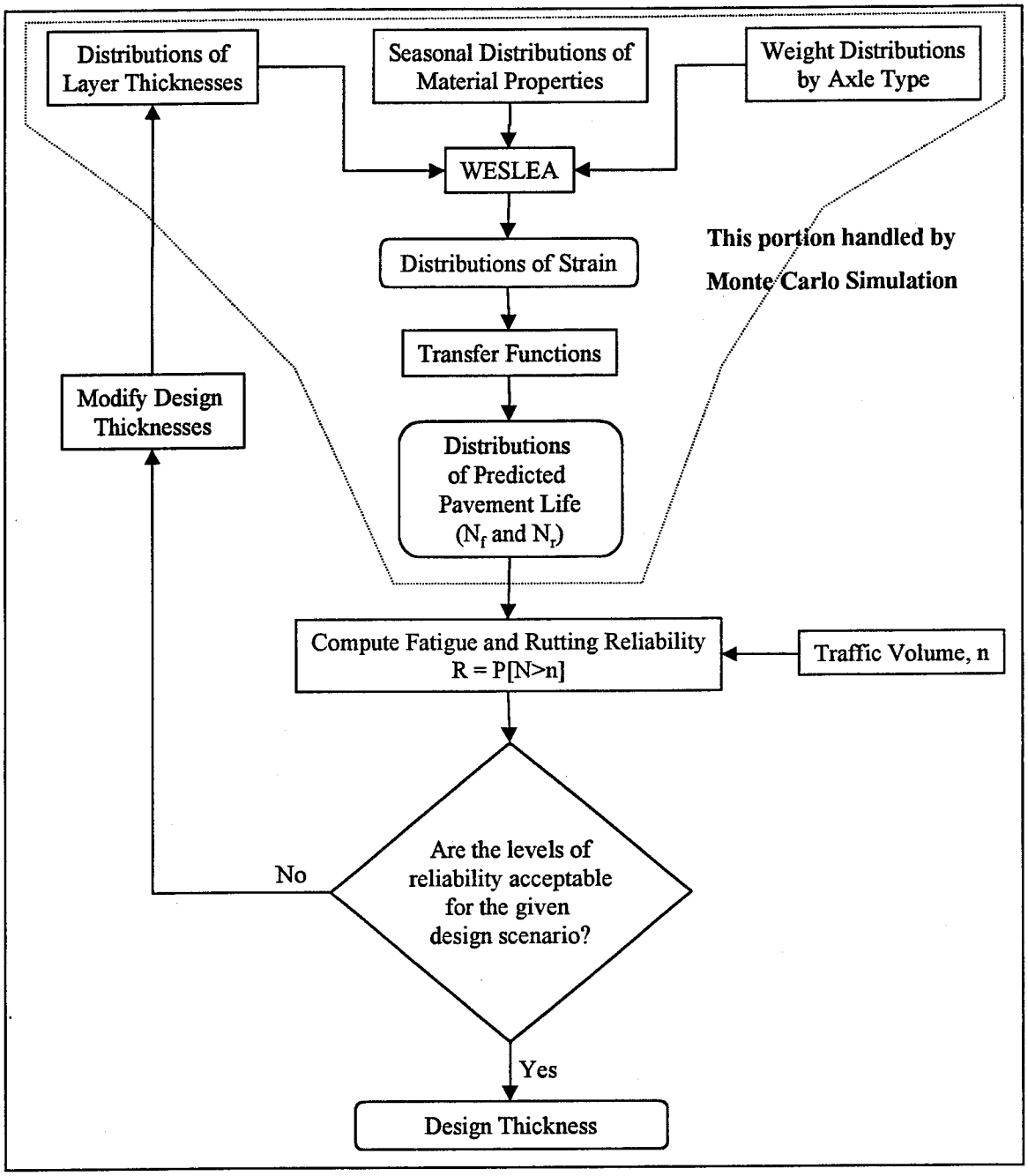

Figure 3.10 Reliability-Based Design Procedure.

CHAPTER 4

PARAMETRIC STUDY AND SENSITIVITY ANALYSIS

As described in the previous chapter, each of the parameters associated with M-E design is stochastic in nature. Consequently, it is imperative that reliability analysis is incorporated into the design procedure. While the means for doing so were presented in Chapter 3, it is important for the designer to understand the interaction between input variability and output reliability. Additionally, the output distribution must be characterized so that reliability may be quantified. Therefore, as part of the overall reliability project, a parametric study and sensitivity analysis study were undertaken and described in this chapter.

Study Objectives

The objectives of this sub-study were to:

1. Assess the effects of input parameter variability on the variability of predicted pavement performance.
2. Identify the parameters that are most critical in terms of predicting pavement performance variability.
3. Characterize the distribution of predicted pavement performance.
4. Determine a reasonable number of Monte Carlo simulations required for design.

Scope

This sub-study utilized the existing ROADENT software with the added capability of performing Monte Carlo simulations within the program. The pavement transfer functions that had previously been calibrated to Mn/ROAD performance data were used and were considered to be deterministic (*1*):

$$N_f = 2.83 * 10^{-6} \left(\frac{10^6}{\varepsilon_t} \right)^{3.206} \quad \text{(fatigue)} \qquad \text{Equation 4.1}$$

$$N_R = 5.5 * 10^{15} \left(\frac{1}{\varepsilon_v} \right)^{3.949} \quad \text{(rutting)} \qquad \text{Equation 4.2}$$

where: N_f = number of cycles until fatigue failure

ε_t = maximum horizontal tensile microstrain at the bottom of the AC layer

N_R = number of cycles until 12.7 mm of rutting develops

ε_v = maximum compressive microstrain at the top of the subgrade layer

The data presented in Chapter 3 were used to provide a practical range of variability for each of the input parameters. Recall that the data were obtained from the Mn/ROAD site and the literature.

Research Methodology

Since there are a large number of possible pavement designs or cross sections, this sub-study was necessarily limited. The investigation focused on a typical three-layer pavement system consisting of asphalt concrete over granular base on top of a subgrade soil. Figure 4.1 illustrates the pavement structure with mean or nominal thicknesses

indicated. The figure also shows the nominal value for each layer's stiffness. Seasonal changes in nominal values were not considered in this part of the analysis.

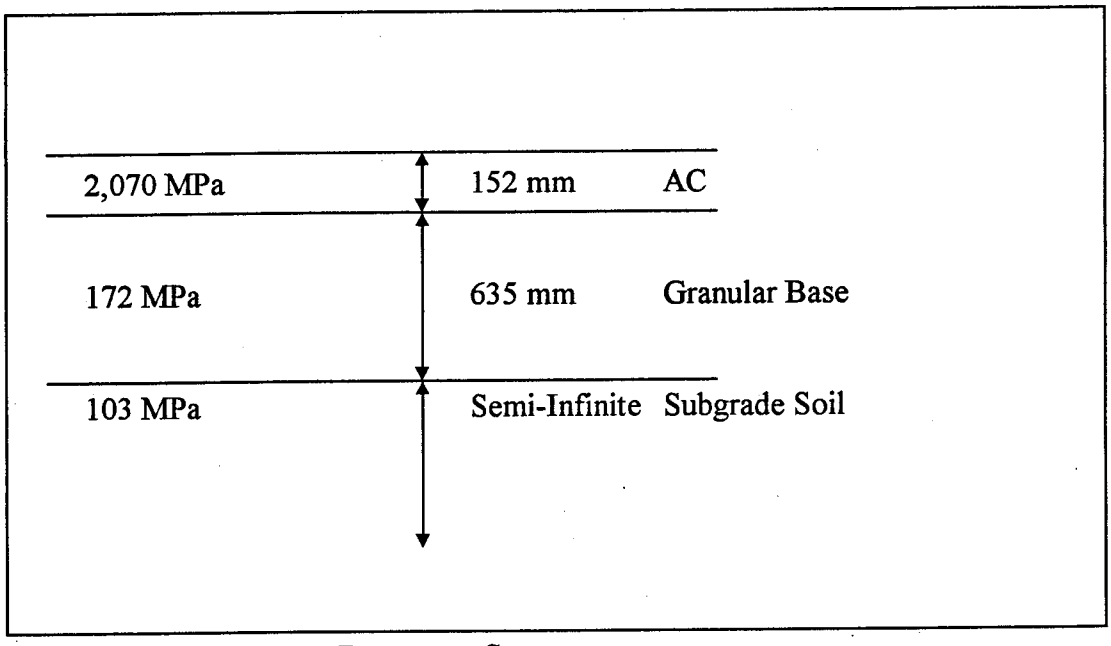

Figure 4.1 Three-Layer Pavement Structure.

The study was divided into three phases, each of which was meant to address different aspects of the objectives outlined above. Phase I focused on one parameter's variability at a time while Phase II established a baseline level of input variability. Neither Phase I nor II considered the variability of axle weight. The third phase added axle weight distributions to the baseline variability in Phase II. The details of each phase are discussed further below.

Phase I – One Parameter Variability

The first phase focused on one parameter variability. All the input values were fixed except for one, which was allowed to vary according to its characteristic distribution. The number of Monte Carlo simulations in this phase was set at 1,000.

Table 4.1 contains the ranges of COV used for each of the pavement layers in terms of modulus and thickness. Additionally, the tire pressure was set with a mean value of 690 kPa and allowed to vary according to a normal distribution with a COV of 10%.

Table 4.1 Phase I Input Variability.

Material - Parameter	Range of COV	Shape of Distribution
AC – Modulus	5%-70%	Lognormal
AC – Thickness	3%-25%	Normal
Base – Modulus	5%-60%	Lognormal
Base – Thickness	5%-35%	Normal
Subgrade - Modulus	5%-50%	Lognormal
Subgrade - Thickness	NA: Modeled as semi-infinite	

Phase II – Baseline Variability

Phase II established a baseline level of variability and then adjusted each parameter's variability as in Phase I. The baseline levels of variability are shown in Table 4.2. The tire pressure was again held at a COV of 10%. The number of Monte Carlo cycles was increased to 20,000 to accommodate the increased level of complexity involved in these simulations.

Table 4.2 Phase II Baseline Variability.

Material - Parameter	Baseline COV	Shape of Distribution
AC – Modulus	30%	Lognormal
AC – Thickness	5%	Normal
Base – Modulus	30%	Lognormal
Base – Thickness	15%	Normal
Subgrade - Modulus	30%	Lognormal
Subgrade - Thickness	NA: Modeled as semi-infinite	

Phase III – Baseline Variability and Single Axle Weight Distributions

The final phase of the investigation added the axle weight distributions found at Mn/ROAD (refer to Figures 3.5, 3.6 and 3.7) to the baseline variability of Phase II. However, each distribution was considered individually. The cumulative distribution

functions are shown in Table 4.3. The number of Monte Carlo cycles was increased to 40,000 to handle the increased complexity.

Table 4.3 Axle Weight Cumulative Distribution Functions.

Group Weight, kN	Cumulative Percentage Less Than Group Weight		
	Single Axle	Tandem Axle	Steer Axle
9	0.06	0.00	0.02
18	0.16	0.02	0.09
27	0.27	0.05	0.16
36	0.36	0.10	0.35
44	0.45	0.18	0.73
53	0.57	0.25	0.97
62	0.68	0.31	0.99
71	0.80	0.37	1.00
80	0.91	0.42	1.00
89	0.96	0.47	1.00
98	0.99	0.52	1.00
107	0.99	0.56	1.00
116	1.00	0.61	1.00
125	1.00	0.67	1.00
133	1.00	0.75	1.00
142	1.00	0.83	1.00
151	1.00	0.90	1.00
160	1.00	0.94	1.00
169	1.00	0.97	1.00
178	1.00	0.98	1.00
187	1.00	0.99	1.00
196	1.00	1.00	1.00
205	1.00	1.00	1.00
214	1.00	1.00	1.00
222	1.00	1.00	1.00
231	1.00	1.00	1.00

Results and Discussion

Phase I Results – One Parameter Variability

Figures 4.2 and 4.3 illustrate the effects of each input parameter's variability on output variability in terms of fatigue and rutting, respectively. It should be noted that the fatigue and rutting output has been log-transformed.

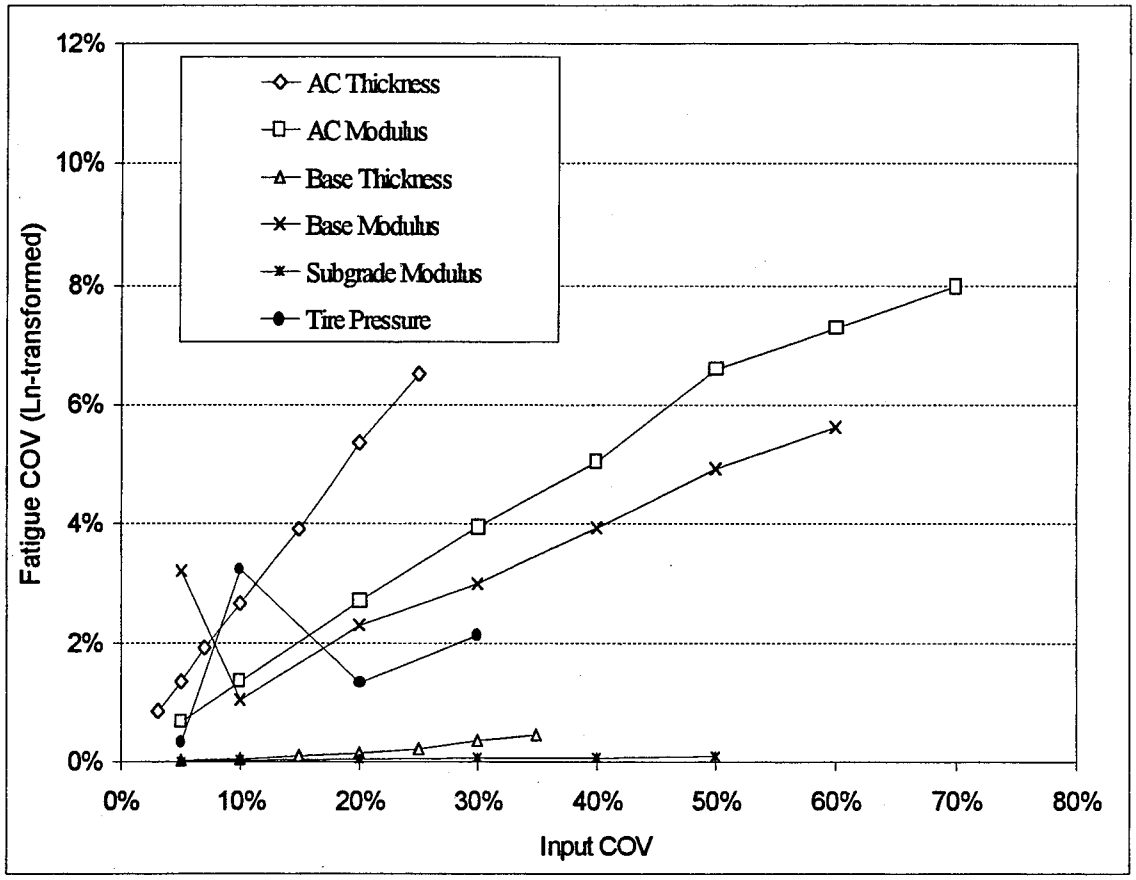

Figure 4.2 Phase I Fatigue Variability Comparison.

Figure 4.2 clearly shows that the parameters having the greatest effect on the variability of predicted fatigue life are AC thickness and AC modulus. Conversely, the base thickness and subgrade modulus seemed to have virtually no effect on the output variability. Recall that the fatigue transfer function, Equation 4.1, was based upon tensile strain at the bottom of the AC layer. Therefore, it is logical that the AC parameters would take precedence.

Some explanation regarding the tire pressure and base modulus curves is warranted since they seem to contain outliers. These data points are prime examples of what may occur with a relatively low number of Monte Carlo cycles. Using only 1,000 cycles increases the chance of producing such outliers.

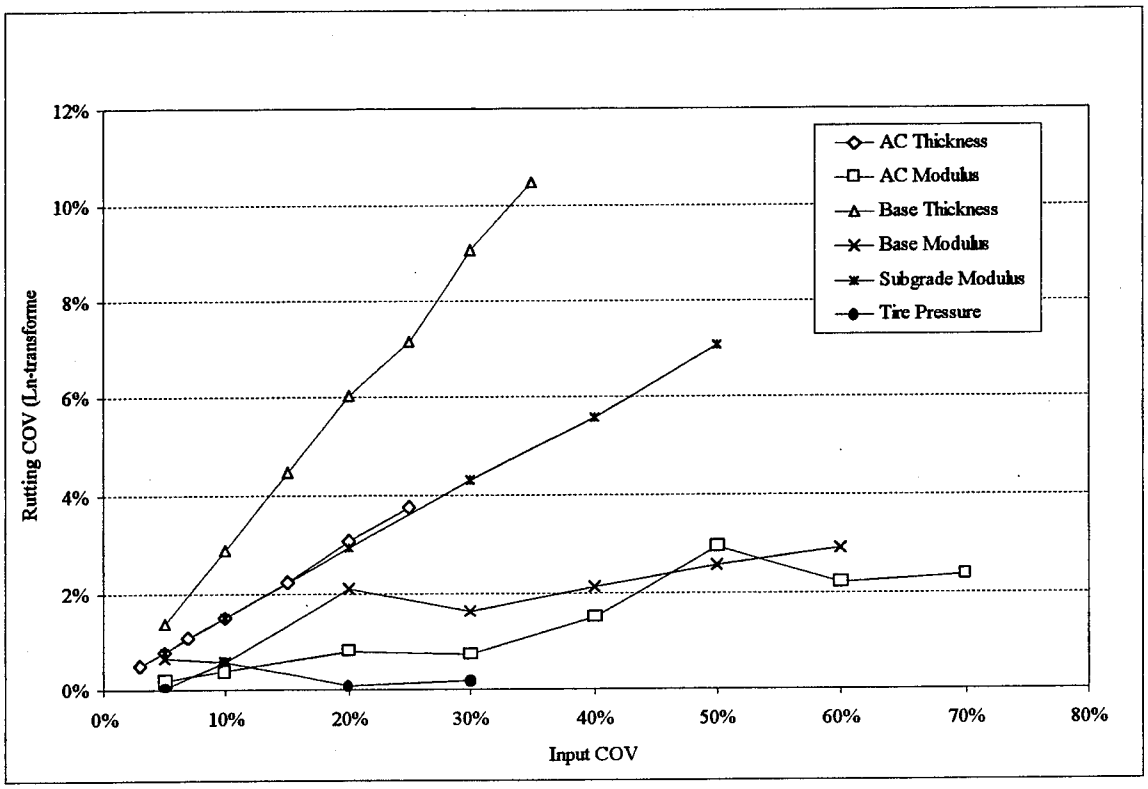

Figure 4.3 Phase I Rutting Variability Comparison.

The parameters most influential in terms of rutting variability were base thickness, AC thickness and the stiffness of the subgrade. This is logical since the rutting transfer function depends upon vertical compressive subgrade strain (Equation 4.2), which has traditionally been controlled using the thickness of the overlying layers.

Table 4.4 summarizes the findings in Figures 4.2 and 4.3. Each of the input parameters are ranked according to relative importance in affecting the output variability.

Table 4.4 Phase I Summary – Relative Importance of Input Parameters.

Rank	Fatigue	Rutting
1	AC Thickness	Base Thickness
2	AC Modulus	AC Thickness
3	Base Modulus	Subgrade Modulus
4	Tire Pressure	Base Modulus
5	Base Thickness	AC Modulus
6	Subgrade Modulus	Tire Pressure

Phase II Results – Baseline Variability

Figures 4.4 and 4.5 show the results of Phase II for fatigue and rutting variability, respectively. As in Phase I, the fatigue and rutting data were log-transformed.

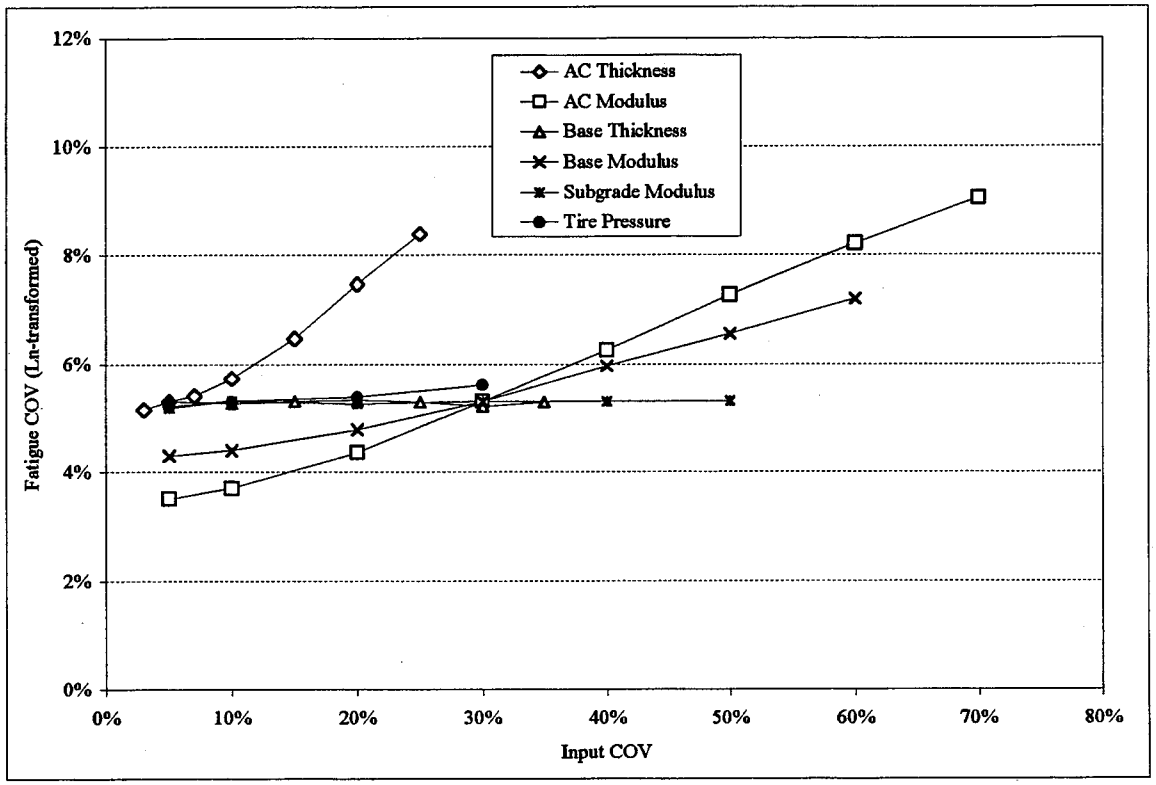

Figure 4.4 Phase II Fatigue Variability Comparison.

Figure 4.4 indicates that the input parameters of primary importance in Phase I are again the most important when the baseline variability has been added. In effect, the curves of Figure 4.2 have simply been shifted up to reflect the baseline variability. Additionally, the input parameters of lower importance in Phase I have been diminished even further, though they do contribute to the baseline level of variability. Similar observations may be made in regard to rutting variability pictured in Figure 4.5

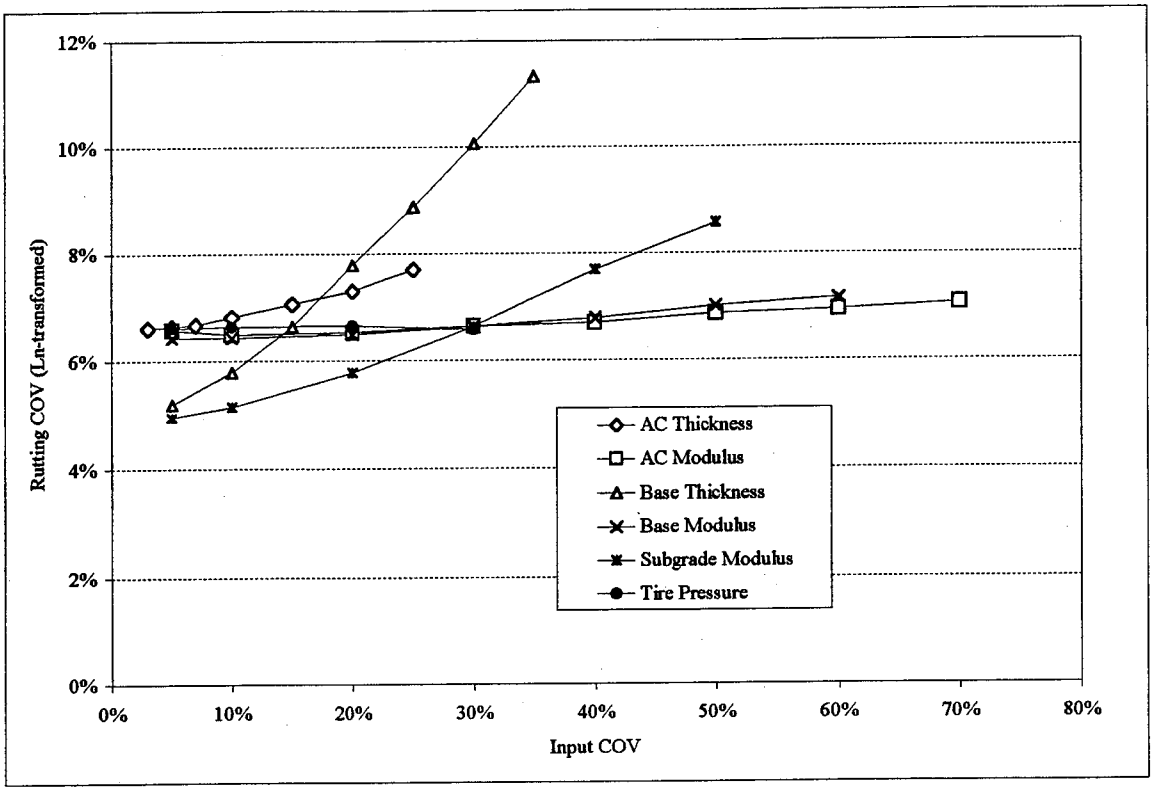

Figure 4.5 Phase II Rutting Variability Comparison.

Phase III Results – Baseline Variability and Axle Weight Distributions

Phase III considered the baseline variability in addition to the axle weight distributions. The results of the single, tandem and steer axle simulations are shown in Figures 4.6, 4.7 and 4.8, respectively. Table 4.5 lists the COVs for each of the distributions with respect to fatigue and rutting.

Table 4.5 Phase III – Fatigue and Rutting COV.

Axle Group	Fatigue COV	Rutting COV
Single	15%	17%
Tandem	12%	14%
Steer	10%	11%

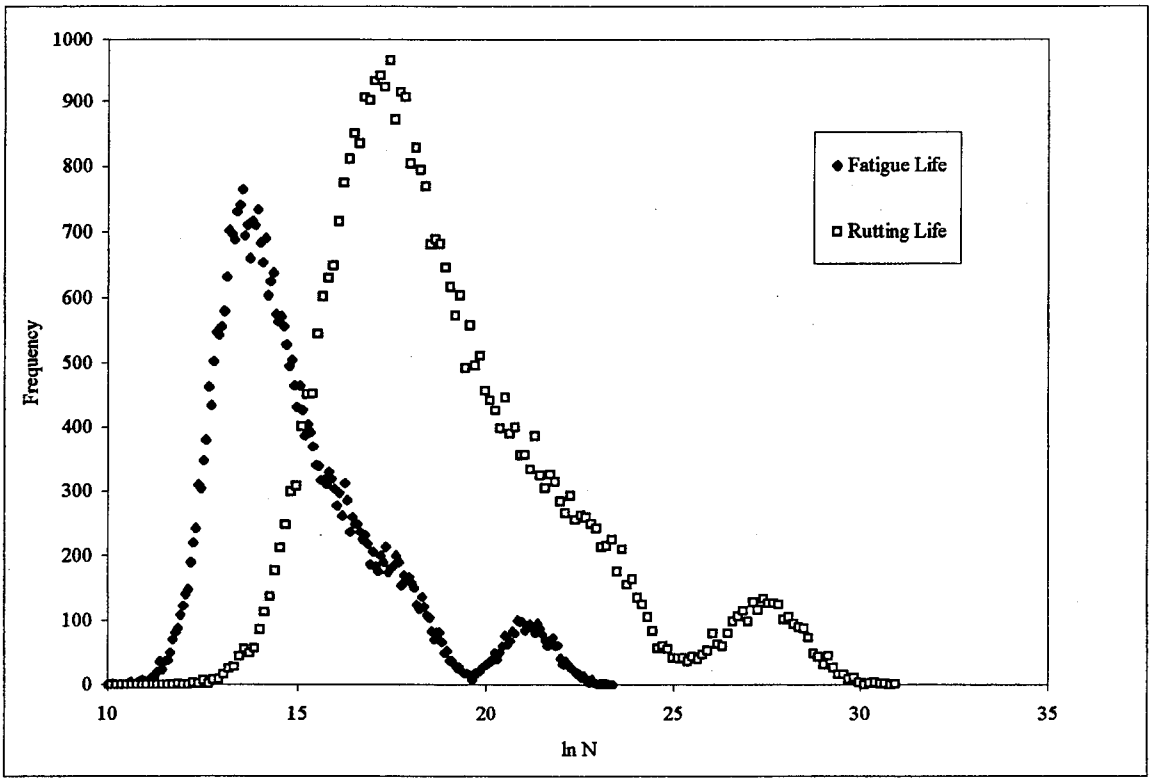

Figure 4.6 Phase III - Single Axle with Baseline Variability.

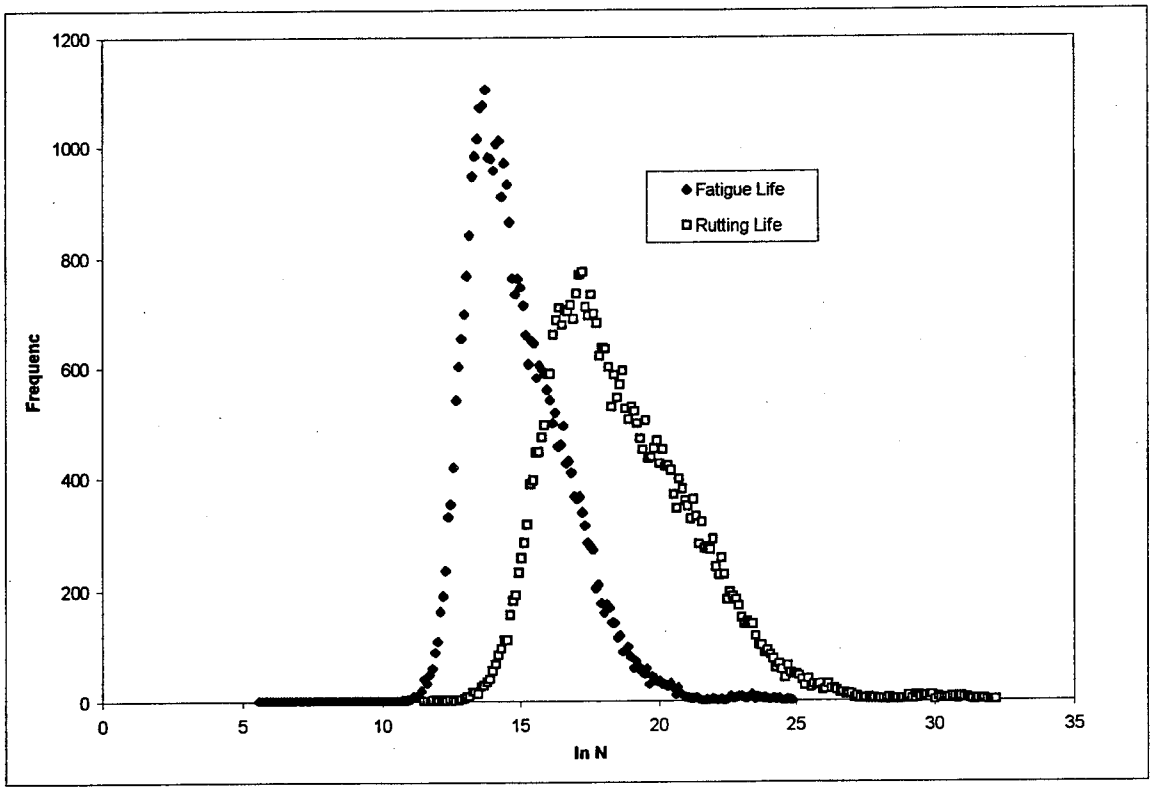

Figure 4.7 Phase III – Tandem Axle with Baseline Variability.

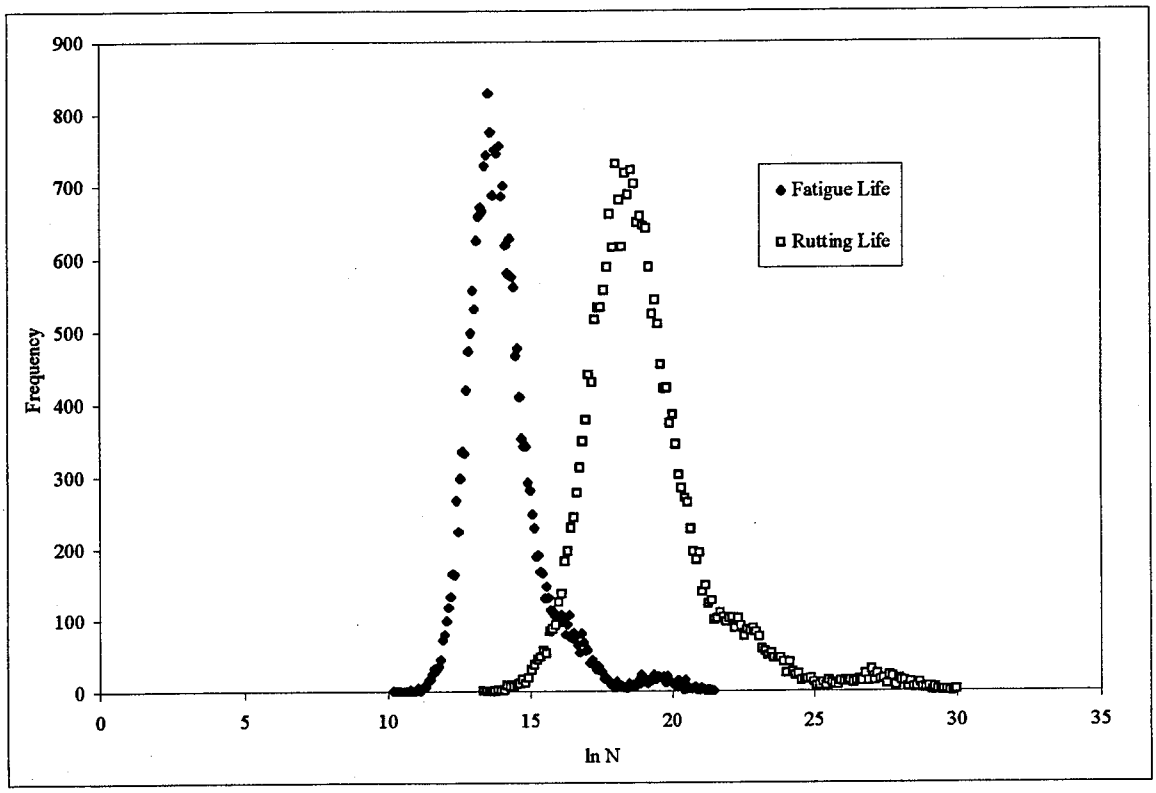

Figure 4.8 Phase III – Steer Axle with Baseline Variability.

It is important to note the magnitude of the variability listed in Table 4.5. In all cases, the addition of a realistic weight distribution more than doubles the output variability when compared to Phase II. This is critical since the increase in variability could have significant effects on the determination of design reliability. In effect, traffic weight is the single most significant input parameter.

The data represented in Figures 4.6, 4.7 and 4.8 may be approximated by an extreme-value type I distribution. Other functions tried were the normal and gamma distributions but none fit as well as the extreme-value distribution. As an example, Figures 4.9 and 4.10 illustrate the fatigue and rutting distributions, respectively, overlaid with the extreme-value type I distribution in addition to the normal and beta distributions for the tandem axle case. As described by Christensen and Baker (*46*), the extreme value type I distribution may be described by the following equations:

Probability Density Function (PDF):

$$f(y) = \alpha e^{-\alpha(y-\mu)-e^{(-\alpha(y-\mu))}} \qquad \text{Equation 4.3}$$

Cumulative Density Function (CDF):

$$F(y) = e^{-e^{(-\alpha(y-\mu))}} \qquad \text{Equation 4.4}$$

where: $\alpha = \frac{\pi}{\sqrt{6}\sigma_y}$ σ_y = standard deviation of data set

$\mu = M_y - \frac{.5772}{\alpha}$ M_y = arithmetic mean of data set

As an additional, more comprehensive, check of the extreme value type I distribution against Monte Carlo data, an additional simulation was performed. In this case, all the axle types were modeled simultaneously in addition to the baseline

variability used in Phase II. The results of the simulation are shown in Figures 4.11 and 4.12 for the fatigue and rutting life distributions, respectively. In each figure, the bars represent the Monte Carlo data while the line represents the extreme value type I distribution. The graphs show that the extreme value type I distribution may be used as an approximation of the Monte Carlo data. This is beneficial since it allows for the straightforward calculation of reliability as described in Figure 3.9.

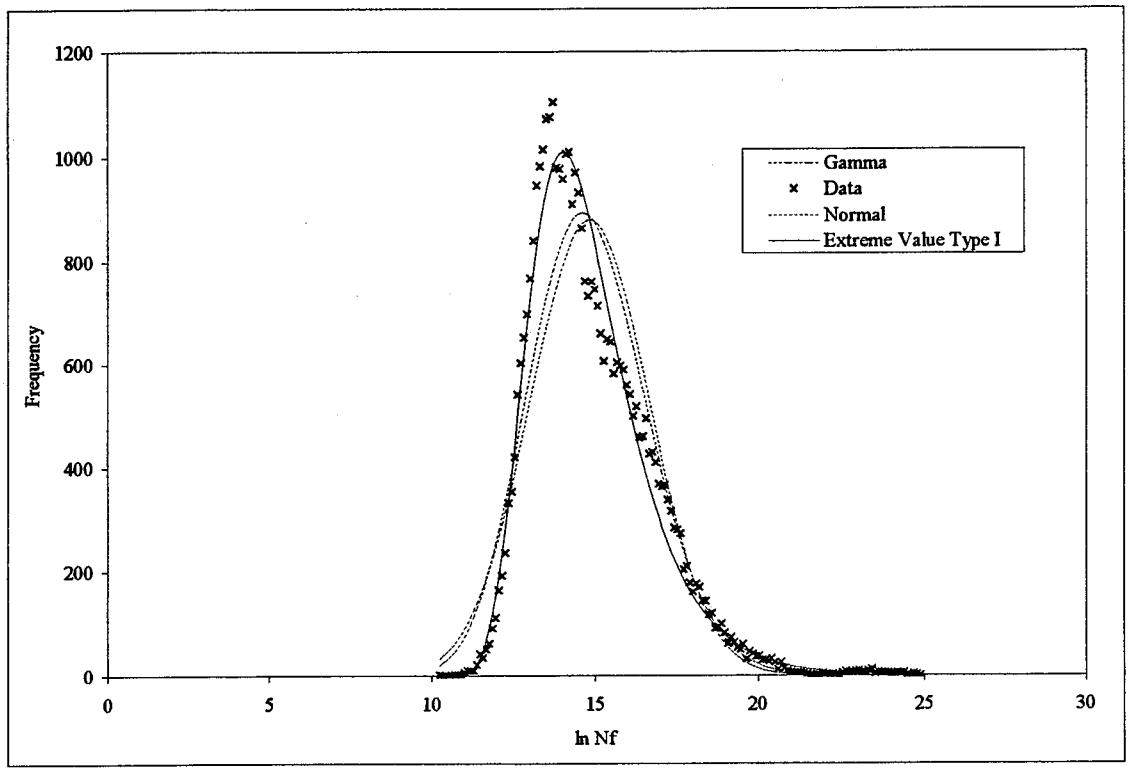

Figure 4.9 Phase III – Fatigue Curve Fitting, Tandem Axle Output.

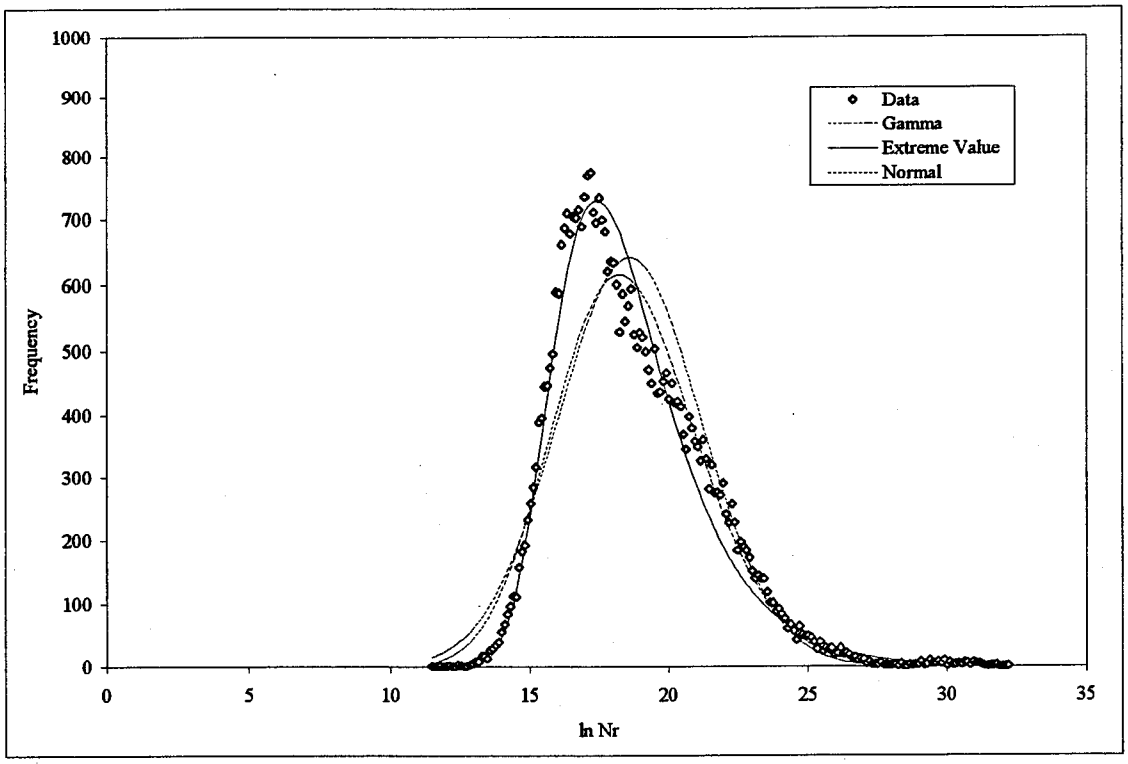

Figure 4.10 Phase III – Rutting Curve Fitting, Tandem Axle Output.

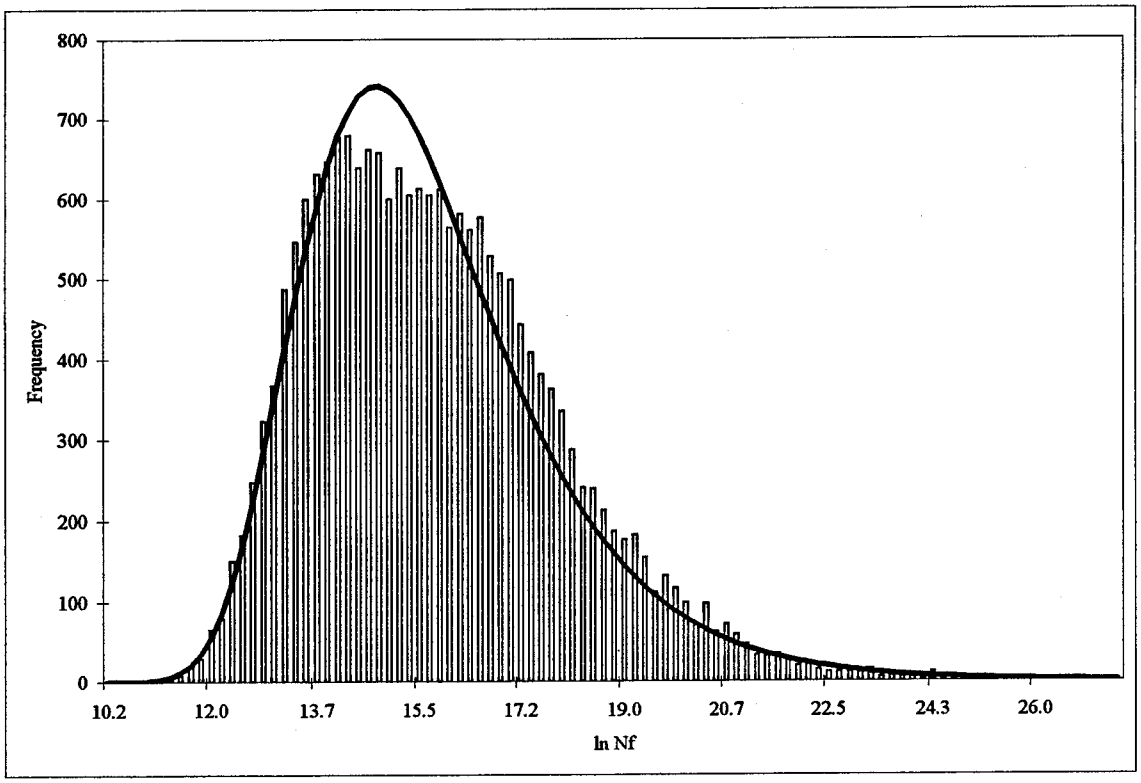

Figure 4.11 Phase III – Fatigue Curve Fitting, All Axle Output.

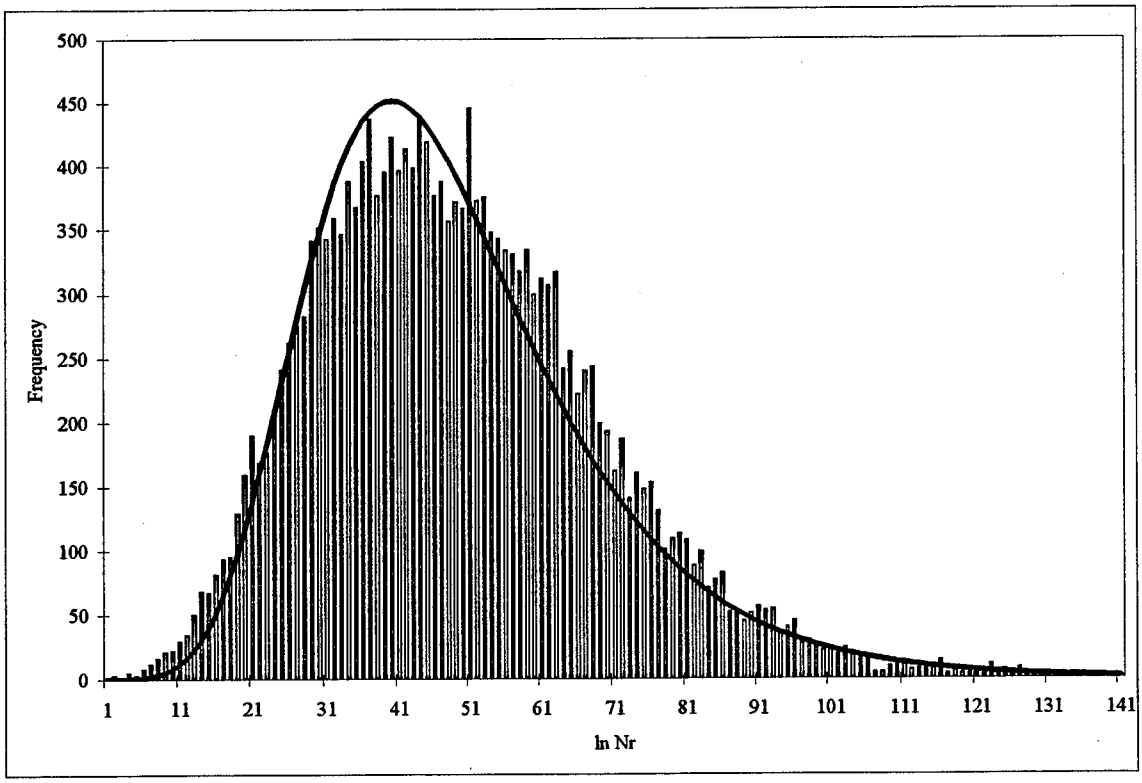

Figure 4.12 Phase III – Rutting Curve Fitting, All Axle Output.

Number of Required Monte Carlo Cycles for Design

The final objective of this sub-study was to determine a reasonable number of Monte Carlo cycles the designer should use. In the course of running the simulations for Phase III, the distribution was monitored as a function of the number of cycles. It was found that the distribution converged after approximately 1,000 Monte Carlo cycles. However, recall that the simulation did not take into account seasonal effects, which would require a greater number of cycles. Therefore, a reasonable number of Monte Carlo cycles may need to be somewhat higher for a typical, four-season, design. It was found that using 5,000 cycles yields relatively repeatable results without being overly time consuming.

Conclusions of the Sub-Study

The following conclusions, as they pertain to the sub-study objectives, may be made based upon the data presented above:

1. Fatigue variability is most affected by the inputs closer to the pavement surface. Namely, asphalt modulus, asphalt thickness and base thickness.
2. Rutting variability is most affected by the stiffness of the subgrade material and the thicknesses of the overlying materials.
3. The other parameters' variability should not be discounted since they each contribute to the so-called baseline variability.
4. Axle weight distributions have an overwhelming effect on the output variability in terms of fatigue and rutting. Therefore, these deserve careful characterization.

5. The fatigue and rutting probability density functions may be approximated with an extreme-value type I function.

6. The number of Monte Carlo cycles that should be used in design is 5,000.

It is important to keep in mind that this sub-study was somewhat limited. It was meant to serve as a guide to designers and provide insight into the reliability-based design framework. The investigation was based upon a typical pavement cross-section, but different design conditions surely exist and may yield different findings than those presented here. The investigation was also limited to the M-E design framework within the program, ROADENT, and is therefore sensitive to everything within ROADENT. For example, a different set of transfer functions would likely produce results different than those presented here.

CHAPTER 5

DESIGN COMPARISONS

A fundamental question regarding the development and use of a new pavement design method pertains to how the new method compares to methods currently in use. Since existing design methods have an historical perspective, they are invaluable in determining the "reasonableness" of a new method. This chapter presents a number of designs comparing the results between the current Minnesota methodology, the 1993 AASHTO Guide method, and ROADENT.

It is important to keep in mind the differences between the methods when comparing the results of the designs. These differences, highlighted below, make a direct comparison nearly impossible since they each have different underlying assumptions. However, the thicknesses obtained between the three methods should be comparable to each other since they are all meant to produce pavements that perform well.

Differences between Design Methodologies

Empirical vs. Mechanistic-Empirical

The AASHTO 1993 and Minnesota methods are based purely upon an empirical database. ROADENT depends on both mechanistic pavement modeling and empirical observations.

Definition of Failure

Recall that the AASHTO 1993 method and the Minnesota method are predicated upon a serviceability rating (e.g. ride quality) and a pavement is judged as failed when it reaches a terminal level of serviceability. Alternatively, ROADENT is based upon pavement performance in terms of fatigue cracking and rutting.

Structural Support

ROADENT uses the seasonal moduli of the pavement layers in addition to the layer thicknesses to represent the structural support of the pavement. The Minnesota method relies upon the granular equivalency (G.E.) concept where the structural support of a particular material may be empirically related to that of another material. The 1993 AASHTO Guide does essentially the same thing, but determines a required structural number (SN) for the pavement.

Each of these differences, and other more subtle issues, will all contribute to differences seen between the different designs. Additionally, it is important to note that the Minnesota method does not formally incorporate reliability into the design. Therefore, it was logical to perform each design according to the Minnesota method and then check the reliability of the design using ROADENT and AASHTO. Using ROADENT, the determination of reliability was simply a matter of entering the thicknesses and running the Monte Carlo simulations. Determining the reliability using the AASHTO guide required working backward through the design nomograph for flexible pavements.

Example Design Methodology

Since the Minnesota method does not involve reliability directly, it was decided to obtain design thicknesses according to the Minnesota method and then check the reliability numbers obtained from the AASHTO and ROADENT methods.

Each design, using the Minnesota method, was predicated upon a soil R-value, ESAL traffic level, and assumed average annual daily traffic (AADT). The soil R-value was then converted to resilient modulus and seasonal changes were assumed so that the AASHTO and ROADENT methods could be used. Seasonal changes in the other pavement materials were assumed according to data obtained from Mn/ROAD. In order to quantify the reliability of each design, appropriate levels of input variability were selected for the ROADENT design, while the AASHTO design simply required a standard deviation between 0.4 and 0.5, so 0.44 was chosen. The ROADENT designs were performed in a forward manner, using the design thicknesses obtained from the Minnesota method, to obtain reliability. However, it was necessary to use the AASHTO 1993 nomograph in reverse (assuming a drop in serviceability of 2.0) to obtain reliability.

Example Design Inputs

The designs were broken up into two groups, A and B, of three traffic levels each. The primary difference being that Group A assumed a stiffer soil than Group B.

Design A Inputs

Minnesota Method

Soil R-Value: 40

ESAL: 823,000 1,500,000 4,000,000

AADT: between 500 and 2500

ROADENT Method

Table 5.1 Design A, ROADENT Inputs.

Layer	Poisson's Ratio	Seasonal Layer Modulus, MPa			
		Summer	Fall	Winter	Spring
1	0.35	2003	6807	10438	6807
2	0.4	172	179	276	69
3	0.45	160	165	276	165
Seasonal Duration (weeks/year)		21	5	19	7

Table 5.2 Design A, ROADENT Input Variability.

Layer	Thickness		Modulus	
	Distribution	COV,%	Distribution	COV,%
1	Normal	5	Lognormal	30
2	Normal	8	Lognormal	30
3	Normal	0	Lognormal	40

ESAL: 823,000 1,500,000 4,000,000

AASHTO 1993 Method

Effective Soil Resilient Modulus (based upon seasonal inputs of ROADENT): 61 MPa

Drop in Serviceability (Δp_t): 2.0

Overall Standard Deviation: 0.44

ESAL: 823,000 1,500,000 4,000,000

Design B Inputs

Minnesota Method

Soil R-Value: 12

ESAL: 1,000,000 1,500,000 4,000,000

AADT: between 500 and 2500

ROADENT Method

Table 5.3 Design B ROADENT Inputs.

Layer	Poisson's Ratio	Seasonal Layer Modulus, MPa			
		Summer	Fall	Winter	Spring
1	0.35	2003	6807	10438	6807
2	0.4	172	179	276	69
3	0.45	53	103	276	103
Seasonal Duration (weeks/year)		21	5	19	7

Table 5.4 Design B ROADENT Input Variability.

Layer	Thickness		Modulus	
	Distribution	COV,%	Distribution	COV,%
1	Normal	5	Lognormal	30
2	Normal	8	Lognormal	30
3	Normal	0	Lognormal	40

ESAL: 1,000,000 1,500,000 4,000,000

AASHTO 1993 Method

Effective Soil Resilient Modulus (based upon seasonal inputs of ROADENT): 24 MPa

Drop in Serviceability (Δp_t): 2.0

Overall Standard Deviation: 0.44

ESAL: 1,000,000 1,500,000 4,000,000

Comparison of Results

Table 5.5 compares the results of the three design methods. Again, it is important to keep in mind that the corresponding reliability estimates are a crude approximation of the reliability associated with the thicknesses obtained from the Minnesota method.

Table 5.5 Comparison of Design Methods.

Design	Traffic, ESAL	Minnesota Design Thicknesses	Corresponding ROADENT Reliability	Corresponding AASHTO Reliability
A	823,000	114 mm AC 254 mm Base	62% (fatigue) 67% (rutting)	70%
	1,500,000	140 mm AC 330 mm Base	71% (fatigue) 85% (rutting)	87%
	4,000,000	178 mm AC 356 mm Base	69% (fatigue) 87% (rutting)	90%
B	1,000,000	114 mm AC 686 mm Base	63% (fatigue) 89% (rutting)	92%
	1,500,000	140 mm AC 686 mm Base	71% (fatigue) 89% (rutting)	97%
	4,000,000	178 mm AC 737 mm Base	68% (fatigue) 88% (rutting)	92%

The rutting reliability numbers from ROADENT correspond reasonably well to the numbers obtained from the AASHTO method. However, ROADENT predicts that fatigue is more likely to occur for each design. Given that very few fatigue cracks are observed on the Minnesota State highway system, these numbers do not represent real performance in Minnesota. Therefore, one may conclude that the current fatigue transfer function used by ROADENT needs further calibration in order to reflect the actual performance of roads in Minnesota. Aside from adjusting the fatigue transfer function, it appears that ROADENT would produce similar designs when compared to existing design methods.

CHAPTER 6

CONCLUSIONS AND RECOMMENDATIONS

The primary objective of this research was to develop a rational means of accounting for the variability of the mechanistic-empirical (M-E) input design parameters. This was accomplished by incorporating Monte Carlo simulation and reliability analysis into the existing M-E design program, ROADENT. The main product of this research was the new edition of ROADENT (3.0), which incorporates the research findings of this study into a user-friendly computer program that performs a comprehensive reliability analysis in addition to the more traditional Miner's hypothesis analysis.

Based upon the research findings presented in this report, the following conclusions and recommendations may be made:

1. Monte Carlo simulation is an effective means of incorporating reliability analysis into the M-E design process for flexible pavements.
2. The resulting distributions of fatigue life and rutting life, obtained from Monte Carlo simulation using the input distributions, are governed by an extreme value type I function.
3. For most practical design scenarios, the number of Monte Carlo cycles should be set at 5,000. However, the designer may use his or her judgement to adjust the number of cycles accordingly.

4. Reliability may be defined as the probability that the allowable number of loads exceeds the expected actual number of loads ($R = P[N > n]$). This definition is consistent with other definitions of reliability.

5. The reliability analysis scheme used in ROADENT produced consistent estimates of reliability when compared to the AASHTO 1993 design guide when rutting performance was considered.

6. The current fatigue transfer function produces reliability estimates inconsistent with observed performance in Minnesota and the AASHTO 1993 guide. Further refinement of the function will improve the reliability estimates.

7. For the purposes of design, data from the literature and the Mn/ROAD project showed that:

   - Layer moduli are lognormally distributed.
   - Layer thicknesses are normally distributed.
   - Tire pressures are normally distributed.
   - Axle weight distributions may be handled as discrete probability density functions in the Monte Carlo analysis scheme.

8. Generally speaking, the input parameters having the greatest influence on the fatigue performance variability are asphalt concrete modulus and thickness.

9. Likewise, the input parameters having the greatest influence on the rutting performance variability are base thickness, asphalt concrete thickness and subgrade modulus.

10. The axle weight variability has an overwhelming effect on the variability of either fatigue or rutting performance predictions. Therefore, careful load characterization is critical to the pavement design.

Until this design procedure is used on a wider basis it will be difficult to make firm recommendations regarding acceptable levels of design reliability. For now, the recommendations made by AASHTO (discussed at the end of Chapter 2) may be used as points of reference. However, the designer must ultimately make the informed decision based upon the available information regarding the design scenario.

It is important to reemphasize the need to continually refine this design procedure. One of the fundamental principles of M-E design is that it must be calibrated to local conditions. This is clearly evident in the fatigue performance predictions made by ROADENT. Further investigations and calibration are required to fine-tune the design procedure. Additionally, the calibration database should be expanded beyond the realm of Mn/ROAD to better represent conditions around the state of Minnesota. However, with the framework in place, the calibration process is relatively straightforward and changes may be implemented without great difficulty.

REFERENCES

1. Timm, D.H., Newcomb, D.E. and Birgisson, B., "Mechanistic-Empirical Flexible Pavement Thickness Design – The Minnesota Method," Draft Final Report, Minnesota Department of Transportation, January 1999.
2. --, AASHTO Guide for Design of Pavement Structures, American Association of State Highway and Transportation Officials, 1993.
3. Lemer, A.C. and Moavenzadeh, F., "Reliability of Highway Pavements," Highway Research Record No. 362, Highway Research Board, 1971, pp. 1-8.
4. Kher, R.K. and Darter, M.I., "Probabilistic Concepts and Their Applications to AASHO Interim Guide for Design of Rigid Pavements," Highway Research Record No. 466, Highway Research Board, 1973.
5. Darter, M.I. and Hudson, W.R., "Probabilistic Design Concepts Applied to Flexible Pavement System Design," Report 123-18, Center for Transportation Research, University of Texas at Austin, 1973.
6. Kulkarni, Ram B., "Rational Approach in Applying Reliability Theory to Pavement Structural Design," Transportation Research Record No. 1449, Transportation Research Board, 1994, pp. 13-17.
7. Harr, Milton E., Reliability-Based Design in Civil Engineering, McGraw-Hill, Inc., 1987.
8. Rosenblueth, E., "Point Estimates for Probability Moments," Proceedings, National Academy of Science U.S.A., Vol. 72, No. 10, 1975.

9. Van Cauwelaert, Frans, "Distributions de Rosenblueth et fonctions correlées" Symposium on Reliability-Based Design in Civil Engineering, E.P.F.L. Lausanne, Switzerland, 1988.

10. Van Cauwelaert, Frans, "Use of the ROSENBLUETH Theory for the Determination of the Frequency Distribution of a function of Random Variables," Proceedings of the C.R.O.W. Workshop, Probabilistic in het verhardingsontwerp: Transfer of Information, Ede, The Netherlands, 1994.

11. Eckmann, Bernard, "New Tools for Rational Pavement Design," Proceedings, Eighth International Conference on Asphalt Pavements, Seattle, Washington, 1997, pp. 25-42.

12. Mann, Nancy R., Schafer, Ray E. and Singpurwalla, Nozer D., Methods for Statistical Analysis of Reliability and Life Data, John Wiley and Sons, Inc., 1974.

13. Al-Sugair, Faisal H. and Almudaiheem, Jamal A., "Variations in Measured Resilient Modulus of Asphalt Mixes," Journal of Materials in Civil Engineering, Vol. 4 No. 4, November 1992, pp. 343-352.

14. Brown, E.R. and Foo, K.Y., "Evaluation of Variability in Resilient Modulus Test Results (ASTM D4123)," Journal of Testing and Evaluation, JTEVA, Vol. 19, No. 1, Jan. 1991, pp. 1-13.

15. Hadley, W.O., Irick, P. and Anderson, V., "Materials and Construction Variability Based on SHRP-LTPP Data," Proceedings, 4th International Conference on the Bearing Capacity of Roads and Airfields, Vol. 2., 1994, pp. 863 - 882.

16. Stroup-Gardiner, Mary and Newcomb, David E., "Investigation of Hot Mix Asphalt Mixtures at Mn/ROAD," Interim Report for the 5-Year Mainline Test Cells, Minnesota Department of Transportation, August, 1994.

17. Stroup-Gardiner, Mary and Newcomb, David E., "Investigation of Hot Mix Asphalt Mixtures at Mn/ROAD," Report MN/RC-97/07, Minnesota Department of Transportation, February, 1997.

18. Allen, David L. and Graves, R. Clark, "Variability in Measurement of In-Situ Material Properties," Proceedings, 4th International Conference on the Bearing Capacity of Roads and Airfields, Vol. 2., 1994, pp. 989 - 1005.

19. Noureldin, A. Samy, "Influence of Stress Levels and Seasonal Variations on In Situ Pavement Layer Properties," Transportation Research Record No. 1448, Transportation Research Board, 1994, pp. 16-24.

20. Rada, Gonzalo and Witczak, Matthew W., "Comprehensive Evaluation of Laboratory Resilient Moduli Results for Granular Material," Transportation Research Record No. 810, Transportation Research Board, 1981, pp. 23-33.

21. Newcomb, David E., Chadbourn, Bruce A., Van Deusen, David A. and Burnham, Thomas R., "Initial Characterization of Subgrade Soils and Granular Base Materials at the Minnesota Road Research Project," Report MN/RC – 96/19, Minnesota Department of Transportation, December, 1995.

22. Barnes, Randal J., Jankovic, Igor and Colom, David, "Statewide Statistical Subgrade Characterization,". Report MN/RC – 95/16, Minnesota Department of Transportation, June, 1995.

23. Yoder, E. and Witczak, M., Principles of Pavement Design, 2nd Edition, John Wiley & Sons, Inc., New York, 1975.

24. Das, Braja M., Principles of Geotechnical Engineering, Third Edition, PWS Publishing Company, Boston, 1994.

25. Attoh-Okine, Nii Otokunor and Roddis, W.M., "Pavement Thickness Variability and Its Effects on Determination of Moduli and Remaining Life," Transportation Research Record No. 1449, Transportation Research Board, 1994, pp. 39-45.

26. Noureldin, A. Samy, Sharaf, Essam, Arafah, Abdulrahim and Al-Sugair, Faisal, "Estimation of Standard Deviation of Predicted Performance of Flexible Pavements Using AASHTO Model," Transportation Research Record No. 1449, Transportation Research Board, 1994, pp. 46-56.

27. Lytton, R.L. and Zollinger, D., "Modeling Reliability in Pavement," Presented at the 72nd Annual Meeting of the Transportation Research Board, Washington, D.C., January 1993.

28. Lukanen, Erland O., "Pilot Program for Evaluation of Structural Adequacy of Flexible Pavements for Counties and Municipalities," Investigation No. 650, Minnesota Department of Transportation, 1980.

29. Kwang, Kim Woo and Burati, James L. Jr, "Probabilistic Approach to Evaluating Critical Tensile Strength of Bituminous Surface Courses," Transportation Research Record No. 1171, Transportation Research Board, 1988, pp. 131-138.

30. Shah, N, "An Investigation of Overloads on Highway Bridge," MS Thesis, Illinois Institute of Technology, Chicago, IL, 1989.

31. Liu, W. David, Cornell, C. Allin and Imbsen, R.A., "Analysis of Bridge Truck Loads," Probabilistic Methods in Civil Engineering, Edited by P.D. Spanos, ASCE, 1988, pp. 221-224.

32. Chia-Pei, J. Chou and Ching, Chung-Piau, "Truck Load Distribution and Its Impact on Vehicle Weight Regulations in Taiwan," Transportation Research Record No. 1501, Transportation Research Board, 1995, pp. 87-94.

33. Mohammadi, Jamshid and Shah, Nadir, "Statistical Evaluation of Truck Overloads", Journal of Transportation Engineering, Vol. 118 No. 5, Sept-Oct 1992, pp. 651-665.

34. Hansen, Rex William, Bertrand, Carl, Marshek, K.M. and Hudson, W.R., "Truck Tire Pavement Contact Pressure Distribution Characteristics for Super Single 18-22.5 and Smooth 11R24.5 Tires", Research Report 1190-1, Project 3-8-88/9 - 1190, Center for Transportation Research, Bureau of Engineering Research, The University of Texas at Austin, July 1989.

35. DeCabooter, Phillip H., "Wisconsin Truck Tire Pressure Study," FHWA/WI-88/1, Wisconsin Department of Transportation, Division of Highways and Transportation Services, Madison, Wisconsin, January 1988.

36. Roberts, F.L., et al., "The effect of Tire Pressures on Flexible Pavements," Research Report 372-1F, Texas Transportation Institute, Texas A&M University, College Station, Texas, August 1986.

37. Planning and Statistics Bureau, Montana Department of Highways, "1984 Truck Tire Study," Helena, Montana, 1984.

38. "Tire Pressure Survey," Unpublished Data, Bureau of Design, Division of Highways, Illinois Department of Transportation, Springfield, Illinois, 1986.

39. Kim, Ok-Kee and Bell, Chris A. "Measurement and Analysis of Truck Tire Pressure in Oregon," Transportation Research Record No. 1207, Transportation Research Board, 1988, pp. 100-110.

40. Middleton, Dan R., Roberts, Freddy L. and Chira-Chavala, T., "Measurement and Analysis of Truck Tire Pressures on Texas Highways," Transportation Research Record No. 1070, Transportation Research Board, 1988, pp.1-8.

41. Gillespie, T.D. and Karamihas, S.M., "Heavy Truck Properties Significant to Pavement Damage," Vehicle-Road Interaction, ASTM STP 1225, B.T. Kulakowski, Ed., American Society for Testing and Materials, Philadelphia, 1994, pp. 52-63.

42. Gerrard, C.M. and W. J. Harrison, "A Theoretical Comparison of the Effects of Dual-Tandem and Dual-Wheel Assemblies on Pavements," Proceedings, Fifth Conference, Australian Road Research Board, 1970.

43. Hart, Gary C., Uncertainty Analysis, Loads and Safety in Structural Engineering, Prentice-Hall, 1982, Section 3.3.

44. Galambos, Theodore V., "Monte Carlo Simulation", Course Notes, April 24, 1989.

45. Box, G.E.P. and Muller, M.E., "A Note on the Generation of Random Normal Deviates", Annals of Mathematical Statistics, 29, 1958, pp. 610-611.

46. Thoft-Christensen, P. and Baker, M. J., Structural Reliability Theory and its Applications, Springer-Verlag, 1982, p. 41.

APPENDIX A

ROADENT 3.0 USER'S GUIDE

The computer software, ROADENT 3.0, is an interactive, user friendly, flexible pavement thickness design program intended for use in Windows 95©, Windows 98© or Windows NT©. The program was created in the Microsoft Visual C++ Developer Studio 4.0 and consists of a series of dialog boxes that allow the designer to enter input data and rapidly evaluate the effects of different variables on the design.

This appendix is meant as a user's guide for the computer program and it is assumed that the designer is familiar with windows-based software. Therefore, program execution and navigation to the different program windows (via mouse clicking or using the tab key) should all ready be familiar to the user.

MAIN WINDOW

When the program is executed, the main program window will appear as shown in Figure A.1. The figure shows five primary drop-down menus: File, Input, Output, Units and Help.

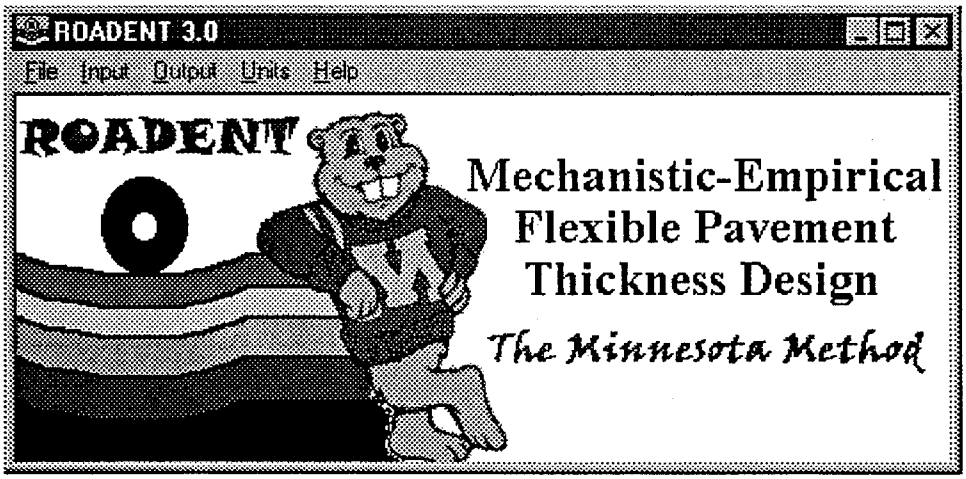

Figure A.1 ROADENT Main Program Window.

The File menu gives access to Open, Save, Save As and Exit. Each of these menu options behaves as in most other windows-based programs.

The Input menu accesses the Structure and Traffic input screens. Additionally, there is a menu item that accesses the transfer function dialog box. The structural input window will be discussed first, followed by the traffic input and transfer function boxes.

INPUT STRUCTURE

The structural input window is pictured in Figure A.2. This input dialog box defines the pavement structure to be analyzed and the seasons to be evaluated. The particular inputs are outlined below. Additionally, the user may alter the variability of the layer inputs by clicking on the variability buttons.

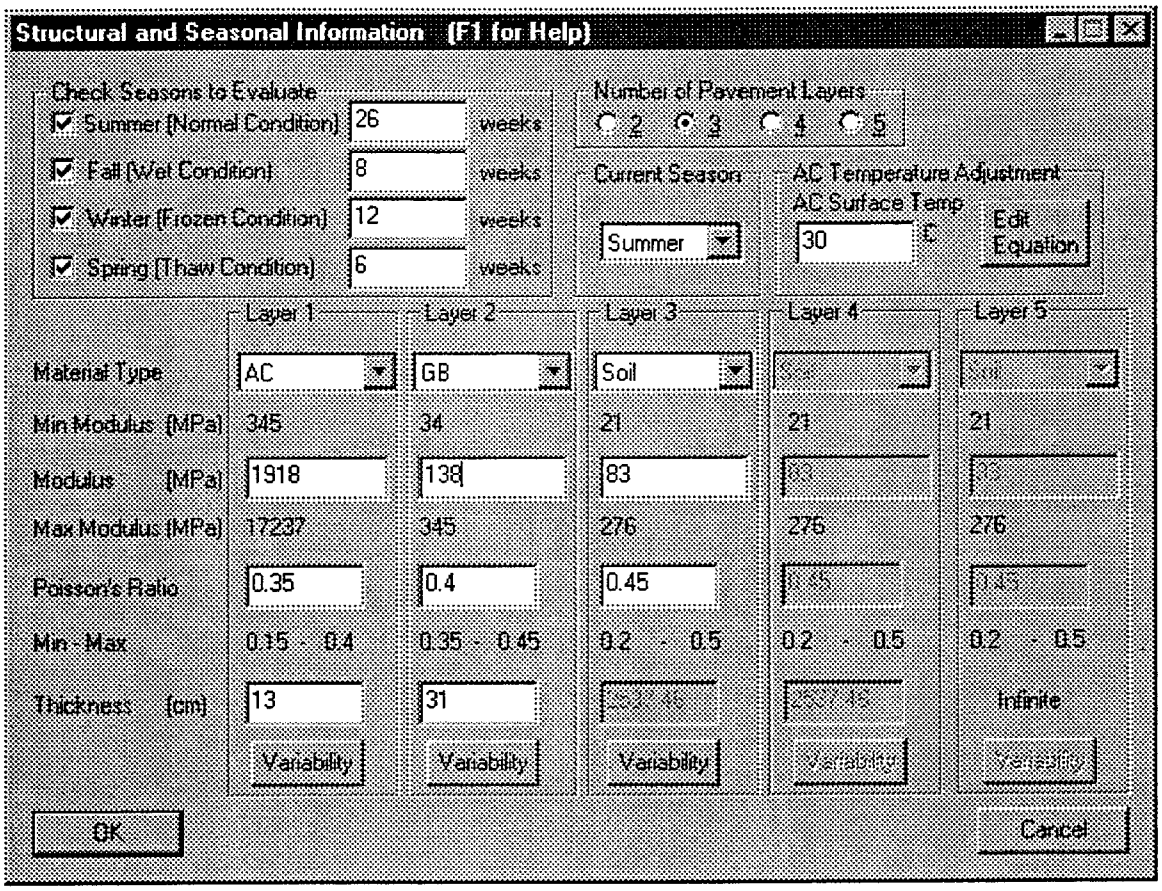

Figure A.2 Structural Input Window.

Check Seasons To Evaluate

In general, the seasons are selected to reflect the seasonal conditions that the pavement will encounter over the course of a typical year. The pavement layer moduli are then defined to represent each season. The duration of the season is used to determine the amount of traffic expected during each season. For example, using the default seasonal durations shown in Figure 4.2, 50% of the traffic would be expected in the summer season (26/52 = 0.5), while the fall condition would experience about 15%. The winter and spring conditions would experience 23% and 12%, respectively. This, of course, assumes that traffic volume is distributed evenly over the course of the year.

Number of Pavement Layers

Since WESLEA is used in the program, ROADENT is limited to the analysis of a five-layer system. However, assigning very large thicknesses to the underlying layers may approximate less than five layers. For example, in Figure A.2, a three-layer pavement has been selected. Notice that layers three and four have thicknesses in excess of 2,500 cm. The program will do this automatically when the number of layers has been changed. However, if more pavement layers are selected for analysis, it is up to the designer to enter the correct thicknesses.

Current Season

The Current Season box, shown in Figure A.2, simply serves to scroll through the seasonal data. For example, when Summer is selected as the current season, the values in

the modulus and Poisson's ratio boxes pertain to the summer condition. Selecting another season will display that season's properties.

AC Temperature Adjustment

The AC Temperature Adjustment box enables the designer to modify the asphalt concrete modulus according to a representative seasonal temperature. The adjustment equation was discussed in a previous report (*1*):

$$M_R = 16{,}693.4 \cdot e^{\left(\frac{(T+26.2)^2}{-1459.7}\right)} \qquad \text{Equation A.1}$$

where: M_R= resilient modulus of asphalt concrete, MPa

T = pavement temperature, °C

The designer also has the option to modify the coefficients shown in Equation A.1. This is accomplished by clicking on the Edit Equation button in the AC Temperature Adjustment group. The dialog box shown in Figure A.3 will then appear and the coefficients of the equation may be modified. Two important notes need to be made. First, the coefficients must be entered so that the equation calculates modulus in terms of MPa. This is the case even when the designer is working in English units. Secondly, as shown in the dialog box, changing the coefficients will automatically update all the asphalt modulus values over all the seasons, according to the temperature and the new equation.

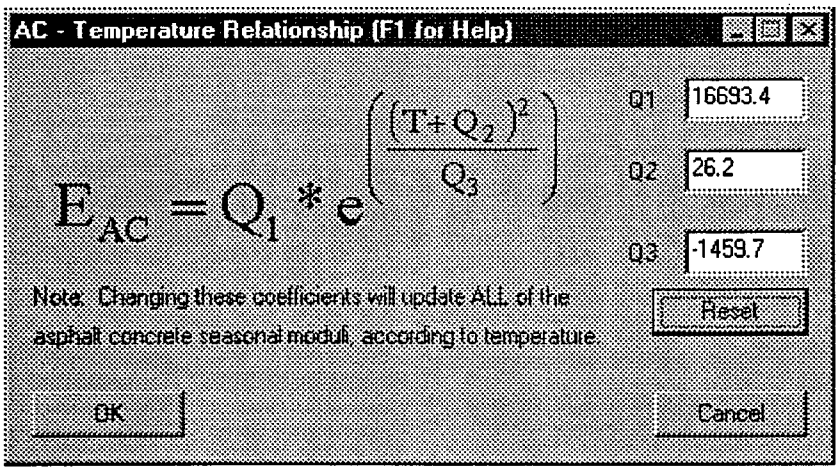

Figure A.3 Modify AC-Temperature Equation Dialog Box.

Material Type

For each pavement layer, the designer should select a material. This will automatically assign default seasonal values for modulus, and default constant values for Poisson's ratio. Additionally, the level of input variability will be set automatically. However, each material permits a range of modulus and Poisson's ratio to allow the designer maximum flexibility when designing the pavement. Table A.1 lists the available materials and ranges of values for Poisson's ratio and modulus. Of course, these values only serve as guidelines and the designer should enter the best available input for the program to be most effective.

Table A.1 Material Database.

	Modulus, MPa		Poisson's Ratio		
Material	Min	Max	Min	Max	Default
AC	345	17,240	0.15	0.40	0.35
Cracked AC	345	690	0.15	0.40	0.35
PCC	13,700	48,200	0.14	0.25	0.18
G.B.	34	344	0.30	0.45	0.40
Soil	20	276	0.20	0.50	0.45
Rock	3,400	27,000	0.10	0.25	0.15
Other	0.3	69,000	0.10	0.50	0.35

There are also default seasonal changes in moduli that go along with each of the materials. However, these are only in effect immediately after the designer has selected a new material. If the designer changes one of the values, this modulus value is now in effect, rather than the automatically adjusted value.

The asphalt concrete layers are temperature dependent as discussed above and the Cracked AC, PCC, Rock and Other remain, by default, constant over all the seasons. The granular base (G.B.) and soil layers, however, use multiples of the summer condition to adjust for seasonal changes.

The following multipliers are used in ROADENT when considering a granular base layer. The multipliers were based upon information obtained from backcalculated moduli data obtained from Mn/ROAD discussed in a previous report (*1*).

- Fall modulus is 1.3 times the Summer modulus.
- Winter modulus is 2 times the Summer modulus.
- Spring modulus is 0.5 times the Summer modulus.

Likewise, the following multipliers are used in ROADENT when considering the subgrade soil layer.

- Fall modulus is 1.25 times the Summer modulus.

- Winter modulus is 2 times the Summer modulus.
- Spring modulus is 1.25 times the Summer modulus.

The last multiplier may seem strange, but the Mn/ROAD data show that the minimum soil modulus occurs in the summer season. Again, the designer should use the best available information in lieu of the ROADENT defaults.

Layer Thickness

The designer must specify the thickness of each pavement layer, except the bottom. The minimum and maximum values that may be entered are 0.64 cm and 2537 cm, respectively.

Layer Parameter Variability

This edition of ROADENT allows the user to input the level of variability associated with each layer thickness and stiffness. By default, the layer stiffness variability is assumed to be constant throughout the design. When a material is selected, ROADENT will assign levels of variability for the thickness and modulus. These values are based upon information obtained from the literature and from Mn/ROAD. However, the designer may alter these default values. Clicking on the variability button for a particular layer brings up the variability dialog box shown in Figure A.4.

At the top of the box, the layer material is identified. The modulus variability may then be set according to distribution type (normal or lognormal) and an associated coefficient of variation (COV). Likewise, the thickness variability may be set in the same

fashion. These distributions will be used in the Monte Carlo reliability analysis. Table A.2 contains the default settings with regard to input variability.

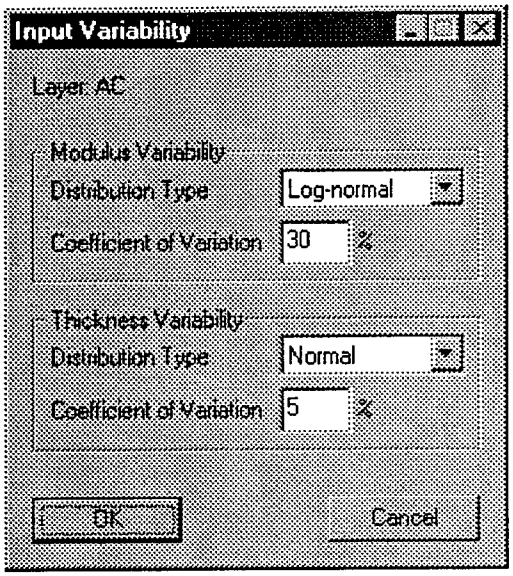

Figure A.4 Layer Input Variability.

Table A.2 Default Input Variability.

Modulus		
Material	Distribution	COV
AC	Lognormal	30%
Cracked AC	Lognormal	60%
PCC	Lognormal	15%
Granular Base	Lognormal	40%
Soil	Lognormal	50%
Rock	--	0%
Other	--	0%

Thickness		
Layer	Distribution	COV
1	Normal	5%
2	Normal	8%
3	Normal	15%
4	Normal	20%

INPUT TRAFFIC

In ROADENT, the traffic loading information may be entered either by load spectra or ESAL, concepts that were explained in a previous report (*1*). The load spectra input window will be discussed first, followed by the ESAL input window.

LOAD SPECTRA WINDOW

The load spectra input window is shown in Figure A.5 and is divided up into Loading Configurations, Choose Current Configuration and Expected Number of Axles in Given Weight Classes. Each of these will be discussed below.

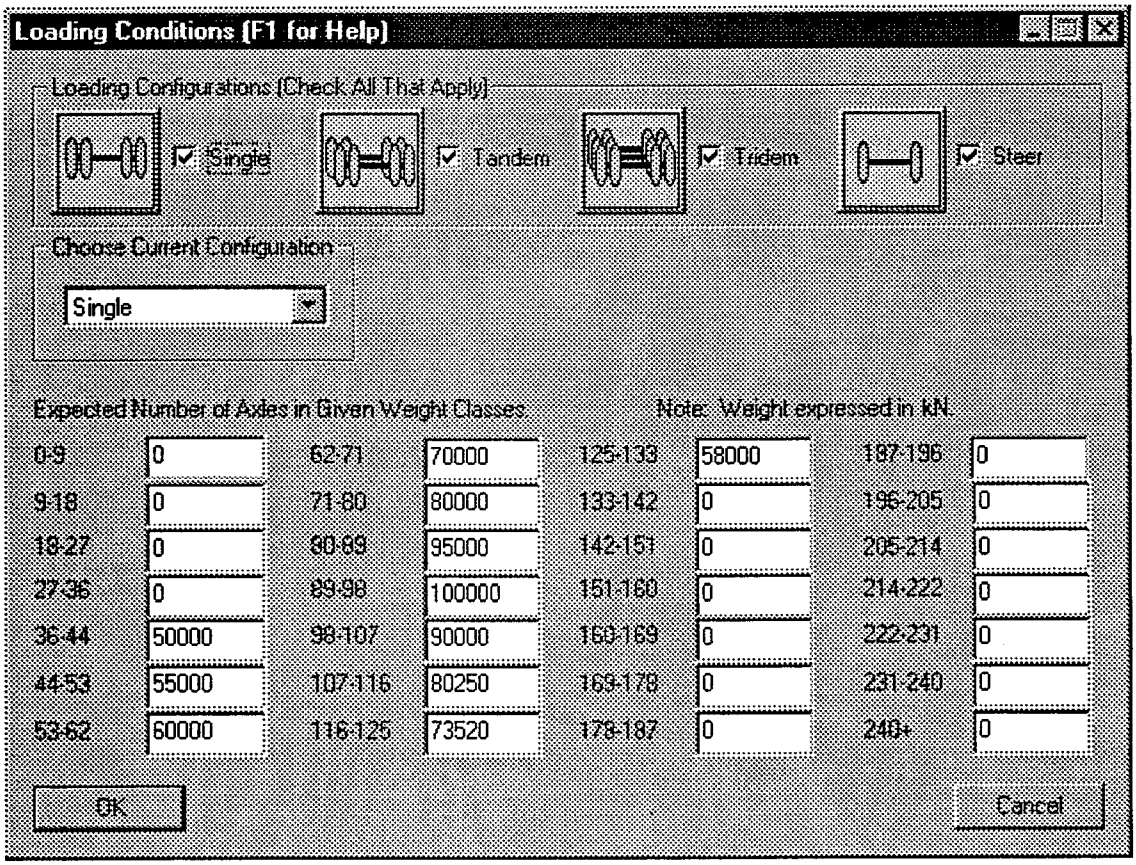

Figure A.5 Load Spectra Input Window.

Loading Configurations

ROADENT allows the designer to account for four different axle types, which may be selected by the check boxes as shown in Figure A.5. The default tire and axle spacing used in ROADENT were based upon the research detailed in a previous report (*1*) and are pictured in Figures A.6, A.7, and A.8 for the single, tandem and tridem axles,

respectively. Due to symmetry of loading, only half the axle is modeled during the analysis. The figures also illustrate the critical locations that ROADENT uses to find the maximum strain at the bottom of the surface layer and top of subgrade for performance predictions. Additionally, in ROADENT, the tire pressure is set to 700 kPa.

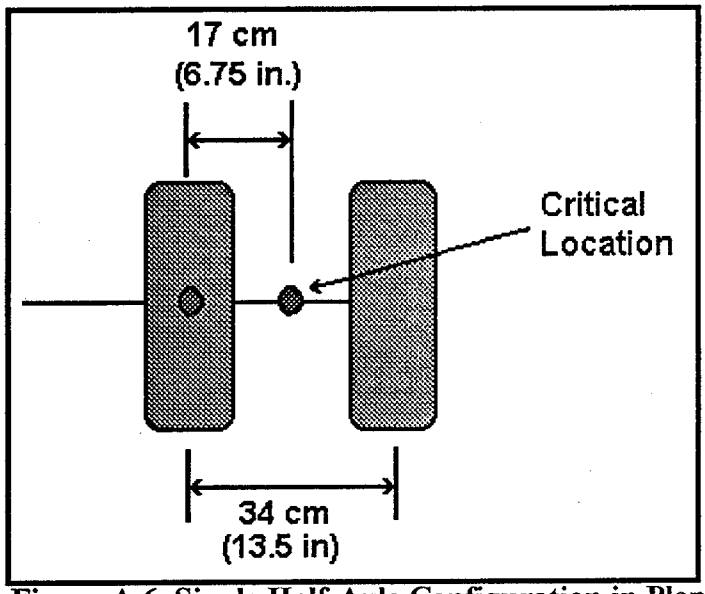

Figure A.6 Single Half-Axle Configuration in Plan View.

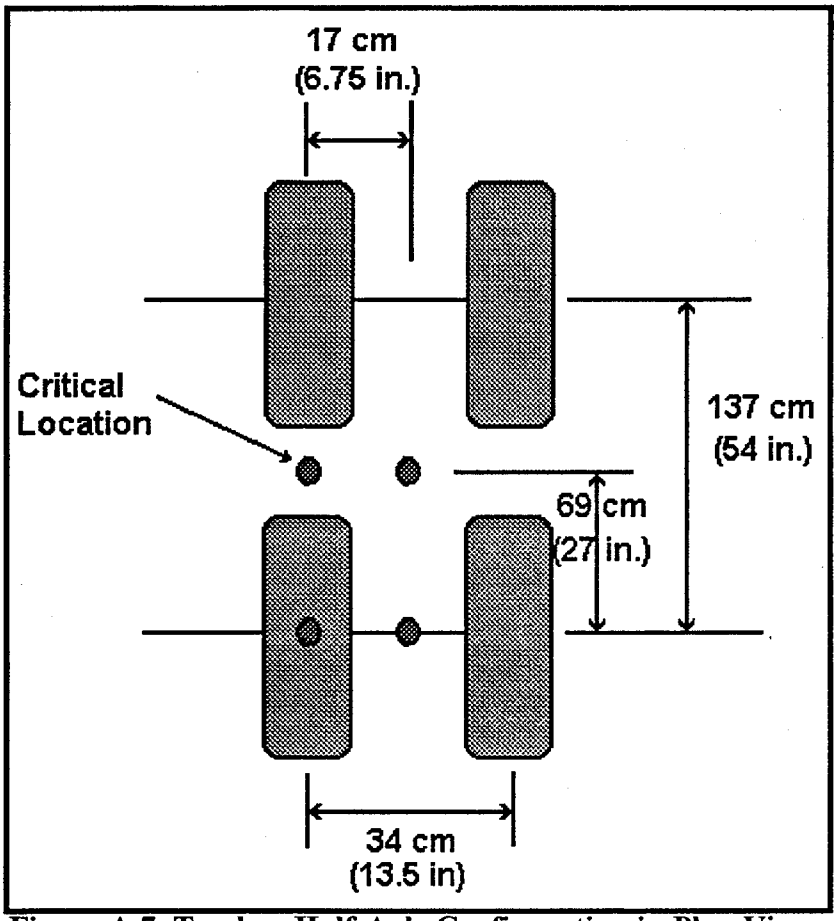

Figure A.7 Tandem Half-Axle Configuration in Plan View.

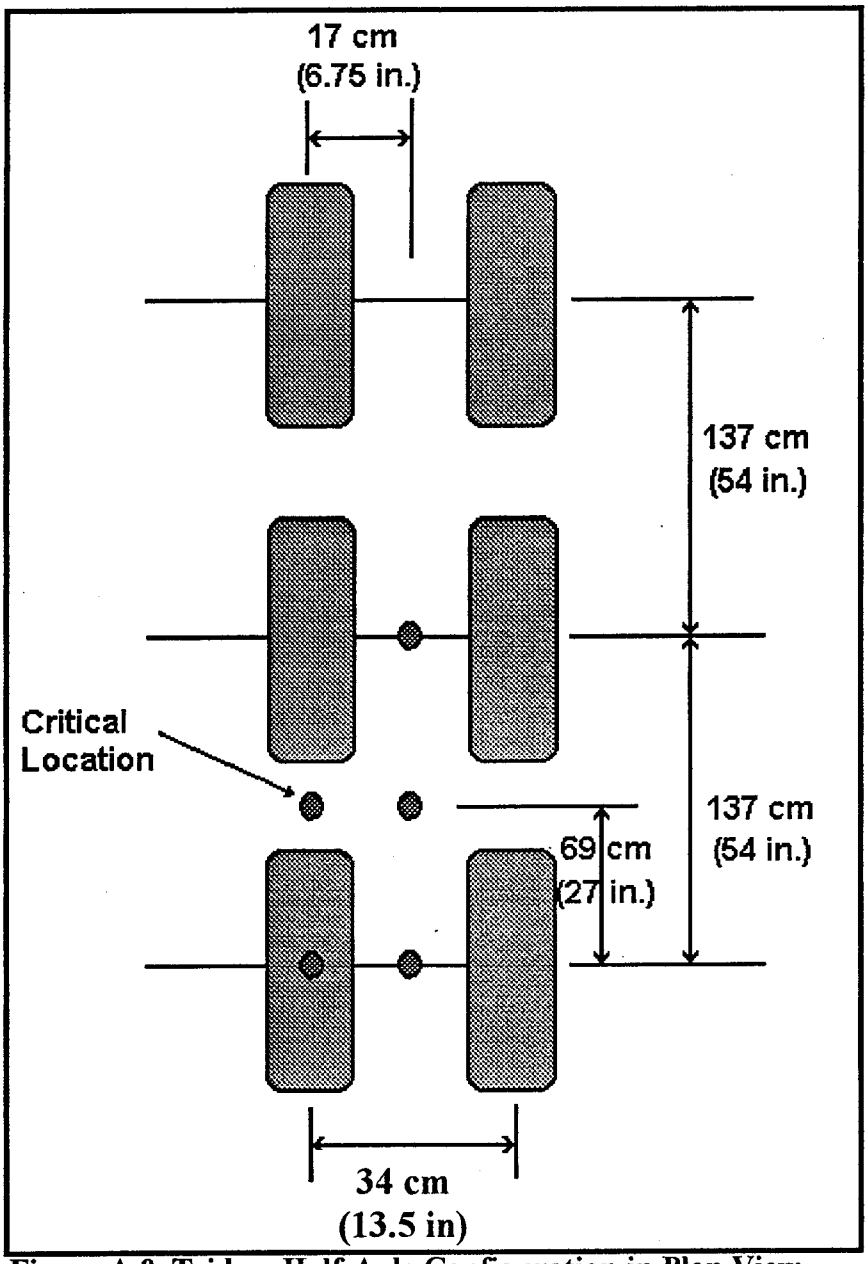

Figure A.8 Tridem Half-Axle Configuration in Plan View.

Choose Current Configuration

This box specifies which axle data are currently displayed. For example, as shown in Figure A.5, single axle is shown and therefore the expected numbers of axles in the boxes below it pertain to the single axle weight distribution. The designer may select any of the other axles to display the respective data.

Expected Number of Axles in Given Weight Classes

The designer should enter, for each axle type selected, the number of expected axles in each weight category over the life of the pavement. These numbers are then used in Miner's Hypothesis to determine the accumulated pavement damage. The numbers are also used in the Monte Carlo reliability analysis. They form the basis of the cumulative distribution functions that are used to perform the analysis and determine the reliability of the design.

ESALS INPUT WINDOW

Although the use of load spectra holds many advantages in terms of pavement design, it may be impossible for the designer to obtain this sort of information. Therefore, the designer may instead enter the traffic data in terms of ESALs. Figure A.9 illustrates the ESAL input window with the default number of ESALs, one million.

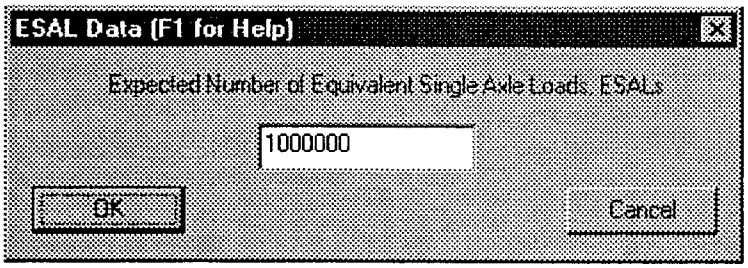

Figure A.9 ESAL Input Window.

Although the designer is using ESALs, ROADENT simply treats this as a very limited load spectrum. If the designer were to view the Load Spectra input window after entering ESALs, he or she would find that ROADENT had simply selected only the single axle for analysis and had divided the number of ESALs evenly between the 71-80

kN and 80-89 kN weight categories. Consequently, this limited load spectrum will be used in the Monte Carlo reliability analysis.

TRANSFER FUNCTIONS

Since it is recognized that the transfer functions may require further calibration and refinement, ROADENT 3.0 allows the designer to adjust the transfer functions accordingly. However, extreme care must be taken when doing this since seemingly small changes in a function can have a significant impact on the resulting design. The transfer functions may be edited by clicking on "Transfer Functions" in the Input dropdown menu. The dialog box shown in Figure A.10 will appear. The designer may change the transfer functions and click OK to accept or Cancel to exit the dialog box without changing the functions. Additionally, the reset buttons are provided to reset the default transfer functions once they have been altered.

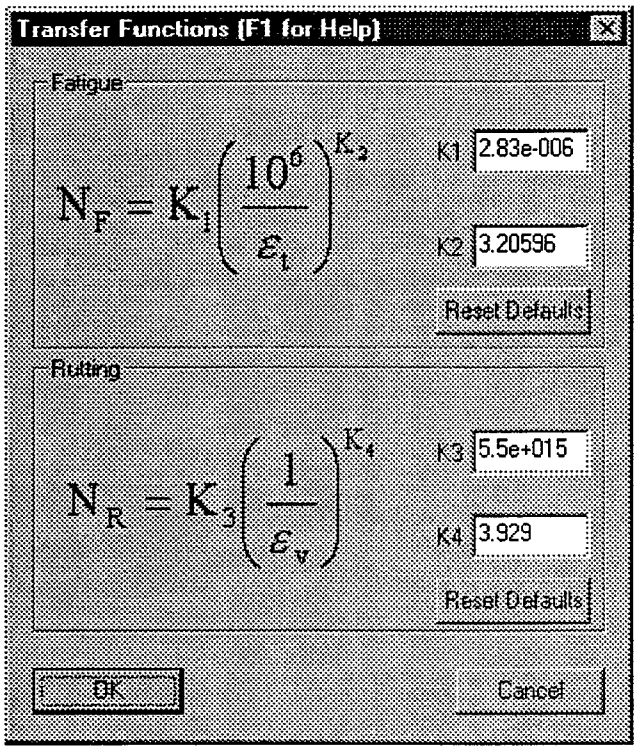

Figure A.10 Input Transfer Functions Dialog Box.

OUTPUT AND DESIGN STUDIO WINDOW

After the structural and traffic inputs have been entered into ROADENT, the designer may proceed to the Output and Design Studio window. To do this, the designer should select Output, View Output from the main window. This action will initiate the Miner's hypothesis calculations and bring up the window as shown in Figure A.11. The window is divided into Damage Analysis, Reliability Analysis, Cost Analysis and Thickness Design Studio, discussed below.

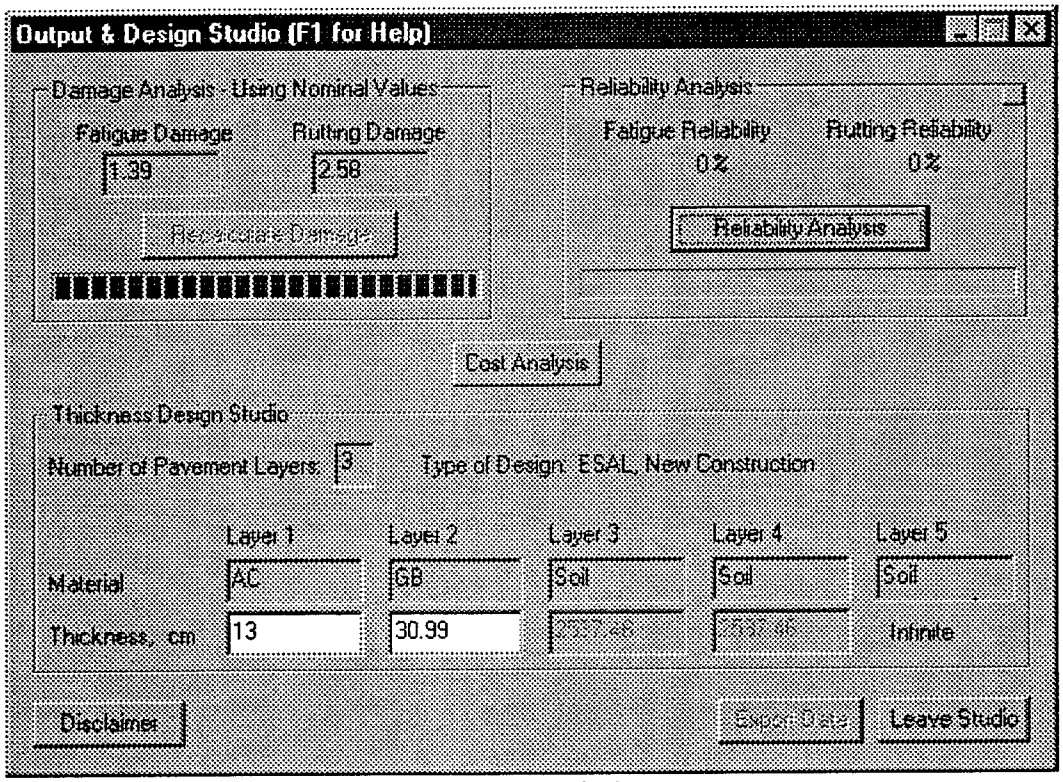

Figure A.11 Output and Design Studio Window.

Damage Analysis

The damage analysis is shown at the top left corner of the window. The fatigue and rutting damage values indicate the amount of damage as predicted from Miner's Hypothesis. These numbers should serve as a design guide before proceeding with the reliability analysis. Typically, the fatigue and rutting values should be below 1.0 before proceeding to the reliability analysis button.

Reliability Analysis

The reliability analysis is in the upper right portion of the output window. When this window first opens, the reliability analysis has yet to be performed. Once the designer is satisfied with the fatigue and rutting damage values obtained from Miner's hypothesis, the Reliability Analysis button may be clicked. This will start the Monte

Carlo simulations and determine the design reliability. The blue status bar will keep track of the progress of the numerous calculations. The number of Monte Carlo cycles has been set at 5,000.

Thickness Design Studio

The thickness design studio allows the designer to change the layer thicknesses and directly evaluate the corresponding pavement damage and level of reliability. The pavement layer materials and thicknesses that were input to the structural window are shown here. To evaluate a new set of thicknesses the designer simply changes the thicknesses and then clicks the Recalculate Damage. The damage is then calculated and shown in the damage analysis portion of the window. Note that changing the design thicknesses will reset the reliability to zero and the designer must perform another reliability analysis after having performed the damage analysis.

Cost Analysis

ROADENT allows the designer to perform a rudimentary initial cost analysis. Clicking on the Cost Analysis button in the Output window (Figure A.11) will bring up the Cost Analysis dialog box (Figure A.12). The designer may then enter the lane width, density and cost of the material. Then, by clicking on calculate, ROADENT will perform the calculations and report the initial cost of the design.

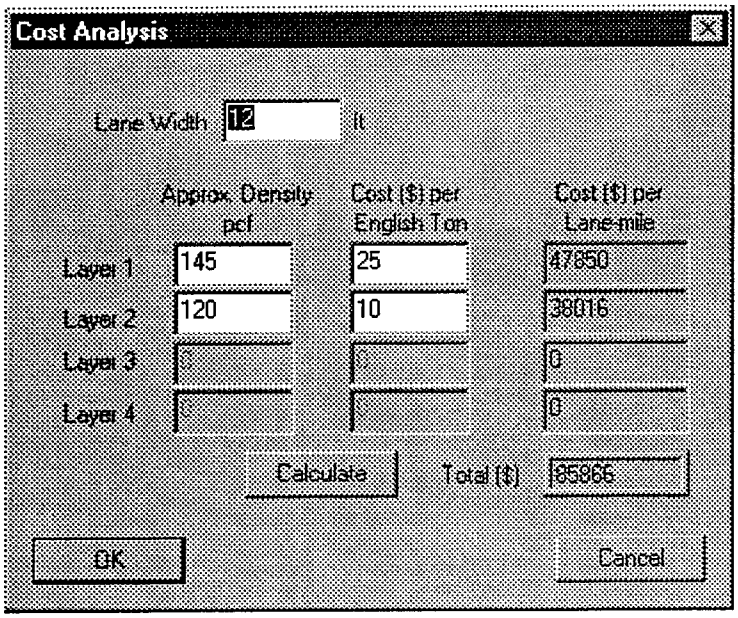

Figure A.12 Cost Analysis Dialog Box.

Miscellaneous Controls

Once a satisfactory set of thicknesses has been achieved, the designer may export the data to a tab-delimited file by clicking on the Export Data button. The data file may then be opened in EXCEL© or any other program that accepts a tab-delimited file.

Clicking on the Leave Studio button will close the design studio and the program returns to the main window pictured in Figure A.1. The Disclaimer button opens the window pictured in Figure A.13.

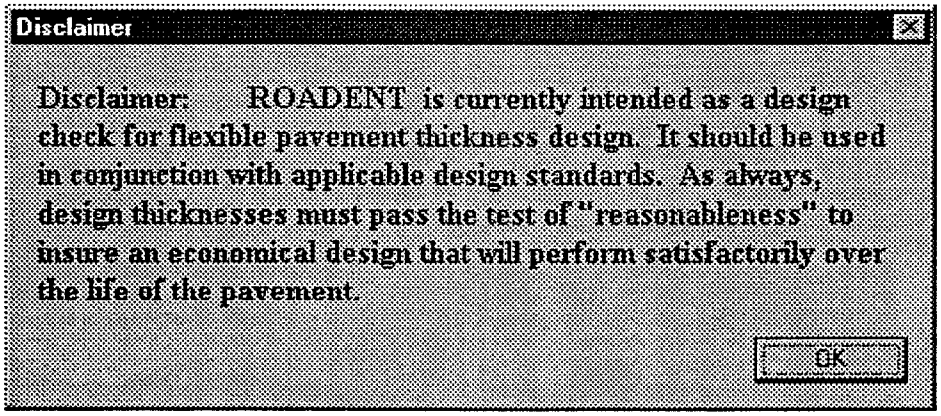

Figure A.13 Disclaimer Window.

HELP FILE

There is a help file associated with ROADENT. The file contains essentially the same information as discussed above, however help regarding each window may be obtained by pressing "F1" on the keyboard. The help file can also be accessed from the main window by selecting the Help menu and then clicking on Contents and Index.

SI AND ENGLISH UNITS

The program may be used in either SI or English units. To change the system of units, the designer should select Units from the main menu and then select either SI or English.

SAVING AND OPENING FILES

ROADENT uses the same "Open", "Save" and "Save As" file protocol common to most windows-based programs. The file names will have the extension ".rdt" to indicate a ROADENT file.

APPENDIX B

GLOSSARY OF STATISTICAL TERMS

1. RELIABILITY
One minus the probability of failure.

2. STATISTICAL [*B.1*]
"Having to do with numbers" or "drawing conclusions from numbers."

3. STOCHASTIC
Involving or containing a random variable.

4. DETERMINISTIC
There is no chance or variability involved.

5. MEAN
Average of a group of measurements (μ).

6. STANDARD DEVIATION
A measure of the variation or dispersion of a group of data (σ).

7. COEFFICIENT OF VARIATION (COV)
The standard deviation divided by the mean value.

8. HISTOGRAM
A graphical form of data presentation. A bar chart that shows in terms of area the relative number of measurements of different classes. The width of the bar represents the class interval; the height represents the number of measurements.

9. NORMAL DISTRIBUTION [*B.2*]
A continuous random variable X is said to have a normal distribution with parameters mean (μ) and standard deviation (σ) where $-\infty < \mu < \infty$ and $0 < \sigma$, if the probability density function is:

$$f(x;\mu,\sigma) = \frac{1}{\sqrt{2\pi}\,\sigma} e^{-(x-\mu)^2/(2\sigma^2)}$$

10. LOGNORMAL DISTRIBUTION [*B.2*]
A nonnegative random variable X is said to have a lognormal distribution if the random variable Y = ln(X) has a normal distribution. The resulting probability density function of a lognormal random variable when ln(X) is normally distributed with parameters μ and σ is:

$$f(x;\mu,\sigma) = \frac{1}{\sqrt{2\pi}\,\sigma x} e^{-(\ln(x)-\mu)^2/(2\sigma^2)} \qquad x > 0$$

where μ and σ are not the mean and standard deviation of X but of ln(X).

11. GAMMA DISTRIBUTION [*B.2*]

A continuous random variable X is said to have a gamma distribution if the probability density function of X is:

$$f(x;\alpha,\beta)=\frac{1}{\beta^{\alpha}\Gamma(\alpha)}x^{\alpha-1}e^{-x/\beta} \qquad x \geq 0$$

12. EXTREME VALUE TYPE I DISTRIBUTION [*B.3*]

A continuous random variable X is said to have an extreme value type I distribution if the probability density function of X is:

$$f(y)=\alpha e^{-\alpha(y-\mu)-e^{(-\alpha(y-\mu))}}$$

where: $\alpha=\frac{\pi}{\sqrt{6}\sigma_y}$ σ_Y = standard deviation of data set

$\mu=M_y-\frac{.5772}{\alpha}$ M_y = mean of data set

REFERENCES

B.1 Western Electric Co., Inc., Statistical Quality Control Handbook, Western Electric Company, Inc., AT&T Technologies, Indianapolis, Indiana, May 1985 (11th Printing).

B.2 Devore, Jay L., Probability and Statistics for Engineering and the Sciences, Fourth Edition, Duxbury Press, 1995.

B.3 Thoft-Christensen, P. and M.J. Baker, Structural Reliability Theory and its Applications, Springer-Verlag, 1982, p. 41.